Exploring the boundaries of networks in the study of resistance against *Ralstonia solanacearum*

Kelis L. G. Fisher

MSc by Research

University of York

Biology

September 2025

Abstract

Solanum dulcamara displays partial resistance to the devastating bacterial pathogen *Ralstonia solanacearum*, with *S. dulcamara* plants showing delayed or no symptoms (Sebastià, et al, 2021). This trait, as well as studies identifying that their root exudates can transfer resistance to *Solanum lycopersicum,* a susceptible crop, makes *S. dulcamara* a key plant for understanding resistance to *R. solanacearum* (Franco Ortega, in press). The following study aims to develop from this finding by exploring the boundaries of network analysis, to broaden our understanding of plant defence against *R. solanacearum*.

A co-expression network compared how gene expression in *S. lycopersicum* and *S. dulcamara* responds to *R. solanacearum* inoculation at five time points post inoculation. This highlighted genes linked to the immune response which differ in expression between *S. dulcamara* and *S. lycopersicum*: Solyc10G001528, Solyc10G000984, Solyc05G001746, Solyc08G000580, Solyc11G001222, and Solyc01G003106. This stretched the capabilities of network analysis to incorporate both cross species and time series data, allowing for the identification of Differentially Expressed Genes (DEGs) related to immunity. Further work is required to mimic *S. dulcamara's* expression of these genes in *S. lycopersicum* to assess whether their function regarding immunity can be transferred to reduce disease.

Additionally, a co-abundance network assessed the influence 2,6-dihydroxybenzoic acid (2,6-DHBA) - a metabolite extracted from *S. dulcamara* root exudates - has on the surrounding microbial communities and to both *R. solanacearum* infection and abundance. This work highlighted six taxa of interest that were influential in the network, and their links to disease have been theorised. However, further research into their roles in the specific interactions between 2,6-DHBA and *R. solanacearum* is required.

This broad study of resistance to *R. solanacearum* has shed light on a multitude of potential resistance mechanisms that *S. dulcamara* has evolved, hopefully contributing to a more sustainable quantitative approach to resistance in *S. lycopersicum*.

Contents

List of Figures

List of Tables

Acknowledgements

I would like to thank both of my supervisors Dr Adrea Harper and Dr Benjamin Lichman, and my TAP member - Dr Daphne Ezer - for their continued support over the course of this project. I would particularly like to thank Dr Andrea Harper for their support, not just during this process, but also over the past five years as my undergraduate supervisor. You have given me countless opportunities to further my career and make the most out of each one of them. Thank you for your patience, advice and guidance. I would also like to show my appreciation to the members of the Harper, Davis and Ezer lab, with particular thanks to Issac Reynolds, Karla Cardenas Gomez, and Daniel Narino Rojas for the continual support, training and advice you have all given me. I would also like to thank Sara Franco Ortega who took an enormous amount of time to teach me. I have gained so much knowledge from you, and I will always be appreciative of the patience you showed me. Finally, I would like to thank my friends and family for all of your support throughout this process. I am unbelievably lucky to be supported by you all.

Declaration

I declare that I am the sole writer of this thesis which is the presentation of original work conducted from data collected by Sara Franco Ortega. This data has been used for Franco Ortega's paper which is currently being prepared for publication, of which, I will be second author of. Any use of Franco Ortega’s work has been acknowledged throughout this thesis and all other sources have been acknowledged as references. This work has not been submitted for any other degree or qualification at the University of York or elsewhere.

1 General Introduction

The human population is expanding and in order to feed this ever-growing population, global food production needs to rise by 70%, with crop yields, in particular, requiring an increase of up to 110% (Buttimer, 2017). However, with climate change being predicted to cause a 12% loss of yield by 2025 and a further 16% loss from pathogens, this target is daunting (Wing, 2021; Ficke, 2018). As of 2011, plant pathogens caused 20% of crop yield losses worldwide, devastating the reliability of food supply (Doornbos, van Loon and Bakker, 2011). This highlights the importance of projects that pursue sustainable management methods to reliably gain high crop yields.

An example of a devastating pathogen that is known to cause $1 billion in yield losses each year is *Ralstonia solanacearum* (Kwak et al., 2018). This pathogen is known to cause an extraordinary loss in yield and is particularly destructive due to its wide host range, encompassing over 200 plant species (Vailleau, 2007). *R. solanacearum*, with its already far-reaching distribution, is continuing to spread via new strains, such as II-B1 (race 3 biovar 2) which have adapted to cooler climates, affecting key crops across the world such as potatoes and tomatoes (Sebastià, et al., 2021). This species of soil borne bacteria interact with the roots via wounds and enter the xylem before travelling to the aerial parts of the plant (Huet, 2014). Here they multiply and, in high densities, produce extracellular polysaccharides (EPS) which are suspected of blocking the transport of water in the xylem, causing characteristic wilt symptoms (Milling, Babujee and Allen, 2011). This pathogen can then be expelled from the roots, entering nearby lakes and rivers, infecting new fields and amplifying the pressure caused by *R. solanacearum* (Huets, 2014).

This tropical pathogen has evolved mechanisms to tolerate the temperate climate of the UK by overwintering in partially resistant host plants such as *Solanum dulcamara* (Huet, 2014). *S. dulcamara* becomes infected with *R. solanacearum* but limits its spread once the pathogen has entered its system (Sebastià, et al, 2021). Then, when temperatures rise to a level where *R. solanacearum* can survive outside of *S. dulcamara*, it emerges and re-enters the watercourse via aquatic roots, ready to travel and inhabit the soil of fields hosting susceptible crops (Sebastià, et al, 2021). This overwintering technique in partially resistant host plants, paired with the ability to survive in soils for years at a time, adds to the complexity of identifying effective methods of prevention (Pascale et al., 2020).

Solanum lycopersicum is an example of a susceptible crop, known to see losses of 26% in fresh hybrid tomatoes from *R. solanacearum* infection (Kim et al., 2016; Artal, 2012). When infected, *S. lycopersicum* displays wilting symptoms, theorised to be due to *R. solanacearum*

blocking the xylem from the production of EPS, inhibiting the flow of water (Caldwell, 2017). *S. lycopersicum* is a crucial crops, providing an affordable source of vitamin A, C and E, and has been found to reduce cancer, cardiovascular disease and osteoporosis risk, as well as requiring low agricultural inputs but selling for comparatively high value, making this the ideal crop for both farmers and consumers (Aslam, 2017). This makes *S. lycopersicum* an invaluable crop which, without protection, could be devastated by *R. solanacearum*.

The large range of hosts and ability to infect water systems have led to the excessive use of chemicals in an attempt to eliminate host plants or reach the deep depths where *R. solanacearum* is known to survive, thereby threatening human and environmental health (Pascale et al., 2020). Currently, there is a reliance on 2-5 year crop rotation, control of host populations, testing for presence in irrigation systems and the creation of resistant crop varieties (Wenneker et al., 1999). However, creating resistance crop varieties based on R (resistance) genes can be ineffective and unsustainable, quickly becoming obsolete with the evolution of pathogens (Laeshita, 2017). The creation of resistant crop varieties stems from understanding the well conserved plant immune response. Plants use Pattern Recognition Receptors (PRRs) to recognise the presence of Microbe-Associated Molecular Patterns (MAMPs) secreted by pathogens (Bigeard, 2015). This activates the Pattern-Triggered Immunity (PTI) which produces defense response proteins. Pathogens inhibit the PTI via the production of effectors, causing effector-triggered susceptibility (ETS). Plants retaliate by producing resistance (R) proteins that recognise the presence of avirulence (avr) proteins and effectors, initiating Effector-Triggered Immunity (ETI). This results in an immune response that provides resistance, known as the Hypersensitive Response (HR). However, if the pathogen's avr proteins are unrecognisable to the plant's R gene, then the plant becomes susceptible (Bigeard, 2015). Understanding which genes are involved in this response often provides the foundation of resistant crop varieties.

As pathogens are continually evolving to overcome resistance, alternative methods are required to reduce *R. solanacearum's* virulence. A well explored example is the investigation into the loss of function of the Type Three Secretion System (TTSS), also known as the *hrp*$^{-}$ mutant (Huet, 2014). This aimed to control *R. solanacearum* by introducing a mutant avirulent variant that outcompetes the pathogenic *R. solanacearum* strain (Frey et al., 1994). The TTSS pathway allows pathogens to translocate proteins into the host plant's cytosol where they influence host cellular processes and cell signalling (Hueck, 1998; Galán, 1999). Mutants with the *hrp*$^{-}$ have a non-functional TTSS, reducing their ability to manipulate the host, resulting in a loss of pathogenicity without impeding its reproduction (Huet, 2014). As these avirulent mutants can still multiply effectively, they were intended to be used as a control for the virulent wild type by competing for the same resources (Huet, 2014).

Unfortunately, despite the promising preliminary greenhouse trials, this proved unsuccessful in its aim to reduce *R. solanacearum* in field trials, likely due to greenhouse trials not considering the continual influx of *R. solanacearum* in field trials (Frey et al., 1994; Huet, 2014).

While this proved unsuccessful and the creation of resistant varieties was especially difficult, *S. dulcamara's* long term partial resistance remained effective. *S. dulcamara* has already been used to shed light on *R. solanacearum* resistance in Sebastià's (2021) study which highlighted increased lignification of xylem vessels, theorised to limit the movement of *R. solanacearum* (Sebastià, et al, 2021). An additional study identified auxin-transport-related genes enriched in *S. dulcamara* when infected with *R. solanacearum* (Franco Ortega, 2025). This was thought to either aid pathogen colonisation or increase root growth which is often found in resistant crops (Franco Ortega, 2025). These findings highlight that, despite how previous control methods have focused on removing the host plant *S. dulcamara* with harsh glyphosate and mechanical intensive labour, that *S. dulcamara* can assist the identification of resistance mechanisms against *R. solanacearum* (Persson, 2008). Furthermore, this emphasises how multifaceted *S. dulcamara's* resistance to *R. solanacearum* is, which may be the reason for their long term and sustainable resistance. Therefore, understanding *S. dulcamara's* resistance mechanisms on multiple levels and mimicking it in the closely related *S. lycopersicum* may provide quantitative resistance that stands the test of time.

To understand *S. dulcamara's* quantitative resistance to *R. solanacearum*, it is key to investigate genetic resistance. Genetic resistance has often been investigated with the intention of identifying genes to intercept the pathogen infection process, such as recognising pathogen-associated molecular patterns (PAMPs) and effectors (Boyd, 2013). An example of R gene studies in relation to *R. solanacearum* includes the identification of a gene called *ERs1* in a resistant eggplant variety (Lebeau, 2012). *ERs1* is theorised to influence marker-assisted selection, reducing susceptibility by reducing colonisation and wilting by interacting with bacterial effectors, influencing the resistance to three strains of *R. solanacearum*: CMR134, PSS366, and GMI1000 (Lebeau, 2012). This study highlights the importance of understanding gene variations between resistant and susceptible plants in the process of identifying key resistance mechanisms. However, R genes such as these have been found to be overcome by the targeted pathogen. This is fueling an increase in interest related to quantitative resistance. For example, there is a *R. solanacearum* resistance *S. lycopersicum* cultivar, LS-89, which upregulates over 140 genes compared to a susceptible cultivar, Ponderosa (Ishihara, 2012). These 140 genes were linked to: jasmonic acid and ethylene signalling; and pathogen-related genes associated with β-1,3-glucanases, lignin and hydroxycinnamic acid amides (HCAAs). This is an example of quantitative resistance

against *R. solanacearum* which, in the case of LS-89, has been recorded as early as 1997 and is still used for its resistance, 28 years later (Nakaho, 1997; Zhang, 2025). This highlights the long-term benefits of understanding quantitative resistance against *R. solanacearum*.

While understanding how genetic differences influence resistance is key, this is not the sole contributor to *S. dulcamara's* partial resistance as physical properties also inhibit infection. For example, the cell wall is one of the first lines of defense so its structural components have been well studied (Shi, 2023). This includes an increase in methylation of pectin, a mixed collection of polymers, found to increase tolerance to pathogens, such as *R. solanacearum*, that degrade cell walls with digestive enzymes (Micheli, 2001; Shi, 2023). Additionally, lignin maintains the strength of the secondary cell wall, also resisting the effects of degrading enzymes, improving the physical robustness of the plant cells which reduce the success of invading pathogens (Sebastià, et al, 2021). Additional structural components have been found to change when under attack from pathogens, such as the formation of tyloses and gels (Xue, 2025). Tyloses are invaginations of the parenchyma cells, often found in the xylems when under stress, which are theorised to block infected plant vessels to prevent the spread of pathogens such as *R. solanacearum* (Caldwell, 2017; Shi, 2023). The production of gel is often alongside tyloses and contains pectin and often antimicrobial compounds (Shi, 2023). These are secreted into the plant vessel via the xylem and have been found to suppress wilt diseases (Shi, 2023). While these structural properties are improving resistance, they do not provide complete control and have been found to be a contributing factor to partial resistance similar to *S. dulcamara's* resistance to *R. solanacearum*.An alternative, yet equally important, area of resistance study is understanding the microbial composition of the rhizosphere and how this changes when *R. solanacearum* is present. The first line of defence for plants is the microorganism community, with high microbial diversity thought to promote plant health (Pascale et al., 2020; van Elsas et al., 2012). High microbial diversity has been found to: increase competition for resources; aid nutrient availability; increase antagonism; and improve the stimulation of plant immune systems (Yu, 2019). However, there is contradictory evidence that makes microbial diversity's link to plant immunity unclear, as high fungal diversity is often linked to higher disease outcomes (Gu, 2022; Filion, 2004). Therefore, soil microbial diversity and composition is likely to be case specific, requiring in-depth and specific analysis to understand why plants are creating specific rhizospheric compositions. Despite this uncertainty, it has been reliably reported that to reap the benefits of rhizosphere microbiomes, plants manipulate their surroundings via root exudates, some of which recruit beneficial soil microbes that provide specific protection and growth promotion (Pascale et al.,

2020). Analysis of the specific interactions between plants, their root exudates, and pathogens which also impact the composition of the rhizosphere is paramount to enhancing growth and protection from disease.

Analysis of this work can take many forms but utilising networks, a well-established bioinformatics tool that, despite being around for over 20 years is continuing to evolve, has the ability to identify interactions and patterns between different conditions (Zitnik, et al., 2024). There are a range of networks, each focusing on interactions between nodes which allow for the exploration of possible functions from these links. For example, co-expression networks identify links (edges) between genes (nodes) and groups them into modules based on the similarity of their expression (Zitnik, et al., 2024; Serin, 2016). The strength of these edges are often depicted by the weight of the lines linking the nodes together (Zito, 2025; Serin, 2016). Modules were linked to traits and the hubs (highly influential nodes) of modules linked to the trait of interest were identified (Serin, 2016). Hub genes can be identified through a myriad of methods, including degree score, centrality and Page Rank. Degree score identifies the most central node within the module, defined by having the most edges to other nodes in the module (Zeng, 2021). Centrality of particular nodes, also referred to as intramodular connectivity (kIM), indicates how connected each node is to the other nodes within the module and those with the highest kIM should be highly linked to the module eigengene, highlighting their influence and representation of the nodes in that module (Langfelder and Horvath, 2008). An alternative method is PageRank which considers the wider influence within the module, identifying both the number and weight of significance of the edges, but also considers how connected each connected node is to gain an understanding of each node's influence in context of the whole module (Kumar and Shahid Mukhtar, 2023). Each method of hub gene identification highlights well connected and influential nodes. Therefore, hub genes of modules linked to the trait of interest are likely to be genes that are high up in pathways involved in the trait of interest. However, interpretation of networks can be complex and require a lot of investigation to gain practical and usable insight into potentially influential genes. Another example of a biological network which faces the same challenges as the co-expression networks, are co-abundance networks which identify interaction patterns in often complex communities and population dynamics (Berry, 2014). These have been used to indicate underlying interactions between microbes and the environment but have yet to be used for exploring changes that root exudate metabolite application has on the microbial communities of a susceptible plant's rhizosphere (Berry, 2014).

In this study, we want to test the boundaries of network analysis, using them in novel situations to identify differences in response to *R. solanacearum* infection at multiple levels:

genetic and microbial. This will include creating a co-expression network to assess differences in gene expression in *S. dulcamara* and *S. lycopersicum* when inoculated with *R. solanacearum*, as discussed in chapter 2. A co-abundance network will then be utilised to understand the changes in the rhizosphere microbiome of *S. lycopersicum* when inoculated with *R. solanacearum* as well as a beneficial metabolite isolated from the root exudates of the partially resistant *S. dulcamara* which will be discussed in chapter 3. These two networks explore separate, novel, areas of study: creating a cross-species co-expression network that incorporates time-series analysis to understand the differences in genetic response to infection; and creating a co-abundance network that explores a new metabolite to understand the impact this has on the surrounding microbiome to test its viability as a marketable protective metabolite. The aim of this thesis which analyses both genetic and soil microbial community's response to *R. solanacearum* inoculation is to identify a multitude of potential resistance mechanisms that *S. dulcamara* uses and how 2,6-DHBA aids resistance in *S. lycopersicum*. This may allow for a more sustainable quantitative approach to further improve resistance studies in *S. lycopersicum*.

Exploring the use of WCGNA with Time-Series data in a Cross-Species comparative analysis

2.1 Introduction

Genetic resistance to *R. solanacearum* which focuses on one resistance gene (R gene) has had limited progress due to the complexity of *R. solanacearum*'s infection mechanisms, and the process of identifying genes in crops and creating successful mutants that are both suitable for growth in the field and for human consumption is a lengthy process (Huet, 2014; Kim et al., 2016). R gene resistance is often quickly overcome by pathogen adaptation, making this form of protection unsustainable (Kim et al., 2016). Therefore, alternative methods of creating innate host resistance need to be identified so that alternative sustainable resistance strategies can be devised, thereby allowing more time in the continuing inevitable arms race between people and pathogens. As the mechanisms behind *S. dulcamara's* resistance, which causes their partial resistance, are still largely unknown, new projects are vital for identifying novel sustainable resistance (Sebastià, et al, 2021). This project, therefore focuses on identifying differentially expressed genes (DEGs) between *S. lycopersicum* and *S. dulcamara* when inoculated with *R. solanacearum* with the aim of exploiting *S. dulcamara's* long standing resistance mechanisms and incorporating this into closely related, susceptible crops. This will require exploring the use of Weighted Gene Co-expression Network Analysis (WGCNA) to understand the co-expression of genes in infected resistant *S. dulcamara*, and susceptible *S. lycopersicum* plants over time to understand *S. dulcamara's* genetic resistance mechanisms.

WGCNA is an established bioinformatics analysis tool that describes the correlation of gene expression with different traits and clusters them into modules based on their expression (Langfelder, 2008). This can incorporate different traits, often quantitative, such as diseased/not diseased, to understand how these traits are impacting the co-expression of genes within the samples (Wang, 2019). This technique has been used in an array of biological contexts, including: animal, plant and bacterial genetics; cancer genetics; and even brain imaging (Langfelder, 2008). For example, WGCNA was used to identify core trait associated genes and regulatory pathways relating to responses to drought in two varieties of Tartary buckwheat, resistant XZSM and susceptible LK3 (Meng et al., 2022). This project regularly assessed the plants once drought conditions were initiated and the extracted RNA-seq data was analysed using WGCNA. The genes were then grouped into modules and Differentially Expressed Genes (DEGs) and Gene Ontological (GO) enrichment analysis was

conducted to identify potential molecular mechanisms linked to the drought trait. These genes encompassed a range of functions, including links to abscisic acid, enzymatic antioxidants and amino acid biosynthesis, and highlighted key pathways that reduce water loss in leaves, initiating cell damage protection, and Reactive Oxygen Species (ROS) scavenging (Meng, et al., 2022). This use of WGCNA shed light on genes and pathways linked to drought-resistance, providing candidate genes that may increase drought resistance in Tartary buckwheat. This highlights how useful WGCNA is when identifying influential genes and pathways that respond to specific traits, without limiting itself to a particular function.

To expand on this use, Wang's (2019) study incorporated a time-series component, further testing the capabilities of WGCNA. Maize leaf samples were extracted at five time points, and WGCNA was conducted to gain clarity on the fluctuations of the carbon metabolism process over time. Genes were clustered into modules and gene-gene analysis identified hub genes which are often high up in biological pathways, and have downstream impacts on more genes (Jin, et al. 2019; Liu, 2019). Further GO analysis identified key candidate genes with links to the trait of interest, carbon metabolism (Wang, 2019). This paper assessed how time impacts the gene expression of carbon metabolism, with the intention of setting a precedent for the use of time-series data in WGCNA as well as identifying candidate genes involved in carbon metabolism for future, in-depth research (Wang, 2019).

WGCNA has also been used across species to improve understanding of the biological processes underpinning osteosarcoma (OS). Zheng Jin's (2019) study described the comparison of human and canine OS samples, justifying the use of two very distinct species by the abundance of conserved biomarkers, such as IL-8 and SLC1A3, which indicates similar pathways and the use of an intermediate mouse consensus network to check the validity of the human-canine network (Jin, 2019). This explored the use of WGCNA to identify co-expressed modules between the human and canine OS positive samples, leading to the identification of highly preserved modules across the species (Jin, et al. 2019). Further functional enrichment analysis indicated module function and hub gene analysis identified influential genes linked to pathways related to OS. As this network included two very distinct species, with just under 4,000 shared genes, further validation for this comparison was needed. This took form as the use of a separate, intermediate human-mouse network that was compared to the original human-canine network to ensure it was not highlighting species-specific anomalies. These saw significant overlap, indicating that this cross-species network was robust enough to identify co-expressed genes that were linked to biological pathways known to be associated with tumours (Jin, et al. 2019). This highlights how

adaptive WGCNA can be, identifying co-expressed genes even across species boundaries to identify influential genes under specific circumstances such as the presence of OS.

WGCNA has previously been used to understand *S. lycopersicum* (cv. Heinz 1705) resistance to disease. For example, Tominello-Ramirez (2024) utilised WGCNA to test the difference in gene expression of *S. lycopersicum* when inoculated with a strain of early blight and brown leaf spot (EBBLS) under four conditions: inoculation of low virulence strain, CS046; inoculation of a highly virulent strain, 1117-1; inoculation of chitin, known to promote plant immunity; and finally, water as a negative control. This WGCNA highlighted the blue module as being significantly linked to the inoculation of CS046 and the yellow module linked to 1117-1. Gene Ontology (GO) analysis found that the blue module was linked to defence while the yellow module, which had no significant GO terms, was enriched with biotic stress and toxin response terms. Further analysis found that the yellow module was home to genes that promoted leaf senescence such as SlWRKY16 and SlWRKY53 while the blue module genes were primarily linked to defence, including SlC3H70, SlERF.A1 and JA2. This use of WGCNA indicated a strong immune response to CS046 compared to the inefficient immune response to 1117-1, so genes that were expressed in response to CS046 were considered to be involved in *S. lycopersicum's* successful defence response. This analysis gained a deeper understanding of *S. lycopersicum's* genetic based resistance which could be harnessed in further resistance studies against EBBLS (Tominello-Ramirez, 2024).

This wide-reaching technique has been stretched to incorporate time-series data and cross-species comparisons but only separately. This project aims to further explore the boundaries of WGCNA and to harness its ability to identify differences in gene expression between two different species, *S. dulcamara* and *S. lycopersicum*, across time points, when inoculated with *R. solanacearum.* This aims to provide candidate genes where their expression levels in *S. lycopersicum* could potentially be altered to mimic the expression of the partially resistant *S. dulcamara*, resulting in an increase in resistance in *S. lycopersicum*.

2.2 Methods

2.2.1 Previous work

This experiment used data collected and analysed in Franco Ortega's (2024) study which required 30 *S. dulcamara* (Millenium Seed Bank, Royal Botanic Gardens Kew, ID-39087) seeds. These were stratified on wet tissue paper and kept in the dark at 4 ^{o}C. After 10 days, the 30 stratified *S. dulcamara* seeds and 30 *S. lycopersicum* (Moneymaker, Mole Seeds,

Colchester, UK) seeds were surface sterilised for 1 minute in a bleach/water dilution (1:99 v/v), then rinsed thoroughly with distilled water. The *S. lycopersicum* seeds were then stratified for 4 days in the same conditions as the *S. dulcamara* seeds to ensure equal germination across seeds and species. All seeds were then potted in John Innes No2 (~125 g compost/pot) at 20 ºC (±2 ºC) with 14 hours light and 10 hours dark cycle in a growth room to mimic early summer in the United Kingdom. After an additional 3 days, a total of 17 days since the beginning, they were inoculated with *R. solanacearum* and moved to a PHCbi growth cabinet (24 ºC and light for 16 hours, 20 ºC and dark for 8 hours), allowing for adequate time to acclimatise.

After 4 days since moving to the PHCbi growth cabinet, 21 days since the start, three *S. dulcamara* and three *S. lycopersicum* plants were root drenched with 5 mL of *R. solanacearum* (UW551) at the base of the stem. This growth stage allowed for an adequate level of infection so that the plants did not succumb to the pathogen immediately and there was enough time to sample. Three of each species were left as a negative control and inoculated with 5 mL of sterile CPG media for comparison between infected and non-infected samples, both within and between species. RNA-sequence data was immediately sampled from the leaves at the time of inoculation (0 hours) and again at 6, 12, 24, and 48 hours post inoculation. These sample times were taken to identify early responses to infection as *R. solanacearum* has been found to spread to the stem of plants within hours (Tans-Kersten, 2001). These additional samples were extracted from a leaf at the same developmental stage for each plant at each time point to assess the genetic response in the same spatial range. To aid extraction, the leaves were frozen in liquid nitrogen and stored at -80 ºC, then ground with a pestle and mortar. RNA was extracted using E.Z.N.A ® Plant RNA Kit (VWR, Lutterworth, UK) as per the manufacturer's instructions as well as treatment with DNase to remove residual DNA. Samples were QCed with TapeStation and quantified with Qubit 4.0. before sequencing by Novogene UK who performed the Illumina library preparation and the sequencing using the NovaSeq 6000 platform (Illumina, CA, USA) with a paired-end library strategy (PE150).

After the final RNA extraction, a PCR was conducted to confirm the presence of *R. solanacearum* using primers RS199F and RS199R (AGTAACTCGGCTGTTCTTT and TATTCGCTTGACCCTATAA respectively) designed on the ITS region (Chen et al., 2010). This used 200 nm of RS199F and Rs199R primers, GoTag Green Master Mix (Promega) at 1x, and 1 µl of 50 g/µL and with the following cycle of 95 ºC for 4.5 min, 40 cycles of 95 ºC for 30 sec, 55 ºC for 30 sec, 72 ºC for 30 sec, and a final extension at 72 ºC for 10 minutes. This was visualised using a 1.5 % agarose gel, sequenced using Eurofins Sanger services and BLASTn was used to identify the species.

Trimmomatic v0.39 was used to read both *S. dulcamara* and *S. lycopersicum* raw reads and Salmon quantified the transcripts against the newly assembled *S. dulcamara* genome (Franco Ortega et al., 26 May 2025) and SL5 pangenome (Zhou et al., 2022). Franco Ortega identified the ortholog genes between *S. dulcamara* and *S. lycopersicum*, resulting in a total of 17,840 genes from the original 17,953 *S. dulcamara* genes as well as identified their corresponding GO ID with p-values indicating significance of association between gene and function term.

2.2.2 Transcriptomic Data Preparation

Comparing the gene expression of the resistant *S. dulcamara* and susceptible *S. lycopersicum* species required the use of their orthologous genes but as these species are closely related, only 113 genes were removed. To accurately compare these two species, one network per species was created, and the movement of DEGs between modules across the two networks were assessed.

2.2.3 DEG Analysis

To identify genes linked to *R. solanacearum* resistance in *S dulcamara*, the DESeq2 package in R (Love, 2014) was used to compare three different factors: species (*S. dulcamara* and *S. lycopersicum*); time point (0, 6, 12, 24, 48 hours); and inoculation status (inoculated and non-inoculated). To incorporate all interactions, the following model was used:Ral_infected + Species + Timepoint + Species:Timepoint + Ral_infected:Timepoint + Ral_infected:Species:Timepoint. To assess the influence of inoculation status, the following reduced model was used: Ral_infected + Species + Timepoint + Species:Timepoint.

The raw abundance, count and lengths data were combined, creating the variance stable distribution (vsd) counts data. The composition of this model took into account DEGs present at 0 hours, removing them to reduce the influence of innate differences between species. The DEGs at each time point were then assessed, using the lfcShrink function (type = “ashr”) from DESeq2 ashr R Package (Stephan, 2023) to improve the logFoldChange (LFC) representation for genes that were lowly expressed, and then filtered to identify significant DEGs (LFC >= 1 and padj < 0.05). Each gene was mapped to their corresponding Gene Ontology (GO) ID during previous work conducted by Franco Ortega (in press) and was matched to their corresponding GO term for further analysis and to aid the understanding of module function. Only GO terms with a p-value < 0.05, determined by Franco Ortega, were kept for further analysis.

2.2.4 Constructing Networks

Before analysis, gene expression quality was assessed by removing lowly expressed genes (missing or 0), resulting in 16,888 genes in the *S. dulcamara* network and 16,765 in the *S. lycopersicum* network. To ensure the data fit the scale-free topology (SFT), the vsd (Variance Stabilising Transformation) data, created using DESeq2 (Love, 2014), was used. This normalises the raw RNA-seq counts data, satisfying the assumption of a scale-free network. Fitting the SFT ensures that there are a few, highly connected hubs, rather than many genes that are moderately well connected. Additionally, a power of 13 was chosen as both networks fit the SFT model at this power (*S. dulcamara* - R2 = 0.8050, mean.k =8.89 and medium.k = 2.870) (*S. lycopersicum* - R2 = 0.85900, mean.k = 22.50 and medium.k = 9.73), allowing for accurate cluster comparisons between both networks.

Weighted Correlation Network Analysis (WGCNA) was conducted, creating separate networks for *S. dulcamara* and *S. lycopersicum*, sorting the genes into modules based on their co-expression (Langfelder, 2008). Therefore, genes with similar expression patterns across the traits were assigned to the same module as it indicated they were co-expressed and the distribution of genes across modules were visually checked using dendrograms.

To identify the over-represented functions of the genes in each module, GO terms were used to identify gene functions that appear more often in one module than expected by chance. Each gene had been linked to relevant GO ID numbers, each of which correlates to a GO term, and using the mutate() function in R (Wickham, 2023), these were combined so that each gene corresponded to the relevant GO term. This, alongside further work, should allow us to identify key genes involved in the infection response, further aiding the identification of modules that influence resistance to *R. solanacearum*.

2.2.5 Module Preservation and Visualisation

The movement of DEGs between modules across the two networks was analysed using the caret package, preprocess function, in R (Kuhn, 2008), which identified differences in the *S. dulcamara* network compared to the control *S. lycopersicum* network. This was done in two ways, with Zsummary and medianRank. For the Zsummary, the nPermutations1 was set to 200, as recommended by Horvath (2011), and seed was set to 1 to ensure the randomisation is reproducible. The function modulePreservation() from WGCNA (Langfelder, 2008) was then used (referenceNetworks = 1, nPermutations = nPermutations1, randomSeed = 1, quickCor = 0, verbose = 3) to identify module preservation between the two networks. This aims to identify modules that are likely to contain genes that differ

between the two transcriptional networks when inoculated with *R. solanacearum* which may indicate if they are likely to be potentially stress or immune related genes.

To further visualise the change between these two networks, a DEG Movement alluvial graph was created using the ggalluvial R package (Brunson, 2023). This was used to identify a module that splits into multiple modules in the other network, highlighting those that potentially contain genes that act differently under the different conditions between the two species. This would aid the understanding of the difference in preservation of genes between the two networks.

2.2.6 DEG Enrichment and Movement

To improve understanding of the modules of interest, the DEG enrichment for each time point was studied. This filtered for significant DEGs (LFC >= 1, padj <= 0.05) at each time point and identified modules that had more DEGs than the average. The number of DEGs at each time point was also assessed using ggvenn() (Yan, 2025) to create a four-way venn diagram to visualise the change in DEGs over time. Finally, DEGs that split into different modules in the other networks, as depicted on the DEG Movement graph (Fig. 1.4), were then assessed further by identifying DEGs with significant GO terms related to immunity and stress.

2.2.7 Hub Analysis

Once the modules were selected, the genes with the highest degree score (genes with the most connections to other genes) were recorded and labelled as hub genes. The hub genes with GO terms linked to immunity and stress were selected, and the expression of these genes were plotted for individual assessment. Those that had variation between species were selected for further analysis.

2.2.8 Statistical Data Analysis

To understand and visualise the data, a PCA graph (Fig. 1.1) was created using the variance-stabilised counts (vsd) data and the plotPCA() function in the DESeq2 package in R (Love, 2014). Additionally, a volcano-plot (Fig. 1.2), using ggplot2 (Wickham H, 2016), was created with the LFC and adjusted p value data to visualise genes with large changes in expression that are highly significant. This was conducted with all DEGs at each time point after filtering.

2.3 Results

2.3.1 Network Construction

To understand the difference between *S. dulcamara* and *S. lycopersicum's* genetic response to *R. solanacearum* infection, two WGCNAs were conducted which assessed orthologous genes under *R. solanacearum* inoculation over time. After filtering to ensure high quality reads, the *S. dulcamara* network assessed 16,888 genes, split between 38 modules while the *S. lycopersicum* network had 16,765 genes, split between 70 modules.

2.3.2 Effect of *R. solanacearum* Infection

To aid the understanding of the data, a PCA was conducted: PC1 representing the difference between the *S. dulcamara* and *S. lycopersicum* samples, explained 55% of the variance; PC2 representing the difference between each time point, explained 11% of the variance; and PC3 which further clarified the split between time point, explained 8% of the variance (Fig. 1.1). PC2 and PC3 indicate that the two species have a similar change over time but PC1 emphasises that there is still clear separation between the species. The similarity in changes over time further validates that comparisons between species is appropriate. Additionally, the difference between time points decreased with 24 and 48 hours being almost indistinguishable which could be due to the initial immune response slowing but has not returned to normal levels as it is still dissimilar to the levels found at 0 hours. Additionally, there is a large difference between 0 and 6 hours, likely to be due to *R. solanacearum* inoculation not reaching the leaves immediately and then inducing a strong initial response at 6 hours post inoculation. It should be noted that all time points were taken in the light due to 16:8 hours light:dark cycle so diurnal changes are unlikely to be influencing such large changes between time points, as seen between 0 and 6 hours. There may be some slight diurnal influences between time points at different times in the light periods, such as 6 and 12 hours, but each time point has both infected and uninfected samples so diurnal changes should be identified through their comparisons.

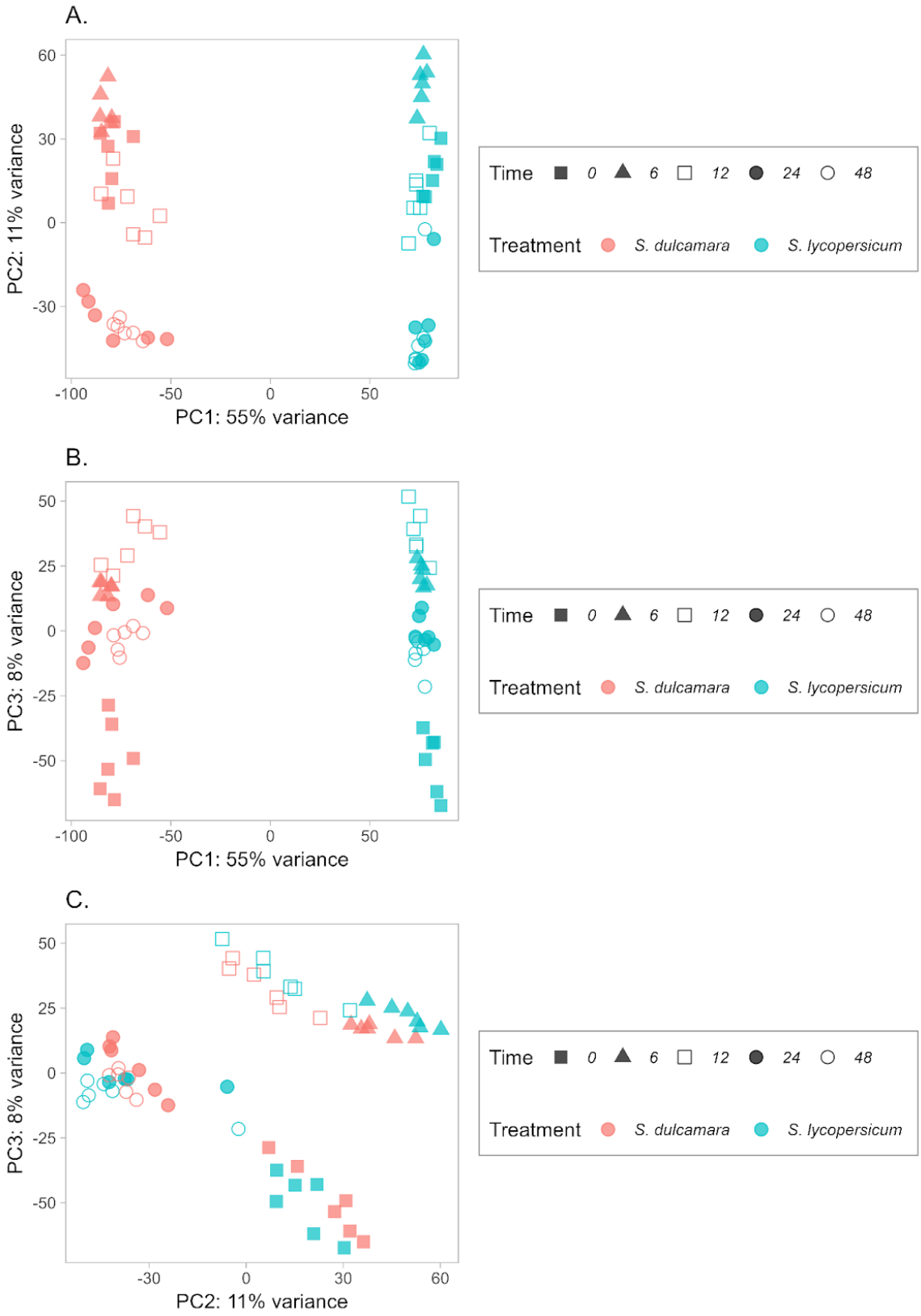

Figure 1.1 PCA graph. Displaying the difference between *S. dulcamara* (red) and *S. lycopersicum* (blue) as well as the difference between each time point (shapes): 0 hours (time of inoculation); 6, 12, 24, and 48 hours. **A.** PC1 separates the species, explains 55% of the variance while PC2 explains 11% of the variance and separates time. **B.** PC1 and PC3 separates species and time points, with PC3 explaining 8% of the variance. **C.** Both PC2 and PC3 separate time points.

To aid the identification of significant DEGs under the model ~ Ral_infected + Species + Timepoint + Species:Timepoint + Ral_infected:Timepoint + Ral_infected:Species:Timepoint, all 17,840 orthologous genes were plotted. All significant DEGs, those that surpass the threshold (logFold Change (LFC) >=1, LFC >=-1 and padj <=0.05), were highlighted. Before further filtering, there were a total of 3,436 DEGs that were significantly up regulated compared to 2,298 that were significantly down regulated. It is also interesting to note how many genes had low significance but high LFC, which is likely due to comparing two different species but the appropriate filtering was able to remove these from further analysis (Fig. 1.2).

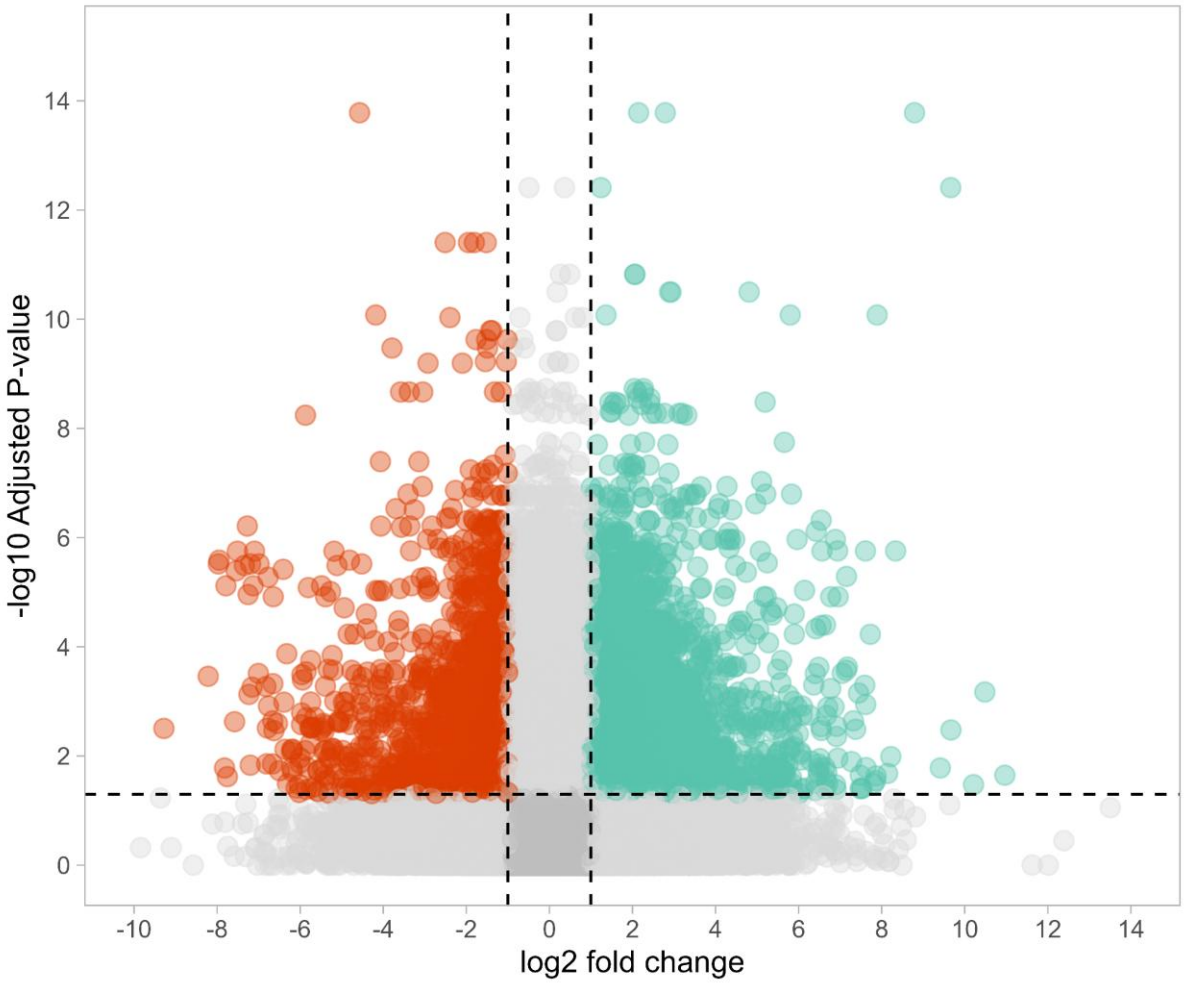

Figure 1.2 Volcano plot. Visualising the expression levels and significance of expression for differentially expressed genes (DEGs). Those above and outside of the dotted lines are considered significant DEGs (log2FoldChange of ±1 and -$\log^{10}$ of the adjusted p value of 0.05). As this has been conducted on the shrunk and filtered data, there are no points between the dotted lines.

2.3.3 Module Preservation

Module preservation assesses how similar the module composition is between the two networks which highlights how different the expression profiles are between them. This was indicated by medianRank and Zsummary (Fig. 1.3). MedianRank measures the level of module preservation between networks (higher medianRank implies lower module preservation) and is intended to be independent from size but the larger module's observed preservations are, the more statistically significant they are compared to a smaller module so there is some size based influence (Langfelder, 2011). Therefore, medianRank is beneficial to assess as it considers module size within this statistic. The Zsummary, however, also measures the preservation of each module in the reference network (>10 = strong module preservation, <2 = no indications of preservation), compared to the test network and considers density and three connectivity-related statistics (Luo, 2021). This statistic heavily depends on module size so should be used in conjunction with the medianRank, especially for networks with a large range of sizes to reduce bias towards larger modules (Nguyen, 2025). For example, the steelblue, lightyellow and green modules show a high medianRank preservation (30, 23 and 21 respectively) and a low Zsummary score (-0.96, 0.72, and 6.74 respectively), indicating low module preservation.

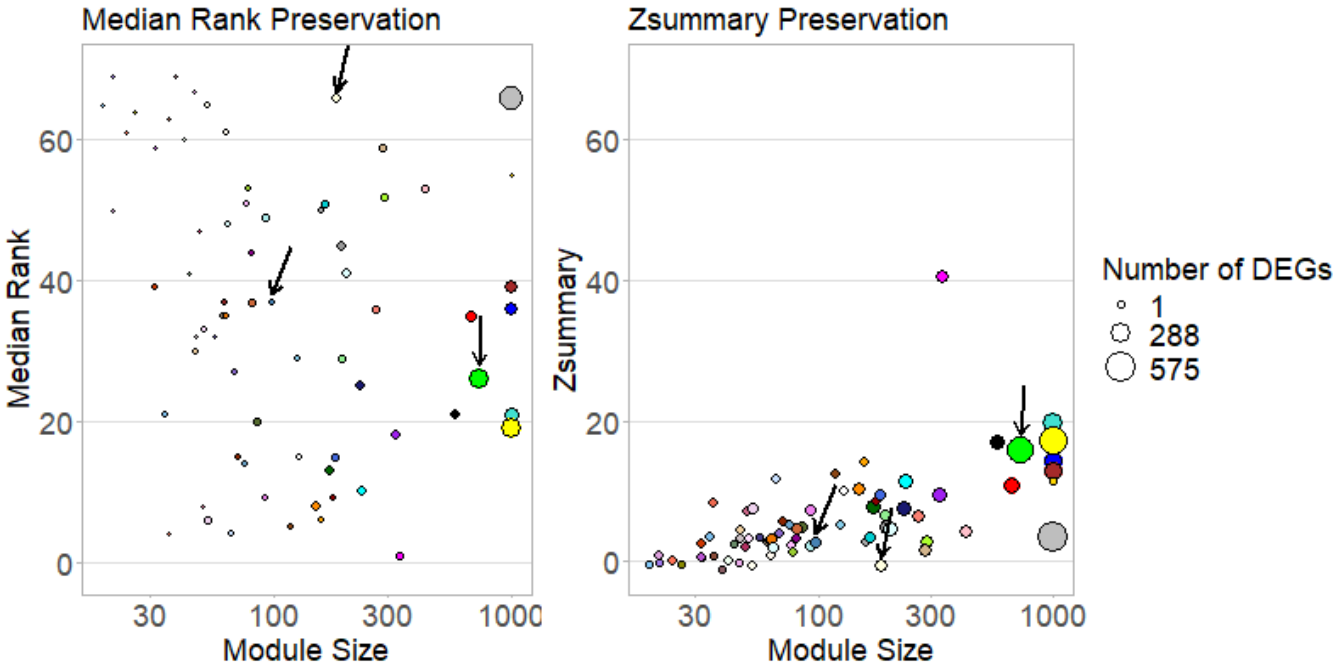

Figure 1.3 Module Preservation across *S. dulcamara* and *S. lycopersicum* WGCNA network. This indicates how much the genes in each module change between the *S. lycopersicum* and *S. dulcamara* networks. Median Rank does not consider module size with a high value indicating lower preservation. Zsummary does consider module size and a lower value indicates low module preservation. The size of each point indicates the number of DEGs that are present in the module across both networks and therefore, modules with no DEGs have been removed. The modules of interest have been indicated by arrows.

2.3.4 DEG Movement

While module preservation is key to understanding differences between networks, further assessment into the movement of DEGs between the networks was visualised to shortlist modules which are likely to contain particularly interesting DEGs linked to the traits of interest (Fig. 1.4). Links between the two distinct networks, with all DEGs split into their corresponding modules, were displayed. This aids the search for interesting modules as identifying those which split into multiple modules in the other network may be an indication of large-scale differences in expression patterns, therefore, DEGs in these modules may be of particular interest. Large movements of DEGs to different modules may link them to immune response and stress, as *S. dulcamara* and *S. lycopersicum* have been found to respond differently to *R. solanacearum*, making these modules of interest. Overall, there were 81 DEGs at 6 hours, 976 at 12 hours, 553 at 24 hours and 74 at 48 hours, making a total of 1,436 genes differentially expressed in at least one time point.

An example of interesting DEG movement includes the green module in the *S. dulcamara* network which splits into a multitude of modules (including yellow, turquoise and blue) in the *S. lycopersicum* network. This indicates that, when S. *lycopersicum* is infected with *R. solanacearum*, these DEGs act differently to one another, while in *S. dulcamara*, they have similar expressions. These genes may be co-regulated in *S. dulcamara* in response to *R. solanacearum* infection, and may be linked to the successful immune response, whereas, in *S. lycopersicum*, these genes are not being co-regulated which may be due to the lack of an immune response. Therefore, the green module in the *S. dulcamara* network is likely to contain genes that are influential to *S. dulcamara's* resistance. Similarly, the lightyellow module in *S. dulcamara*, which has no module preservation, moves largely to the thistle2 and salmon modules in *S. lycopersicum*. Finally, the steelblue module in the *S. lycopersicum* network splits mostly between the grey and red modules in the *S. dulcamara* network. This further highlights that different groups of genes are being co-regulated in *S. dulcamara* and *S. lycopersicum*, which may be due to their differing immune response to *R. solanacearum*. This difference in expression is indicative of differences between their regulatory pathways so further hub gene analysis is required to shed light on the function of these genes, and therefore, the green (*S. dulcamara* network), lightyellow (*S. dulcamara* network), and steelblue (*S. lycopersicum*) modules will be taken forward for further investigation.

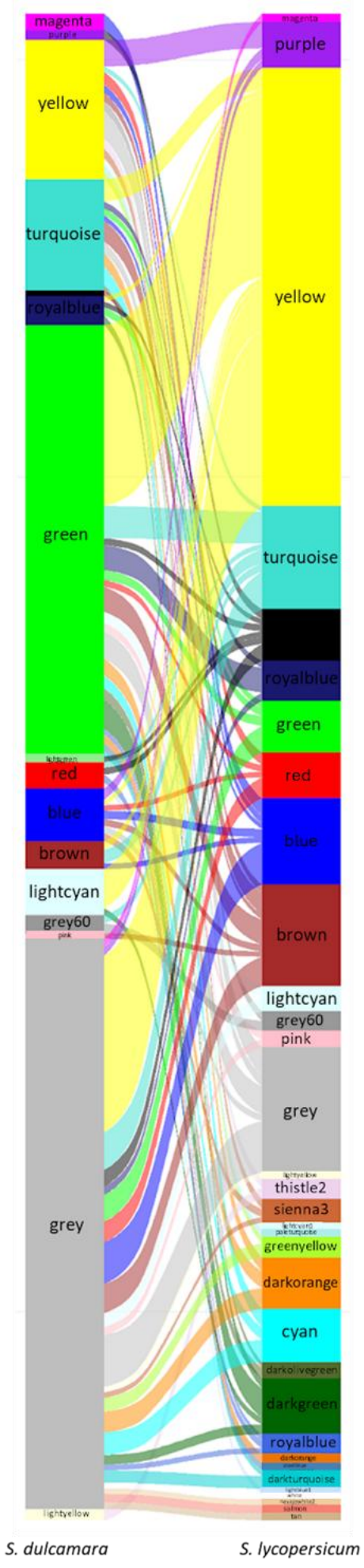

Figure 1.4 DEG Movement between *S. dulcamara* and *S. lycopersicum* WGCNA networks. This highlights the movement of DEGs between the *S. lycopersicum* and *S. dulcamara* network. The bottom shows the *S. dulcamara* modules and the top shows the *S. lycopersicum* modules. The size of the lines connecting the two networks are proportional to the number of DEGs that have moved between modules. A threshold of >3 DEGs in a module was required, resulting in 37 modules removed from *S. lycopersicum* and 22 from *S. dulcamara*.

2.3.5 DEG Enrichment

Understanding the distribution of DEGs across modules is key, but understanding the presence of DEGs at different time points may also shed light on how diurnal changes are influencing the immune response or if response time is different between species. Time point 12 has the largest number of DEGs, with 747 unique to 12 hours and 229 shared across different time points (Fig. 1.5). The second highest time point is 24 hours which has 327 unique DEGs and 226 shared across all time points (Fig. 1.5). The highest number of shared DEGs is between 12 and 24 hours which indicate that these time points may be of particular interest for identifying differences in immune response.

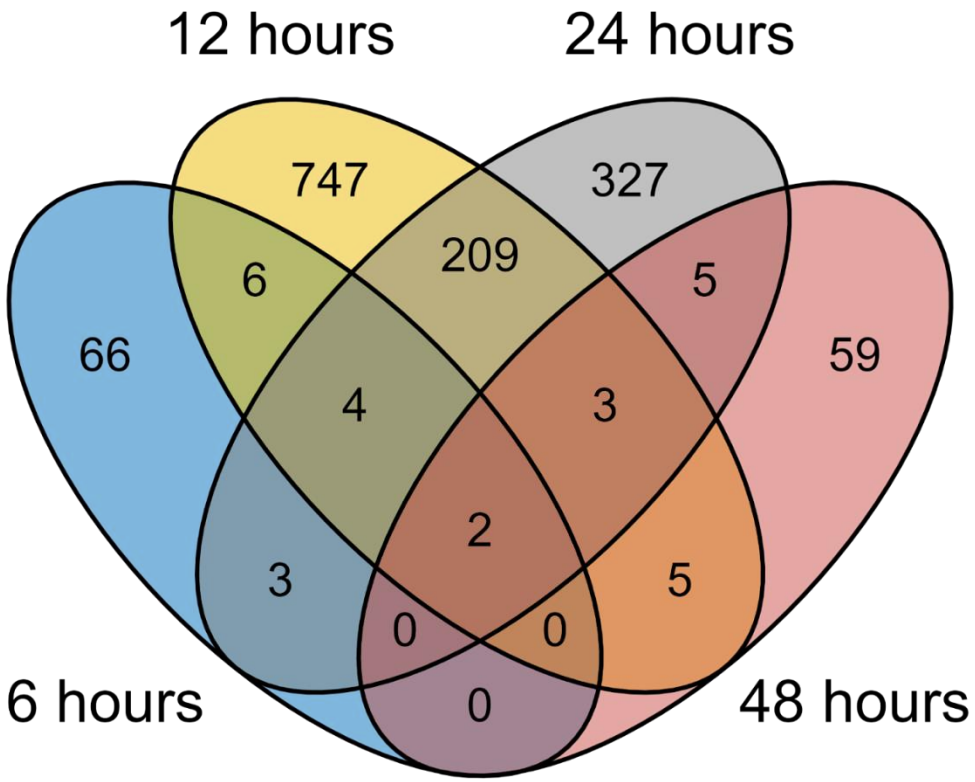

Figure 1.5 DEG presence at each time point. Each time point has been assessed to identify the number of DEGs that are unique or shared between time points. At 6 hours, there are a total of 81 DEGs, 66 of which are unique to 6 hours, 6 which are shared with 12 hours, 3 shared with 24 hours, 4 shared with 12 and 24 hours, and 2 shared with 12, 24, and 48 hours. At 12 hours, there are a total of 976 DEGs, 747 of which are unique to 12 hours, 209 shared with 24 hours, 5 shared with 48 hours, and 3 shared with both 24 and 48 hours. At 24 hours, there are a total of 553 DEGs, 327 of which are unique to 24 hours, and 5 shared with the 48 hours time point. Finally, there are 74 DEGs at 48 hours but 59 unique to this time point. It is important to note that there were no shared DEGs in the following time point combinations: 6, 14 and 48; 6, and 48; and 12, 24 and 48.

To choose which module to analyse further, the interesting modules were identified as having both low module preservation (Fig. 1.3), and interesting DEG movement (Fig. 1.4). The DEG enrichment at each time was then assessed, as modules enriched in DEGs are likely to have genes linked to the differences in immune response as the only difference in treatment was disease pressure. Understanding which time point each module is enriched in may shed light on their function. For example, DEGs enriched earlier are more likely to be involved in the fast-acting immune response, whereas those that are enriched later, such as the steelblue module in the *S. lycopersicum* network, may be as a result of a more delayed response (Table 1.1). The green, lightyellow, and steelblue module were selected for further analysis due to: their low module preservation (Fig 1.3); encompassing DEGs that move between different modules across the two networks (Fig 1.4); and enrichment at different time points to gain a more comprehensive overview of the time-series data (Table 1.1).

Module of interest	Species	Enriched 6 hours	Enriched 12 hours	Enriched 24 hours	Enriched 48 hours
green	*Solanum dulcamara*	5.96×10^{-6}	5.11×10^{-297}	<0.0001	0.62
lightyellow	*Solanum dulcamara*	0.77	1.64×10^{-8}	0.23	0.23
steelblue	*Solanum lycopersicum*	0.75	0.45	5.53×10^{-4}	0.75

Table 1.1 DEG enrichment status. Three modules of interest have been selected: green and lightyellow in the *S. dulcamara* network; and steelblue in the *S. lycopersicum* network. Modules were enriched in DEGs if the number of DEGs present at that time point was more than the average number of DEGs for that time point. Each module of interest was significantly enriched (pval <0.05) at least one time point in both networks, as described in the table. P values highlighted in green were <0.05 and significant whereas those highlighted in red were not significant are >0.05.

2.3.6 Hub Genes

To understand the functions and key genes in the modules of interest, the hub genes were identified and those with GO terms linked to immunity or stress were kept for further analysis. If no GO terms were present for the hub genes, the gene directly linked to the hub gene was assessed to indicate the function of the original hub gene as they are likely to be

involved in the same pathway. All gene sequences were then analysed using BLAST to identify their function and those linked to immunity and stress responses were then plotted for individual gene expression.

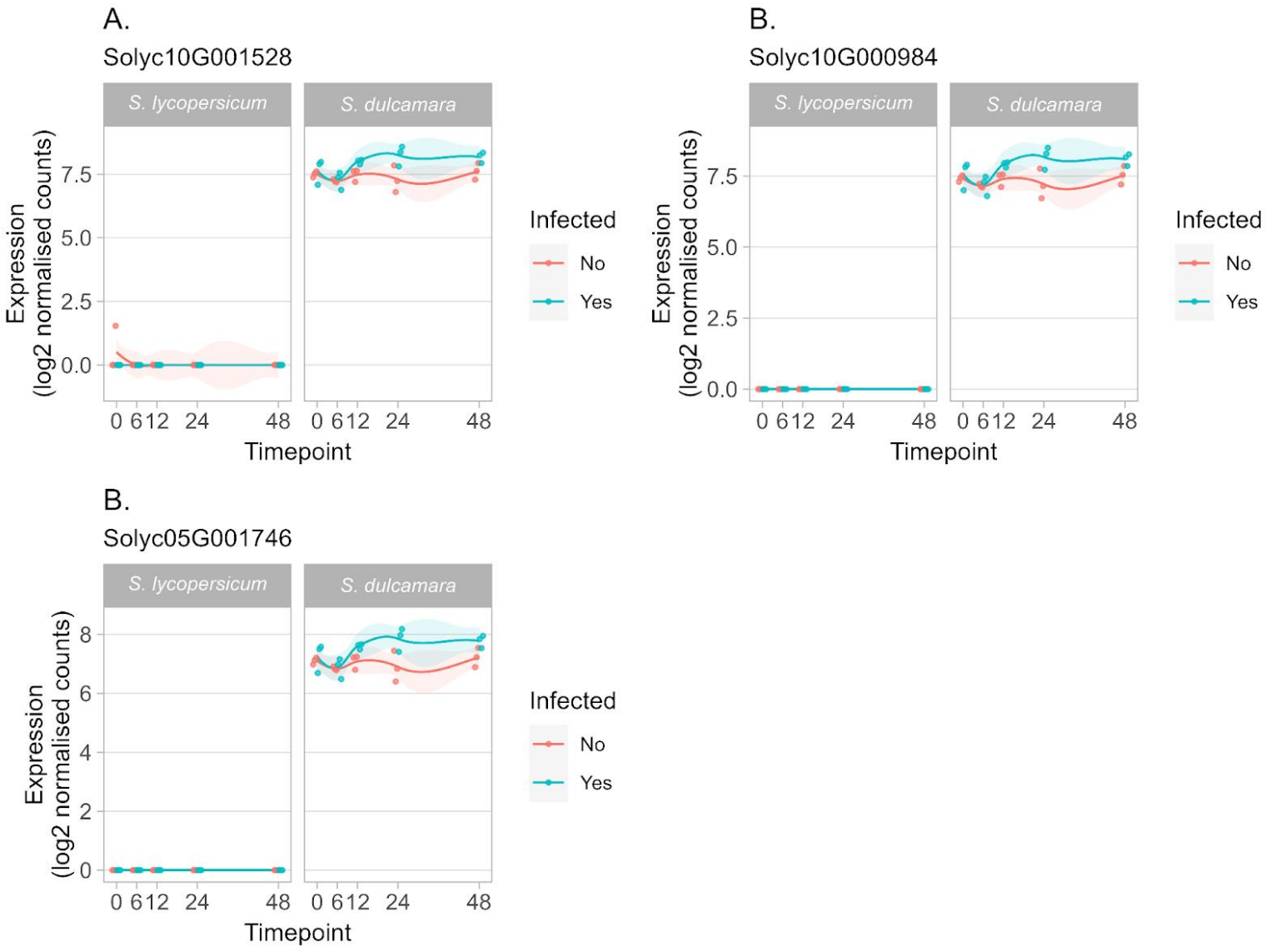

Figure 1.6 Expression of the genes of interest in the green module of the *S. dulcamara* network. A. Solyc10G001528, **B.** Solyc10G000984, and **C.** Solyc05G001746. The expression for each gene in *S. dulcamara* (right) and *S. lycopersicum* (left) is displayed. This depicts normalised expression of the genes of interest in the *S. dulcamara* and *S. lycopersicum* network and in infected (blue) and not infected (red) samples. These genes do not appear in the *S. lycopersicum* network due to low expression and were, therefore, removed from the *S. lycopersicum* network.

The hub genes for the green module in the *S. dulcamara* network includes Solyc05G001746, Solyc10G000984, and Solyc10G001528 (Fig. 1.6 A-C) all of which saw a rise in expression when *S. dulcamara* was inoculated with *R. solanacearum* compared to the non-infected *S. dulamacara* plants. However, expression was near 0 in both infected and non-infected *S. lycopersicum* plants and were removed from the network due to being too lowly expressed to meet the threshold. This may shed light on genes that are upregulated in *S. dulcamara* when infected and aids their partial resistance.

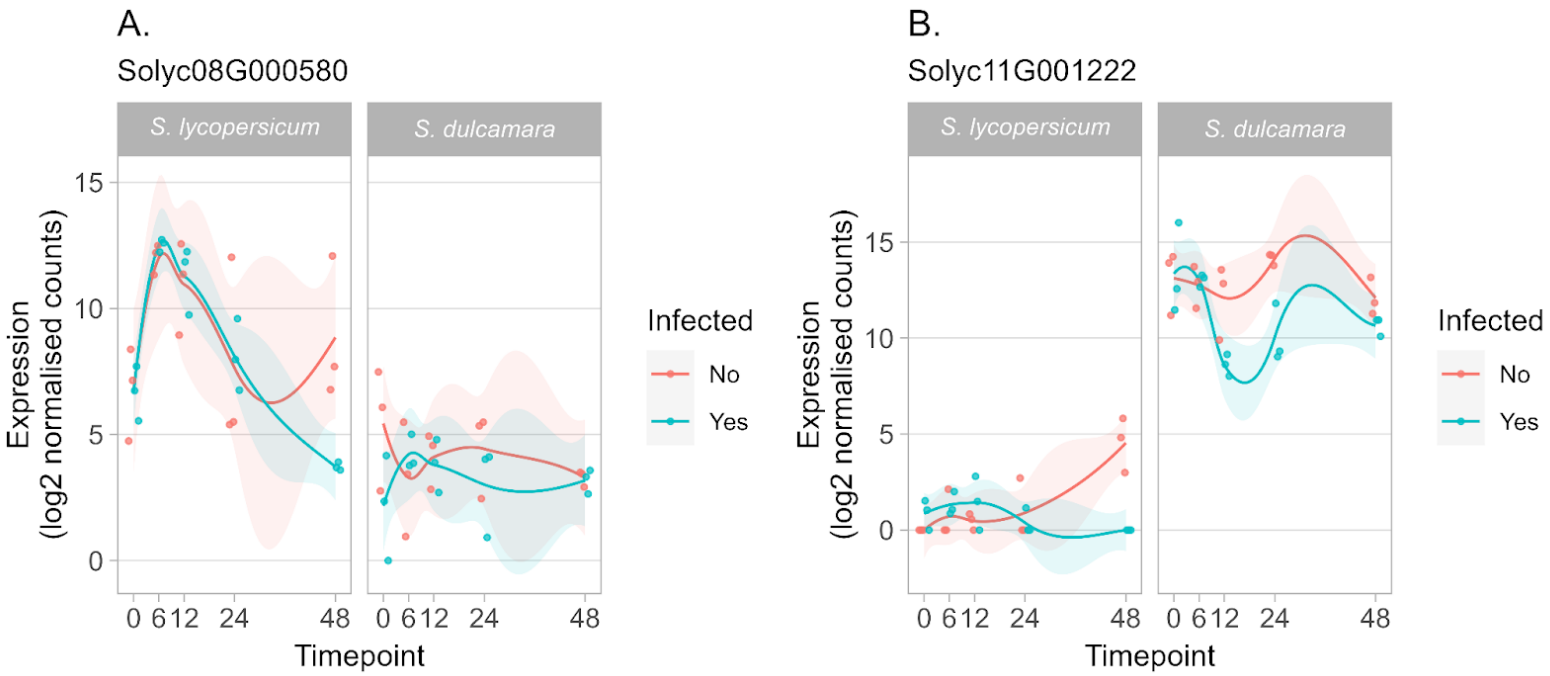

Figure 1.7 Expression of the genes of interest in the lightyellow module of the *S. dulcamara network*. A. Solyc08G000580 is in the lightyellow module in the *S. lycopersicum* **B.** Solyc11G001222 is in the lightyellow module in the *S. dulcamara* network. The expression for each gene in *S. dulcamara* (right) and *S. lycopersicum* (left) is displayed. This depicts normalised expression of the genes of interest in the *S. dulcamara* and *S. lycopersicum* network and in infected (blue) and not infected (red) samples.

The hub genes for the lightyellow module in the *S. dulcamara* networks were Solyc08G000580 and Solyc11G001222 (Fig. 1.7 A-B) which saw large differences in gene expression between species and limited differences between infection status where only a slight reduction in infected *S. dulcamara* plants was seen. Solyc08G000580 in both infected and non-infected *S. lycopersicum* plants had very similar expression patterns, only differing after 24 hours where the non-infected plants saw an increase in expression while the infected plants continued on the downward trajectory. In *S. dulcamara*, the expression

pattern overall is less similar but they are within the boundaries, indicating that infection status does not change the expression of this gene. Solyc11G001222 in *S. lycopersicum* drastically changes also at 24 hours with the non-infected plants increasing in expression. The expression in *S. dulcamara*, however, sees the same overall pattern but has a large decrease in infected plants after 6 hours. Therefore, this reduction may be hindering infection and aiding *S. dulcamara* in defending against infection. It may also indicate that *S. dulcamara* is more sensitive to infection, responding by decreasing expression compared to the non-infected plants after 6-12 hours, while infected *S. lycopersicum* drops below non-infected levels of expression after 24 hours.

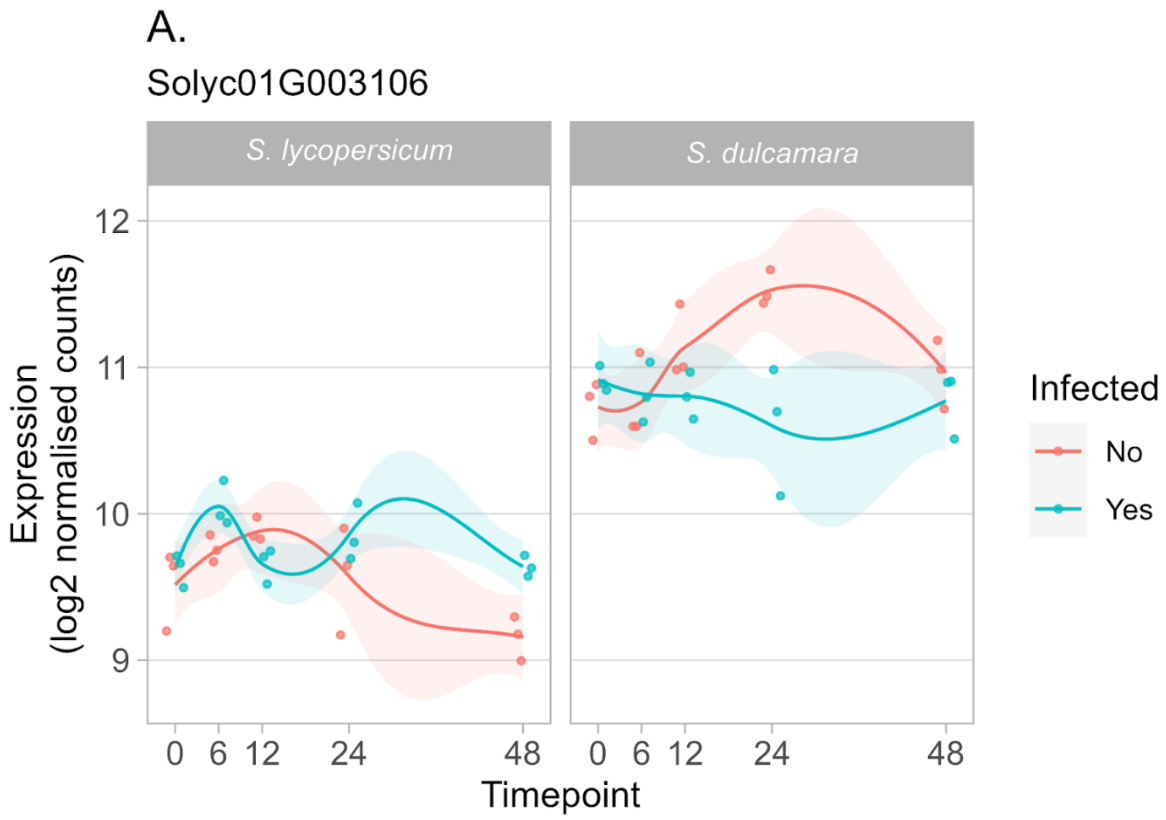

Figure 1.8 Expression of the Solyc01G003106 gene of interest in the steelblue module of the *S. lycopersicum* network. The expression for each gene in *S. dulcamara* (right) and *S. lycopersicum* (left) is displayed. This depicts normalised expression of the genes of interest in the *S. dulcamara* and *S. lycopersicum* network and in infected (blue) and not infected (red) samples.

The hub gene for the steelblue module in the *S. lycopersicum* network, Solyc01G003106 (Fig. 1.8), had a higher expression in *S. dulcamara* than *S. lycopersicum*. In *S. dulcamara*, non-infected plants saw a rise in expression between 6 and 24 hours before a gradual

decline. In infected plants, however, there was limited change in expression over time. Both infected and non-infected *S. lycopersicum* plants reduced in expression after 24 hours with limited overall change between both infection statuses. Despite the limited overall change, the expression patterns do vary within this range with infected samples peaked at 6 and 24 hours while non-infected samples peaked only at 12 hours. The downregulation in infected *S. dulcamara* plants may be protecting them from infection so further analysis into the function of Solyc01G003106 may shed light on this.

2.4 Discussion

2.4.1 Network Summary

To understand how gene expression in *S. dulcamara* and *S. lycopersicum* differs when inoculated with *R. solanacearum*, two WGCNs were created using 17,840 orthologous genes from RNA seq data extracted from the leaves of the plants at the time of inoculation and then 6, 12, 24, and 48 hours after inoculation. Filtering left 16,888 genes in the *S. dulcamara* network and 16,765 genes in the *S. lycopersicum* network. A power of 13 was chosen for the construction of the WGCNA as both networks fit the SFT model at this power (*S. dulcamara* - R2 = 0.8050, mean.k =8.89 and medium.k = 2.870) (*S. lycopersicum* - R2 = 0.85900, mean.k = 22.50 and medium.k = 9.73).This grouped the genes into modules by their expression patterns, comparing the changes of expression between the different: species, inoculation statuses; and time points. Module preservation, DEG enrichment, and GO term analysis highlighted three modules of interest: green (*S. dulcamara* network), lightyellow (*S. dulcamara* network), and steelblue (*S. lycopersicum* network). The hub genes for these modules were then identified and their function assessed. An alternative method for module of interest identification could have included the use of gene significance to measure module significance which allows for the isolation of modules with genes strongly associated with that particular module (Langfelder, 2008).This would allow for the selection of modules associated with the traits of interest and their hub genes should be highly likely to also be associated with the trait of interest. However, due to the composition of this network, module selection conducted here was adequate enough to select modules with key hub genes with links to the traits of interest.

It should be considered that cross species analysis is controversial but there are examples of successful cross-species network analysis, which explore between species with vast genetic differences such as humans and canines (Jin, 2019). The benefit of the comparison between *S. dulcamara* and *S. lycopersicum* is that they are very closely related, sharing 17,840 orthologous genes out of the 27,429 known genes in *S. dulcamara* and 34,240 in *S.*

lycopersicum (Franco Ortega, 2025; Fernandez-Pozo et al., 2014). This allows for a large proportion of their genes to be incorporated in these networks.

There are still some innate differences between species. Therefore, the composition of the model underpinning these networks removed DEGs present at 0 hours, before the inoculation of *R. solanacearum* was able to impact gene expression in the sampled leaves. It should also be noted that all interpretation is considered with the background of the non-inoculated plants, giving a baseline for each plant species. Every comparison made should be made between the plants of the same species with different infection statuses which should provide context of the differences between the species before the inoculation of *R. solanacearum* is considered.

It should also be considered that time-series data is known to be complicated to interpret, especially due to the influences of diurnal changes. This was considered when sampling as all samples were extracted within the 16 hours of light, with sample times of 0, 24 and 48 hours being the same time of day, therefore, changes in expression are unlikely to be due to diurnal changes. Furthermore, DEGs with potential links to diurnal changes were not assessed further.

2.4.2 Green Module in the *S. dulcamara* network - CDPK 1 upregulation in infected *S. dulcamara* plants

The genes Solyc05G001746, Solyc10G000984, and Solyc10G001528 (Fig. 1.6A-C) were present in the green module in the *S. dulcamara* network but not present in the *S. lycopersicum* network as the expression levels were deemed too low, resulting in their removal from the *S. lycopersicum* network. This was further validated by the gene expression being near 0 for all but one sample, whereas in *S. dulcamara,* these genes have a consistent expression within their species and inoculation status. When not inoculated, the expression seems to follow the light cycle but when inoculated with *R. solanacearum*, instead of decreasing at 12 hours, the expression increases. As *R. solanacearum* is a soil borne pathogen, primarily impacting the roots, a delayed response in the leaves is to be expected, further validating the pattern of expression of these three genes.

After analysing the gene transcripts with BLAST, these genes were strongly linked to Ca^{2+}-dependent protein kinase 1 (CDPK1). CDPKs have long been recognised as being involved in plant immune and stress signalling as well as being differentially expressed in response to stress stimuli such as: drought; heat; pathogens; and abscisic acid, a sesquiterpenoid hormone known for regulating stress responses and, particularly in well-watered conditions,

to prompt growth (Boudsocq, 2012; Brookbank, 2021). CDPK1, in particular, has not been greatly studied in *S. dulcamara* or *S. lycopersicum* but has in *Arabidopsis thaliana*. These studies identified AtCDPK1's role in pathogen resistance as: initiating salicylic acid pathways; regulating the initiation of cell death; and to phosphorylate NADPH oxidases to induce the production of reactive oxygen species (ROS) (Wang, 2015). All genes of interest (Fig 1.6A-C) see a reduction to near 0 normalised expression in *S. lycopersicum*, compared to the relatively high expression found in *S. dulcamara*, which translates to a large upregulation of these genes. As the BLAST search matched these genes to CDKP1, we can infer that these genes rising in *S. dulcamara* when under *R. solanacearum* infection, may be improving stress signalling and initiating immunity pathways, as discussed in Qi and Zhang's (2020) paper and similar to what has been found in ginger, ZoCDKP1 positively regulating drought stress signalling (Qi and Zhang's, 2020; Dontoro Dekomah, 2022). Increasing the expression levels in *S. lycopersicum* to mimic the expression in *S. dulcamara* may see an improved resistance to *R. solanacearum.*

2.4.3 Lightyellow Module in the *S. dulcamara* network- upregulation of SINA 1 increasing cell death in *S. dulcamara*

The hub gene of the lightyellow module in the *S. dulcamara* network, Solyc08G000580 (Fig. 1.7A), has been linked to Cuscuta receptor 1 (CuRe1), a cell surface receptor that detects pathogens such as *Cuscuta reflexa* and initiates immune response via inducing the production of ethylene (Hegenauer, 2020). Therefore, upregulation of CuRe1 results in initiation of a defence response in resistant plants such as *S. lycopersicum* (Hegenauer et al., 2020). This hub gene is located on the same chromosome as Solyc08G016270, a CuRe1, and other genes such as Solyc08G016210 and Solyc08G016310 are a close match in amino acid sequences to Solyc08G016270 but do not respond to the Cuscuta factors as expected of a CuRe1 (Hegenauer, 2016). As Solyc08G000580 expression increased despite no Cuscuta factors being present, this suggests that Solyc08G000580 may not be a functioning CuRe1 similar to Solyc08G016210 and Solyc08G016310. There has been no link to CuRe1 being activated by other pathogens, due to the high level of specificity of this interaction. CuRe1 has only reliably been identified with positive immune response, specifically the parasitisation of *C. reflexa,* in *S. lycopersicum* but seems to not have an immune response even in the closely related, wild counterpart, *Solanum pennellii* (Hegenauer, 2016). This may explain the differing responses found in *S. lycopersicum* and *S. dulcamara*. As the plants were not stimulated with *C. reflexa,* the upregulation in *S. lycopersicum* is unexpected and may be due to other factors, including: diurnal changes, as the peak was at 6 hours and all other time points have a similar level of expression when at

the same point of the day; or this gene is influenced by pathogens other than *C. reflexa* which are yet to be identified. However, CuRe1 has been linked to the biosynthesis of ethylene which is influential in the ripening of fleshy fruits, including tomatoes (Li, 2022). Ethylene has been found to increase during ripening, activating ethylene response factors (ERFs) linked to key components of fruit ripening, such as colour, flavour and smell (Li, 2022). Therefore, the diversion seen between infection statuses of *S. lycopersicum* and *S. dulcamara* may be a reallocation of resources, prioritising defense over ripening of fruit. Furthermore, the delay in reduction of expression in infected *S. lycopersicum*, compared to the uninfected *S. lycopersicum* occurred at 24 hours, while the *S. dulcamara* plants diverge between 6 and 12 hours, indicating that it may be postponing this reallocation quicker in *S. dulcamara*, resulting in a more efficient immune response. This would require further investigation to clarify if this gene is a functioning CuRe1, if its expression is limited by *C. reflexa* presence or linked to diurnal changes, and if this may be a reallocation of resources to aid the immune response. Additionally, in *S. dulcamara,* there seems to be no change between immune status or time, and considering the function, this indicates that this gene is unlikely to be a contender for in-planta experiments and alternatives should be prioritised.

The expression of the second hub gene of the lightyellow module in the *S. dulcamara* network, Solyc11G001222 (Fig. 1.7B), is linked to SINA1, an E3 ubiquitin ligase, specifically SlSINA1 (Wang, 2018). Ubiquitin is a family of well conserved proteins which modify the structure of other proteins and Seven in absentia (SINA), being a ubiquitin ligase, causes post-translational changes to ubiquitin (Pickart, 2004; Wang, 2018). SINA has been linked to plant growth and development, plant-microbe interactions as well as response to both abiotic and biotic stress (Roche, 2023; Wang, 2018). There are six SINA genes found in *S. lycopersicum* called SlSINA1-6, each with their own function (Wang, 2018). SlSINA1 is the most uniquely structured and is shorter than the other five, having 20% less similarity in sequence than other SISINA (Wang, 2018). SlSINA1 has been found to suppress cell death and defence signals, therefore, the decrease seen in both *S. lycopersicum* and *S. dulcamara* is likely causing an increase in cell death (Wang, 2018). However, *S. dulcamara* overall has higher expression of SISINA1, indicating that cell death is more greatly suppressed in *S. dulcamara*, in relation to the uninfected control plants. Cell death can be a useful defence mechanism as it can limit the spread of disease, but it has been adapted by pathogens to proliferate infection further (Ashida, et al. 2011).

It should be noted that despite *R. solanacearum* being a soil borne pathogen and initially found in the roots of infected plants, it takes only a few hours to migrate towards the aerial parts of the plant (Tans-Kersten, 2001). This is likely to be why we only start to see a

response around 6 to 12 hours post infection as the RNA-seq data was collected from the leaves of the plants. It would be beneficial to explore RNA-seq data from root samples. However, incorporating this into time-series analysis would be destructive and likely to cause stress to the plants. Therefore, it is difficult to interpret the extent of cell death and how it impacts the spread of disease, especially as *R. solanacearum* has been identified as being a hemibiotroph, encompassing both biotrophic and necrotrophic traits, with the ability to promote cell death in an effector related dosage dependent response (Narancio, 2013; Byth-Illing and Bornman, 2013; Xue et al., 2025). However, it has been theorised that *S. dulcamara* is able to withstand infection by limiting the spread of *R. solanacearum* , a relatively slow growing bacterium, by expediting cell death (Sebastià, et al, 2021). As *R. solanacearum* is a hemibiotroph, it benefits from the growth of its host, therefore, death of plant cells across the entire plant may inhibit its proliferation and, despite *S. dulcamara* having a higher expression of Solyc11G001222 than *S. lycopersicum*, it decreases under infection with *R. solanacearum*. Therefore, cell death is exacerbated in infected *S. dulcamara* and may be contributing to the inhibition of infection. Furthermore, there has been no record of *R. solanacearum* influencing the expression of SISINA1, indicating that *R. solanacearum* is unlikely to be causing this cell death.

To consolidate whether *R. solanacearum* may be promoting cell death, dead cells should be viewed via microscopy and a bioluminescent strain, such as UY031 Pps-lux, can be used to identify if *R. solanacearum* is present in the dead cells (Ferreira, 2017). If some dead cells have been identified without *R. solanacearum* present, we can assume that this protects cells by inhibiting *R. solanacearum's* proliferation and migration to other cells. However, if all dead cells showed signs of *R. solanacearum*, this indicates that *R. solanacearum* may be influencing cell death. This assay can be conducted alongside future iterations of this work and to further understand the influence this gene has on both *S. dulcamara* and *S. lycopersicum's* immune response, it would be beneficial to assess the susceptibility of knockout Solyc11G001222 mutants.

2.4.4 Steelblue Module in the *S. lycopersicum* network - PNGase linked to *S. dulcamara's* susceptibility or prioritisation of resources

The hub gene for the steelblue module in the *S. lycopersicum* network, Solyc01G003106 (Fig. 1.8), is linked to a putative peptide:N-glycanase (PNGase), an enzyme which causes the loss of N-linked glycans in glycopeptides and glycoproteins, in a process called deglycosylation (Joshi, 2005; Suzuki, 2015). This loss of N-linked glycans can cause the misfolding of glycoproteins, aiding their breakdown and keeping control of protein quality

(Suzuki, 2015; Berger, 1995; Diepold, 2007). This process releases the free N-glycan which has been found to have links to fruit ripening, seed development and innate immunity by influencing the formation of pattern recognition receptors (Hirayama, 2015; Strasser, 2014). Both species saw a change when inoculated with *R. solanacearum* (Fig. 1.8), indicating a response to infection in both the *S. lycopersicum* and *S. dulcamara* as the uninfected samples rise and fall once whereas infected samples have a more undulating pattern. *S. dulcamara* is expected to have a higher expression when inoculated with *R. solanacearum* due to the link to protein quality checks and the formation of pattern recognition receptors but was found to be downregulated under these conditions. This may be an example of how *S. dulcamara* is not a fully resistant plant and can experience symptoms when under infection. However, this unexpected expression may be due to the links to fruit ripening and seed development, both of which would not be a priority when under attack from a pathogen like *R. solanacearum*. *S. lycopersicum's* expression stays around the same expression level despite infection status, but does change in pattern, which implies that *S. dulcamara's* exaggerated change in response to *R. solanacearum*, may be providing protection by prioritising resources. Downregulating Solyc01G003106 in *S. lycopersicum* could elucidate the physiological implications of this gene's function.

2.5 Conclusion

S. dulcamara and *S. lycopersicum* are closely related, sharing 17,840 orthologous genes between them, but *S. dulcamara* is partially resistant to *R. solanacearum* whereas *S. lycopersicum* is susceptible and suffers great losses due to this pathogen (Huet, 2014). Despite sharing a large proportion of genes, their expression differs greatly. Identifying and understanding the expression of key genes that are potentially linked to *S. dulcamara's* partial resistance opens the door for adapting the expression of *S. lycopersicum* to mimic *S. dulcamara's* response to infection. This project aims to identify expression patterns of genes linked to *S. dulcamara's* resistance and incorporate them into the expression of *S. lycopersicum's* genes. This was conducted by expanding the horizon of WGCNA by combining cross-species and time-series analysis.

2.5.1 Suggestions for Further Work

This use of WGCNA identified five genes of interest from three modules theorised to be involved in the immune response: Solyc10G001528, Solyc10G000984, Solyc05G001746, Solyc08G000580, Solyc11G001222, and Solyc01G003106. These candidate genes could be used in future in-planta experiments to assess the physiological implications of changing expression in *S. lycopersicum* to mimic *S. dulcamara's* response to infection.

Solyc10G001528, Solyc10G000984 and Solyc05G001746 are linked to CDPK1 which promotes stress signalling and therefore, in-planta experiments should focus on being upregulated in *S. lycopersicum* with the aim of improving cell signalling and initiating other immune pathways more efficiently. In-planta experiments for Solyc08G000580 should not be of priority due to there being very few links to general or *R. solanacearum* specific immune response. Solyc11G001222 analysis, on the other hand, would benefit from investigating knock out mutants in both *S. dulcamara* and *S. lycopersicum*, to assess the impact of increased cell death when infected with a hemibiotrophic bacterium such as *R. solanacearum*. Further clarification could be gained from assessing dead cells for the presence of bioluminescent *R. solanacearum* via microscopy. Finally, downregulating Solyc01G003106 in *S. lycopersicum* may indicate whether its putative function of a PNGase is aiding *S. dulcamara's* resistance by prioritising resources and reducing the promotion of fruit ripening and seed development. This work highlights the effectiveness of WGCNA and how broad a scope this bioinformatics tool encapsulates, unlocking the potential to explore and understand transcriptomic data to even greater extents than previously attempted.

Exploring the Boundaries of CANA to Test the Influence of 2,6-DHBA

3.1 Introduction

Root exudates are known to influence the microbiome of the rhizosphere, with plants changing root exudate production to recruit specific microorganisms (Pascale et al., 2020). Additionally, it has been found that root exudates change in response to external pressures, which has been identified in *Solanum lycopersicum* (tomato) under *Ralstonia solanacearum* pressure by Gu (2016). This study tested root exudates from both healthy and *R. solanacearum* infected *S. lycopersicum* plants to identify whether exudate production changes, and how this influences disease susceptibility and rhizospheric microbial composition. Plants were grown in hydroponics, and the liquid was analysed with high-performance liquid chromatography (HPLC). These exudates were then added to fresh soil and DNA was extracted, amplifying the 16S V4 region of rRNA to identify the different species of bacteria present in each sample. This identified different exudate production between the treatments, finding that those created under infection with *R. solanacearum* caused a reduction in rhizosphere microbe diversity. Additionally, artificially adding compounds found to be produced under infection did not produce the same microbial composition but did reduce pathogen growth. This strongly indicates that plants under pathogen attack could change the composition of the surrounding rhizospheric microbiome to reduce pathogen stress and improve resistance to disease. Studies like Gu's (2016) can highlight compounds that can be artificially added to promote disease protection.

An alternative and recently popular approach to understanding changes between different communities are co-abundance networks (CAN) (Berry, 2014). This method has been used to analyse a range of community level interactions, including Wang's 2022 study that explored the change in composition between healthy and *R. solanacearum* infected tobacco plants (*Nicotiana tabacum L.*) which aimed to understand the influence pathogen presence can have on composition change (Liu, 2023; Wang, 2022). This use of co-abundance network analysis (CANA) further consolidated that root exudates change depending on the stress the plant is experiencing, which in turn impacts the diversity and composition of the rhizosphere (Wang, 2022). Microbial diversity increased in diseased plants which was attributed to the plant attempting to recruit more microbes that may outcompete and reduce pathogen abundance and viability (Wang, 2022; Gu, 2022). Furthermore, this CANA specifically identified keystone taxa in healthy plants including: *Burkholderia-Caballeronia-*

Paraburkholderia; *Acinetobacter*; *Penicillium*; and *Trichoderma* (Wang, 2022). This analysis highlights the ability of CANA to identify patterns in microbial composition under different treatments and emphasises specific influential taxa that may be promoting resistance. Studies such as this are why network analysis is used even across disciplines to identify patterns between complex communities (Barberán, 2012). This technique can be complex, requiring an abundance of data, and does not provide clear explanations of interactions between communities, however, this analysis highlights previously unknown patterns that may lead to novel discoveries of community level functions (Barberán, 2012; Liu, 2023).

Wang's (2022) study highlighted the benefits of CANA and Gu's (2016) study identified that artificial metabolites can be added to mimic the physiological results of plant promoting root exudates that occur as a result of disease priming. Combining these approaches, using CANA to assess changes in microbial composition when a beneficial metabolite is added to a susceptible plant, should identify key taxa that promote disease resistance. There has been limited research that utilises the ability of CANA to understand the links between rhizosphere microbial communities and the application of an artificial root exudate substitute alongside infection. This method can provide more quantifiable links between the abundance and treatments than alternatives such as assessing the raw abundance, allowing for clearer associations to be formed, which allow for more accurate future work.

An example of a metabolite linked to promoting resistance, yet to have its impact on microbial composition assessed in-planta, is 2,6-dihydroxybenzoic acid (2,6-DHBA) which was identified in Franco Ortega's 2024 study (Franco Ortega, in press). This found that partially resistant *Solanum dulcamara* produces significantly higher levels of the metabolite 2,6-DHBA than produced by susceptible *S. lycopersicum*. To understand the influence 2,6-DHBA has on resistance to *R. solanacearum*, 48 *S. lycopersicum* plants were tested under four treatments: *R. solanacearum* inoculated; *R. solanacearum* and 2,6-DHBA inoculated; 2,6-DHBA inoculated; and control (CPG media inoculated). A reduction in *R. solanacearum* symptoms was observed in the previously susceptible *S. lycopersicum* when inoculated with both *R. solanacearum* and 2,6-DHBA. This found that 2,6-DHBA reduced the pathogenicity of *R. solanacearum* and promoted resistance in susceptible plants (Franco Ortega, in press). This previous work then theorised that 2,6-DHBA influences resistance by altering the presence of beneficial microbes.

2,6-DHBA is a benzoic acid, a hydroxylated phenolic compound, which has previously been linked to a well-known plant defence chemical: salicylic acid (SA) (Juurlink, 2014). SA is a plant hormone well-known for its involvement in plant defence, as well as growth and abiotic stress response (Wang, et al., 2025). Whereas other benzoic acids are generally considered

to be precursors in both the Isochorismate synthase pathway and the recently identified, primary route to SA, phenylalanine pathway (Wang, et al., 2025; Wildermuth, 2001; Zhu, 2025). 2,6-DHBA however, is classed as a derivative of SA as 2,6-DHBA is synthesised by the addition of a hydroxyl group (OH) to SA (Dachineni, et al., 2017). Despite being a derivative of SA, 2,6-DHBA has been reported to have low microbial growth inhibition efficacy, requiring the addition of metal ions such as Ni^{2+} and CO^{2+} to improve inhibition and plant defence (Santoso, 2016). Despite this, Franco Ortega (in press) found that the addition of 2,6-DHBA significantly reduced the susceptibility of *S. lycopersicum* plants inoculated with *R. solanacearum*. Therefore, it would be interesting to understand 2,6-DHBA's impact on microbial activity and explore the claims of its inability to defend plants or if it promotes healthy growth, even when plants are under threat.

This study aims to confirm whether 2,6-DHBA impacts the presence of microbes. This is examined by extracting DNA from the soil of each treatment and using Co-abundance Network Analysis (CANA) to understand the influence this metabolite has on the composition of the rhizosphere. This will aim to identify keystone taxa which either are recruited by 2,6-DHBA and provide protection against *R. solanacearum* infection, or are inhibited by 2,6-DHBA and increase the pathogen pressure of *R. solanacearum*.

3.2 Methods

3.2.1 Previous Work

Franco Ortega's study (in press) explored the impact of 2,6-DHBA by testing four treatments: *R. solanacearum* inoculated; *R. solanacearum* and 2,6-DHBA inoculated; 2,6-DHBA inoculated; and control (CPG media inoculated). The *S. lycopersicum* seeds (cv Moneymaker, Moles Seeds, Colchester, UK) were surface sterilised with bleach for 1 minute and then rinsed with distilled water, to remove preexisting variations in microbial communities. They were allowed to germinate on a wet tissue for 4 days, to ensure adequate germination, before being moved to compost (John Innes No2, ~125 g per pot) in a growth room at the Department of Biology (University of York, York, UK) at 20 ^{o}C with a 14/10 hour light/dark light cycle for 17 days. Following these 17 days, the plants were moved to acclimatise in a PHCbi growth cabinet for 4 days at 24 ^{o}C/20 ^{o}C for 16/8 hours, light/dark cycles. After a total of 21 days, 24 plants were inoculated with 5 ml of *R. solanacearum* (UW551) via soil drenching as close to the stem as possible. After 24 hours, 12 of the 24 *R. solanacearum* inoculated plants were inoculated with 12 ml of sterile 2 mg/ml 2,6-DHBA (referred to as "*Rs*2,6-DHBA" samples) and the remaining 12 were soil drenched with water (referred to as "*Rs"* samples). Then, 12 plants were inoculated with 5 ml of CPG media,

followed by 12 ml of 2,6-DHBA (referred to as “2,6-DHBA” samples) and 12 negative control plants were inoculated with 5 ml of CPG media, followed by 12 ml of water (referred to as “NC” samples). The disease status was assessed for 21 days post inoculation and was determined by observations: 0 = no symptoms; 1 = 25% symptom coverage; 2 = 50% symptom coverage; 3 = 75% coverage; 4 = 100% coverage/deceased. Healthy plants were awarded a 0 and diseased plants from 1-4 were grouped. Rhizosphere samples were then collected 21 days post inoculation and stored at -80 ^{o}C for DNA extraction. The plants were kept for a total of 42 days but as the plants began to outgrow their pots, the resulting yellowing and growth effects made disease assessments unreliable.

3.2.2 Data collection

To understand the microbial composition of the rhizosphere across these four treatments, DNA was extracted from all 48 samples following an adaptation Tien (1999) and Porteous and Armstrongs’ (1991) protocol. This required mixing 0.2 g of soil in 1.5 ml of mixing buffer (0.5 M D-Sorbitol; 0.019 M PEG; 0.13 M Diethyldithiocarbamic acid; 0.1 M EDTA; 0.05 M Tris) and adding 125 mg of PVP which was vortexed. Then, 5 uL of lysozyme (50 g/L, Vazyme) was added, as well as 5 ml of Lysis buffer (0.14 M; 0.1 M EDTA; 0.05 M Tris) which was then vortexed and left on ice for 2 hours. This was centrifuged at 3112 G force for 20 mins at 4 ^{o}C and the supernatant was discarded. The pellet was resuspended in a blank buffer (0.1 M EDTA; 0.05 M Tris), vortexed and centrifuged again. The supernatant was extracted and moved to a clean tube. This cleaning process was repeated a total of three times, adding the supernatant to the clean supernatant falcon tubes. Potassium acetate was then added to a final concentration of 0.5 molL^{-1} which was vortexed and incubated on ice for a further 2 hours. This was centrifuged again at 3112 G for 35 mins at 4 ^{o}C to remove the precipitate. The supernatant was then moved to a clean falcon tube, and two volumes of 95% ethanol were added and vortexed. This was centrifuged at 3112 G for 35 mins at 12 ^{o}C and spun for a further 10 mins if a pellet was not visible. Finally, the supernatant was discarded, and the pellet was suspended in 10 ul of TE buffer (0.01 M EDTA; 0.001 M Tris). DNA was then extracted and sent to Novogene (Cambridge, UK) where the 16S, V4 region was amplified using the primers 525F and 806R provided by Novogene. This returned a total of 9251 amplicon sequence variants (ASV) with varying occurrences across the 48 samples.

3.2.3 Transcriptomic Data Preparation

The abundances for a total of 9,251 ASVs were returned from the DNA extractions for each of the 48 samples which were normalised to the amount of soil used in each sample using a simple equation (ASV abundance/DNAweight) and the function mutate() in R (Wickham, 2023). This was used to create a single co-expression network which required a scale-free

topology (SFT). This was best achieved by standardising the ASV abundance values using the scale() function (center = TRUE, scale = TRUE) from the base package in R (R Core Team, 2024) which subtracts the mean from each value and then divides by the standard deviations. ASVs with low abundance (mean <= 1) or missing data (0 or NA) were removed, resulting in 3,680 remaining across 48 samples. A dendrogram of the samples was created using flashClust(), showing the spread of the abundance data (Langfelder P, 2012). As the samples were well grouped, none were removed and the 3,680 ASVs across the 48 samples remained.

The pickSoftThreshold() function in the WGCNA package in R (Langfelder, 2008) was used to identify a power that would satisfy the assumption of a scale-free network (R^2 = 0.7 - 0.9), resulting in the network being well connected but only having a few hubs. This groups ASVs by their patterns of abundance into modules, using the WGCNA package in R (Langfelder, 2008) and was then used to plot the scale independence (R^2 value) for each power (Fig. 2.1A), and the mean connectivity (magnitude) at each power which visually clarified that power 13 (R2 = 0.805, mean.k = 38.2 and medium.k =22.5) was the most appropriate (Fig. 2.1B). Then, the blockwiseModules() function (Langfelder, 2008) was used to identify the grouping of ASVs into numbers by their abundance patterns across all sample types with each module being assigned a unique identifiable colour. The parameters set were standard bar: network type = signed hybrid; soft threshold power = 13; minimum module size = 30; merge cut height = 0.15. Then to create the edge files later used for identification of hub taxa through analysis of degree score, the exportNetworkToCytoscape() function (Langfelder, 2008) with a threshold of 0.15.

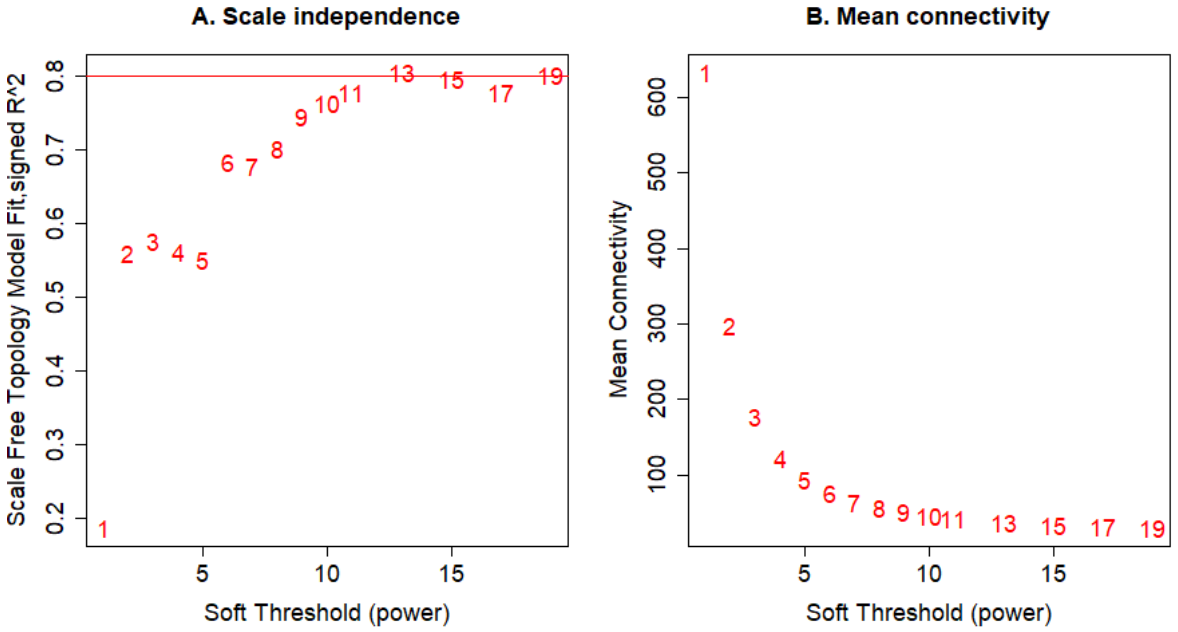

Figure 2.1 Determining the Soft Threshold Power for WGCNA. **A.** highlights the R^2 value at each power which, to satisfy the SFT assumption, is required to be between 0.7 and 0.9. **B.** highlights the mean connectivity for each power and the power that is chosen should be found close to the curve. This identifies the power most appropriate for the network, ensuring the abundance data is split between modules appropriately.

3.2.4 Statistical Data Analysis

To visualise the data, heatmaps were created to understand how each module's abundance was correlated with specific treatment groups including disease status (healthy = disease score 0, diseased = disease score 1) and sample treatment (*R. solanacearum*; *R. solanacearum* and 2,6-DHBA; 2,6-DHBA; and control) separately, using ggplot2 in R (Wickham H, 2016). Traits that explained the sample were indicated by a 1 while 0 indicated that the sample was not associated with the trait. The module eigenabundance was created using the moduleEigengene() function in R (Langfelder, 2008) and the correlation between the eigenabundance and the traits were created using the corr() function in the stats package in R (R Core Team, 2024). The significance was then calculated using the corPvalueStudent() function (Langfelder, 2008) and those that were deemed as not significant were recorded as NS (pval =>0.05). The correlation and significance were then simplified to two decimal places before being plotted on a heatmap to identify modules with abundance patterns that significantly correlated with the traits of interest, highlighting modules for further investigation using ggplot2 in R (Wickham H, 2016).

3.2.5 Visualisation of Module Abundance

Stacked proportional bar plots were created in ggplot2 (Wickham H, 2016) to understand the spread and abundance of taxa in each module, without consideration for disease status and sample treatment. The normalised, but not scaled, abundance data was used and, for each ASV, the abundance values were summed together across all samples to create a total abundance for each ASV. The ASV numbers were then aligned to their species name, as provided by Novogene. The names were then reduced to order level and the abundances of those with the same order were summed together. This was to aid the understanding of taxa abundance as multiple ASVs can represent one taxon due to the variations in sequences.

This was repeated for the four sample treatments (*R. solanacearum*; *R. solanacearum* and 2,6-DHBA; 2,6-DHBA; and control) and disease status (8 diseased, 40 healthy plants) by separating the sample's abundance according to the trait of interest sampled. Then the total abundance for each ASV in each trait was calculated.

3.2.6 Identification of Influential Taxa

A hub taxon is the organism with the highest degree score which is a count of the number of connections each node (taxa) has to other nodes. This was created by identifying links between ASVs. The function exportNetworkToCytoscape() from the WGCNA package (Langfelder, 2008) identified connections between the different ASVs in each module and then using the function gather() from the tidyr package (Wickerham, 2024) to record the number of times each ASV had a connection. The official classification for each ASV was then awarded accordingly, as received by Novogene, and those with the same classification were grouped. The taxon with the highest degree score, the number of connections to other taxa, was the hub taxon. Each module apart from lightyellow and skyblue had multiple taxa with the highest degree score, so to find the most prominent hub, the threshold for the taxonomic level was increased and the abundance of those belonging to the same classification were combined. This was repeated until there was one hub gene present and all top degree scores were plotted on a bar plot using ggplot2 in R (Wickham H, 2016).

3.2.7 Hub Taxa Behaviour

To ensure that the hub taxa for each module of interest was representative of their corresponding module before proceeding with analysis, the abundances of each ASV making up each hub taxon were assessed. This was conducted by identifying the ASVs that belonged to each hub taxon, plotting the abundance data from the CANA under each sample

treatment (*R. solanacearum*; *R. solanacearum* and 2,6-DHBA; 2,6-DHBA; and control) which was plotted as a boxplot using ggplot2 (Wickham H, 2016).

3.3 Results

3.3.1 Correlation between Modules and Traits

To understand how 2,6-DHBA influences the rhizospheric microbiome, a CAN was created using a total of 9,251 ASVs from DNA extractions for each of the 48 samples but only 3,680 remained after filtering. An R^2 value of between 0.7 and 0.9 is required to satisfy the scale-free network assumption so a power of 13 was used (R2 = 0.805, mean.k = 38.2 and medium.k =22.5) (Langfelder and Horvath, 2008). The CANA grouped the ASVs into modules by their abundance patterns across all sample types. Each module is assigned a unique identifiable colour for clear differentiation.

Modules including ASV abundance correlated to healthy or diseased plants were identified (Fig. 2.2A). Only three were found to have a significant correlation (steelblue, darkgrey, and lightcyan), all of which were negatively correlated with being healthy. These modules proceeded as potential modules of interest. Modules correlated with sample treatment (*R. solanacearum*, *R. solanacearum* and 2,6-DHBA; 2,6-DHBA; and the control) identified four modules of interest (skyblue, saddlebrown, steelblue, and lightyellow) (Fig. 2.2B).

As lightcyan and darkgrey are both significantly correlated with the same disease status and conditions, darkgrey was kept for further analysis while lightcyan was discarded as it was slightly more negatively correlated with healthy plants and slightly more correlated with the different treatments. To summarise the modules of interest predicted to be linked to disease proliferation are: darkgrey, lightyellow and steelblue. The modules of interest predicted to be linked to aiding 2,6-DHBA and therefore, promoting protection are: saddlebrown and skyblue.

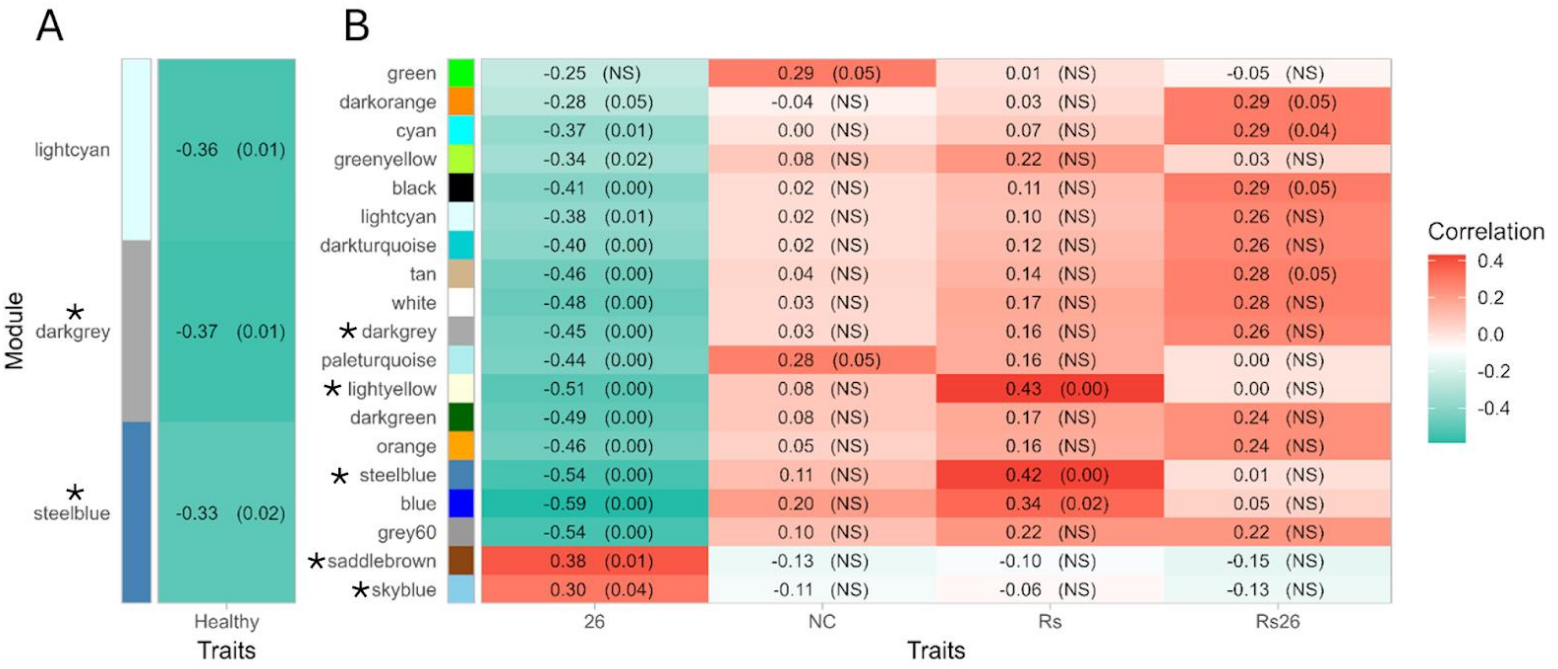

Figure 2.2 CANA Module-Trait Correlation. A. Heatmap of significant correlations between modules and healthy status (healthy disease score = 0; diseased disease score = 1). Each panel is a different module containing specific species of bacteria with red indicating a positive correlation to the trait of interest, health, while blue indicates a negative correlation with the healthy trait, and the significance is denoted in the brackets (NS = not significant, pval (pearsons) < 0.05 = significant and represented with the numerical value). **B.** Heatmap of significant correlations between modules and sample treatment (Rs = *R. solanacearum* inoculation; Rs26 = *R. solanacearum* and 2,6-DHBA inoculation; 26 = 2,6-DHBA inoculation; and NC = control). The red indicates a positive correlation to treatment type while blue shows a negative correlation with treatment type. Therefore, the modules of interest, denoted by an asterix (*), include: saddlebrown; skyblue; steelblue; lightyellow; and darkgrey.

3.3.2 Module Composition

The taxa composition for each module of interest was assessed at phyla level (Fig. 2.3). This was chosen to improve the readability of the graph by reducing the number of different classifications of organisms while not discarding individual organism data and still maintaining enough specificity to investigate their implication on module function.

The disease associated module's largest phyla include: *Proteobacteria* in darkgrey; *Firmicutes* in steelblue; and lightyellow being equally split between *Proteobacteria* and *Chloroflexi* (Fig. 2.3). Despite *Proteobacteria* being the largest phyla in only the darkgrey module, it is also highly abundant in the lightyellow and steelblue modules, comprising 23.4% and 27.7% respectively. Additionally, these modules also contained two phyla that

were not present in the two modules positively correlated with 2,6-DHBA inoculation: *Actinobacteriota* (11.3% of the darkgrey; 14.4% of the lightyellow; and 17% of steelblue), and *Acidobacteriota* (6.5% of the darkgrey; 20.4% of the lightyellow module; and 1.2% of steelblue). The modules positively correlated to 2,6-DHBA largest phyla include: *Bacteroidota* in saddlebrown; and *Firmicutes* in skyblue (Fig. 2.3).

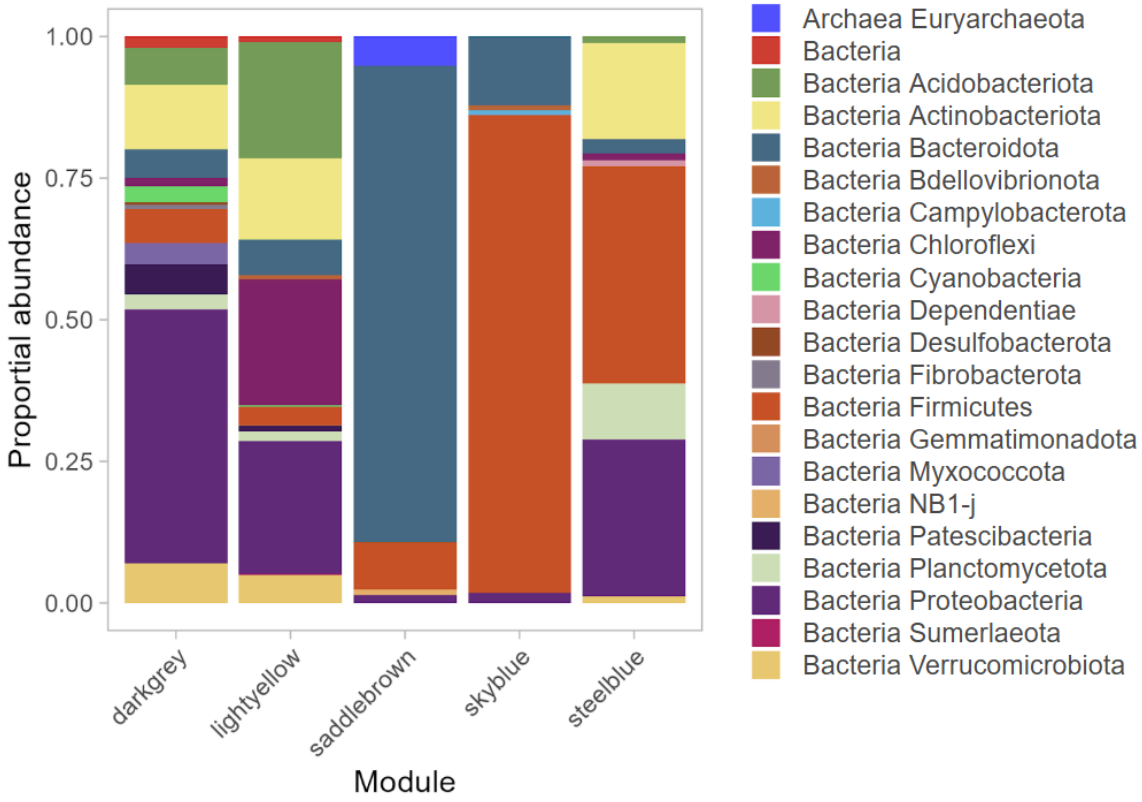

Figure 2.3 Module Composition. To improve the readability of the composition of the modules of interest, they were isolated from Fig. 2.2, allowing for interpretation of the proportion each phyla contributes to the modules of interest.

3.3.3 Hub Taxa

It is key to understand the most influential taxa within the modules of interest as these indicate the module's function. Therefore, the hub taxa must be representative of the module of interest, which was confirmed by assessing the abundance of each ASV associated with the hub taxon. The darkgrey module was significantly negatively correlated with 2,6-DHBA (Fig 2.2: correlation = -0.45, pval = <0.01), and there was a similarly large reduction in ASV abundance for both hub taxa, while the remaining treatments were not significantly associated with sample treatment and were more similar to each other (Fig 2.4). Both the steelblue and the lightyellow modules were similar with a a significant negative correlation

under 2,6-DHBA inoculation (Fig 2.2: steelblue correlation = -0.54, pval = <0.01; lightyellow correlation = -0.51, pval = <0.01) but also saw a significant positive correlation with *R. solanacearum* infection (Fig 2.2: steelblue correlation = 0.42, pval = <0.01; lightyellow correlation = 0.43, pval = <0.01). Both of the hub taxa for these modules mirrored the correlations with abundance, having lower abundance under 2,6-DHBA inoculation and higher abundance under *R. solanacearum* (Fig 2.5, 2.6). The saddlebrown and skyblue modules, however, were only significantly positively correlated with 2,6-DHBA inoculation (Fig 2.2: saddlebrown correlation = 0.38, pval = 0.01; skyblue correlation = 0.3, pval = 0.04) which is where we see a rise in abundance under 2,6-DHBA inoculation (Fig 2.7, 2.8). Each of these hub taxa aligned with the correlations between the treatments and modules, therefore, they were prioritised for further analysis.

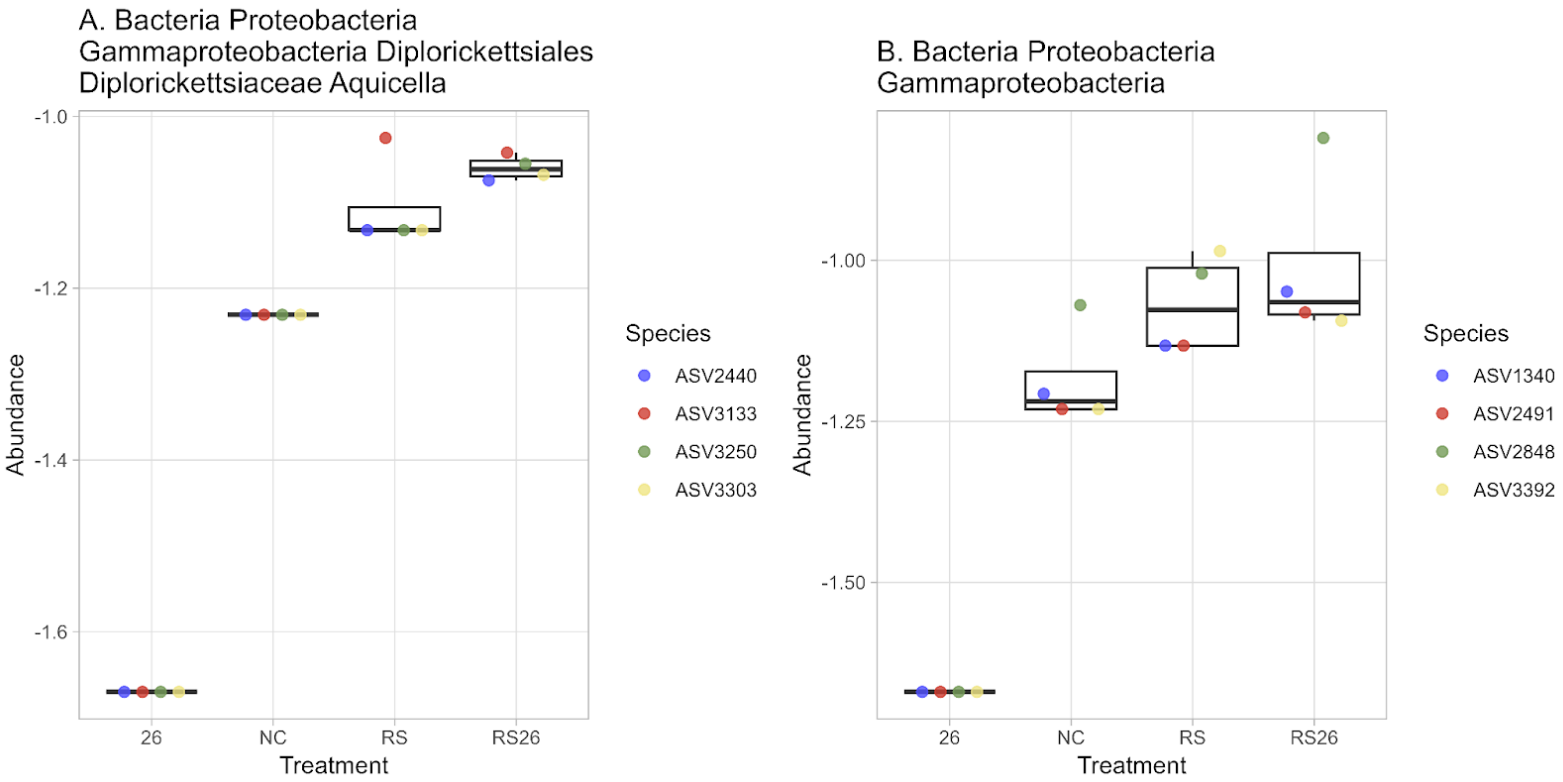

Figure 2.4 Darkgrey Hub Taxa Abundance. A. The abundance of the four ASVs for the hub taxon, *Aquicella*, were plotted under each treatment (2,6-DHBA referred to as 26; control as NC; *R. solanacearum* as Rs; and *R. solanacearum* and 2,6-DHBA as Rs26). The abundance under 2,6-DHBA is considerably low compared to all other treatments (abundance = -1.65) **B.** The second hub taxon's, *Gammaproteobacteria's*, abundance was also recorded, incorporating four ASVs under each treatment and saw a similar reduction under 2,6-DHBA (abundance = -1.7)

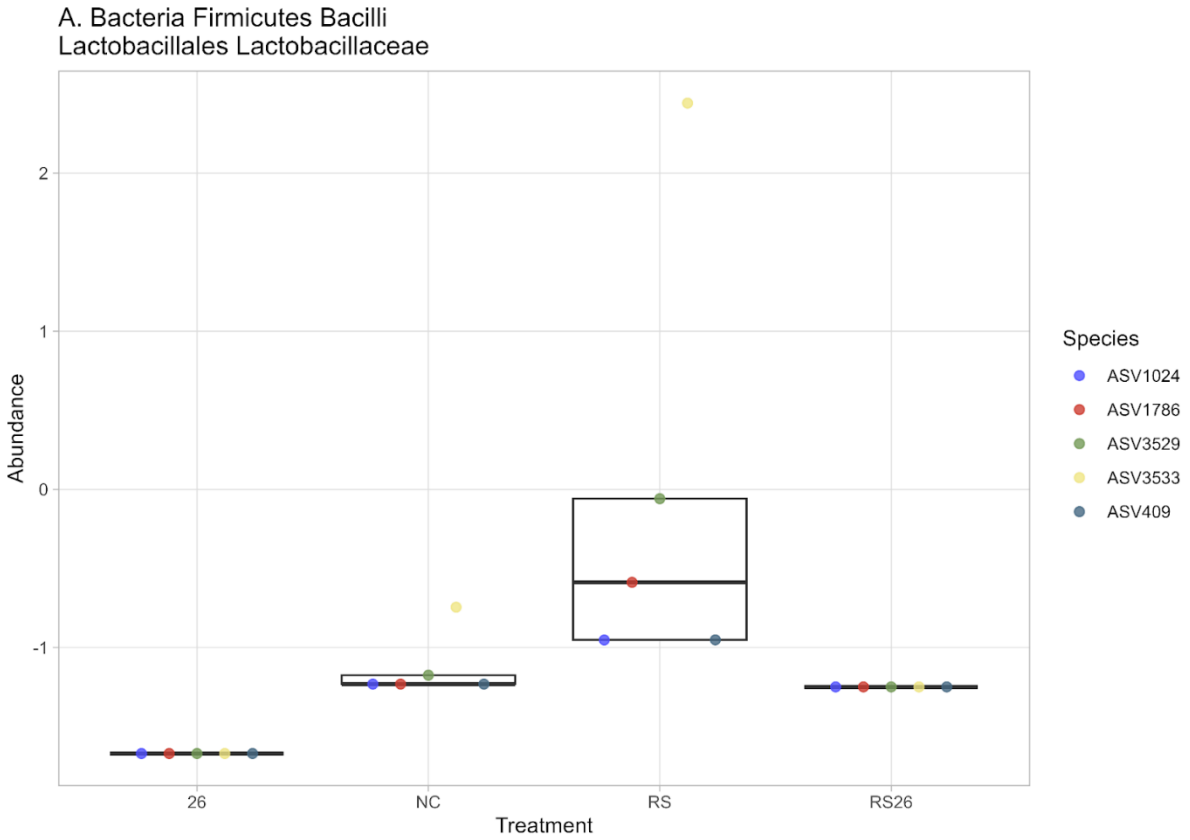

Figure 2.5 Steelblue Hub Taxa Abundance. The abundance of the five ASVs for the hub taxon, *Lactobacillaceae*, were plotted under each treatment (2,6-DHBA referred to as 26; control as NC; *R. solanacearum* as Rs; and *R. solanacearum* and 2,6-DHBA as Rs26). The abundance of these ASVs under *R. solanacearum* infection ranged from -0.99 to -0.01, with one outlier, ASV3533.

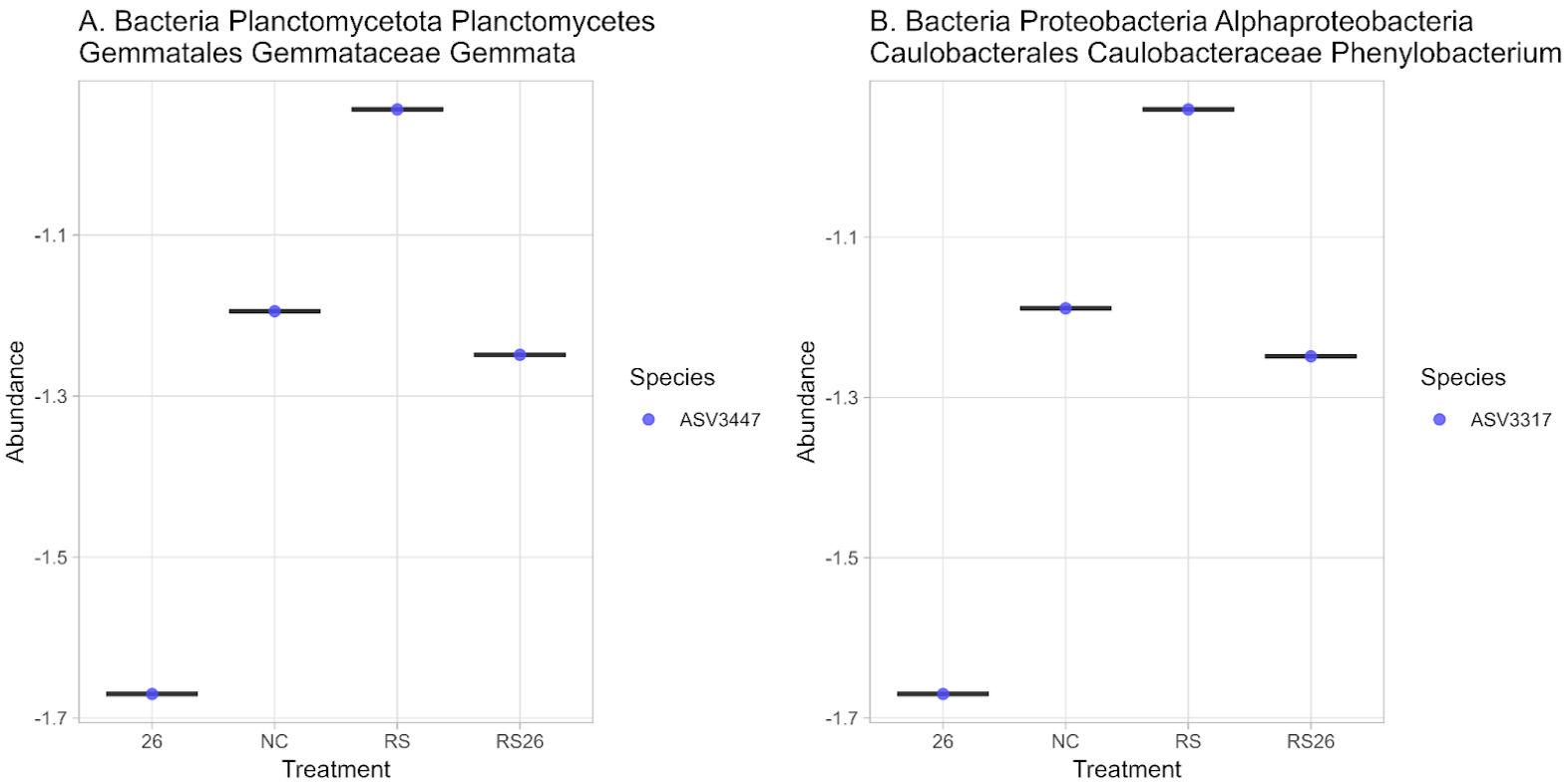

Figure 2.6 Lightyellow Hub Taxa Abundance. A. The abundance of the only ASV for the hub taxon, *Gemmata*, was plotted under each treatment (2,6-DHBA referred to as 26; control as NC; *R. solanacearum* as Rs; and *R. solanacearum* and 2,6-DHBA as Rs26) and saw a comparative rise in abundance under *R. solanacearum* inoculation (abundance = -0.95). **B.** The second hub taxon, *Phenylobacterium*, also only had one hub taxon and saw a similar level of abundance to the *Gemmata* hub taxon (abundance = -0.95).

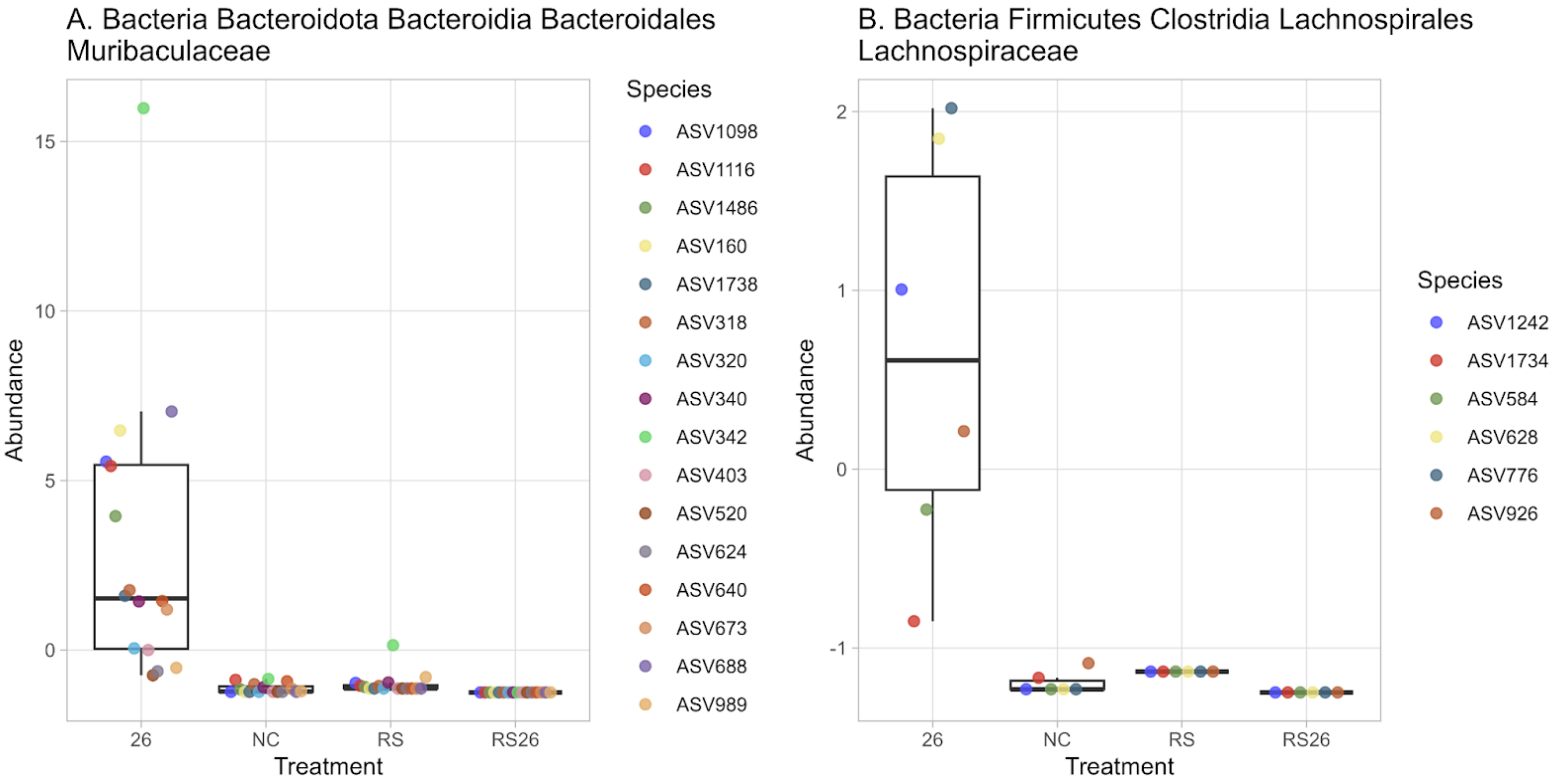

Figure 2.7 Saddlebrown Hub Taxa Abundance. A. The abundance of the 16 ASVs for the hub taxon, *Muribaculaceae*, were plotted under each treatment (2,6-DHBA referred to as 26; control as NC; *R. solanacearum* as Rs; and *R. solanacearum* and 2,6-DHBA as Rs26) and saw a comparative rise in abundance under 2,6-DHBA inoculation (abundance = 0.05 to 15.05). **B.** The second hub taxon, *Lachnospiraceae*, contained six ASVs and a considerable rise in abundance under 2,6-DHBA (abundance = -0.9 to 2).

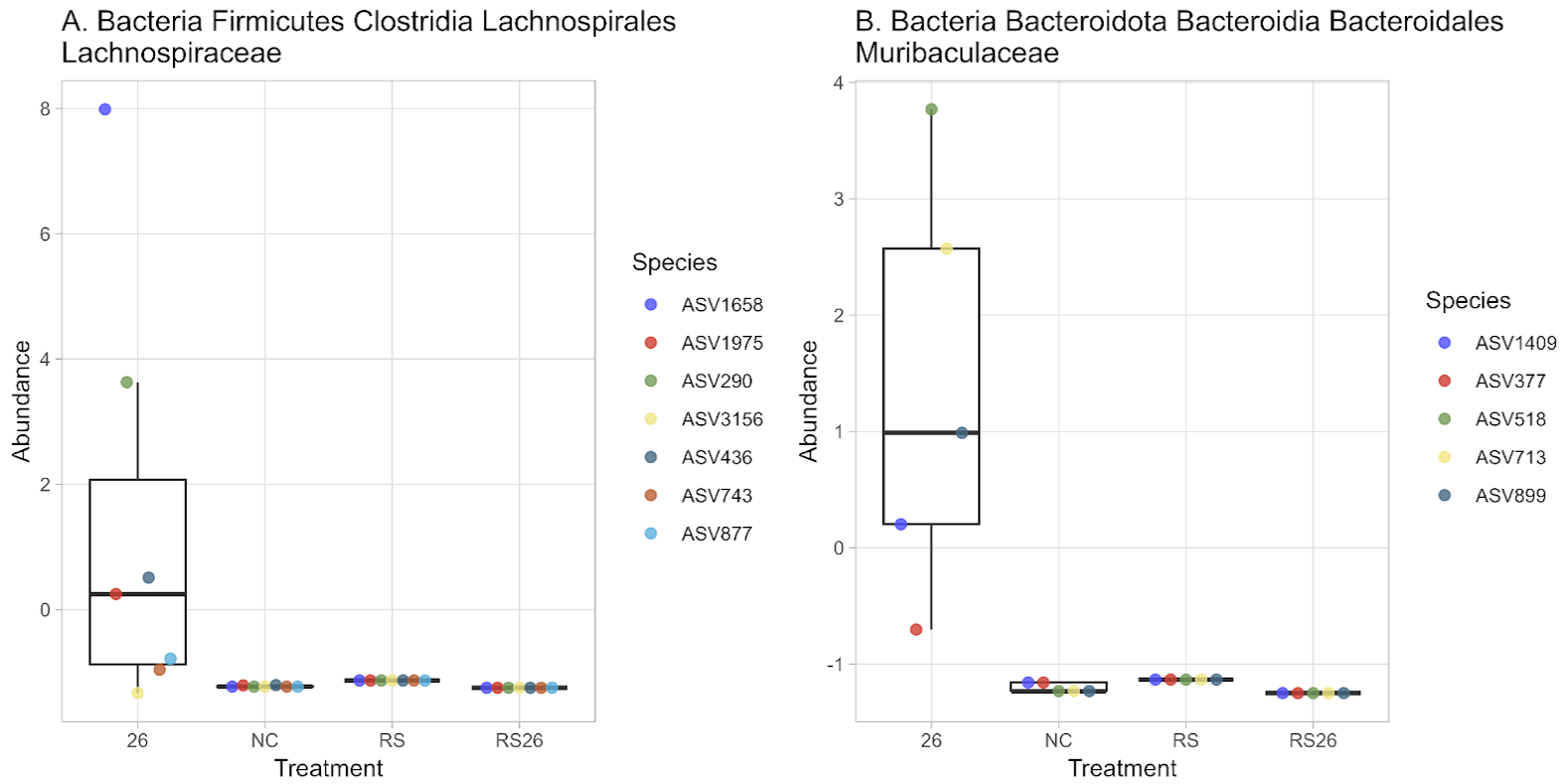

Figure 2.8 Skyblue Hub Taxa Abundance. A. The abundance of the seven ASVs for the hub taxon, *Lachnospiraceae*, were plotted under each treatment (2,6-DHBA referred to as 26; control as NC; *R. solanacearum* as Rs; and *R. solanacearum* and 2,6-DHBA as Rs26) and saw a comparative rise in abundance under 2,6-DHBA inoculation (abundance = -1.75 to 3.75). **B.** The second hub taxon, *Muribaculaceae*, was composed of five ASVs which also saw an increase in abundance under 2,6-DHBA inoculation (abundance = -0.75 to 3.8).

The degree score was then calculated for each module which counted the number of connections between nodes (taxa). The more connections a taxon has, the more influence it has on the module. As there were often multiple hub taxa at low taxonomic levels, to find the most influential hub, the order of classification was reduced and the degree scores of those belonging to the same classification were combined, until there was one highest degree score. This was conducted for all 5 modules of interest: darkgrey, lightyellow, saddlebrown, skyblue, and steelblue.

The hub taxon for darkgrey (Fig. 2.4) is *Aquicella* (genus) with a degree score of 219, followed by *Gammaproteobacteria* (class) with a degree score of 211. Both belong to the class *Gammaproteobacteria*, however, the second hub taxon was only identifieed to the

class level due to the amplicon sequence resolution. As these both belong to the same class, *Gammaproteobacteria*, this is evidently influential in the darkgrey module and requires further investigations. The hub taxon for the lightyellow (Fig. 2.5) module was *Bacteria* (domain) but this low specificity does not provide adequate indication of module function, so the second hub taxon was *Gemmata* (genus) with a degree score of 57, closely followed by *Phenylobacterium* (genus) with a degree score of 54. The saddlebrown hub taxa (Fig. 2.6) was *Muribaculaceae* (family) with a degree score of 489 followed by *Lachnospiraceae* (family) with 212. The hub taxa for the skyblue (Fig. 2.7) module was *Lachnospiraceae* (family) with a degree score of 225 which was followed by *Muribaculaceae* (family) with a degree score of 179. Finally, the hub taxa for the steelblue (Fig. 2.8) module was *Lactobacillaceae* (family) with a degree score of 67, followed by four other orders, indicating that *Lactobacillaceae* has a clear influence on this module and will be the only one taken for further investigation from this module.

Figure 2.9 Darkgrey Species Degree Score. Bar chart of degree scores calculated for the darkgrey module at genus level. The highest degree score for the darkgrey module, found at the top of the graph, is *Aquicella* (genus) with a degree score of 219.

Figure 2.10 Lightyellow Species Degree Score. Bar chart of degree scores calculated for the lightyellow module at genus level. The highest degree score for the lightyellow module, found at the top of the graph, is *Gemmata* (genus) with a degree score of 57. Taxa with a degree score less than 10 was removed.

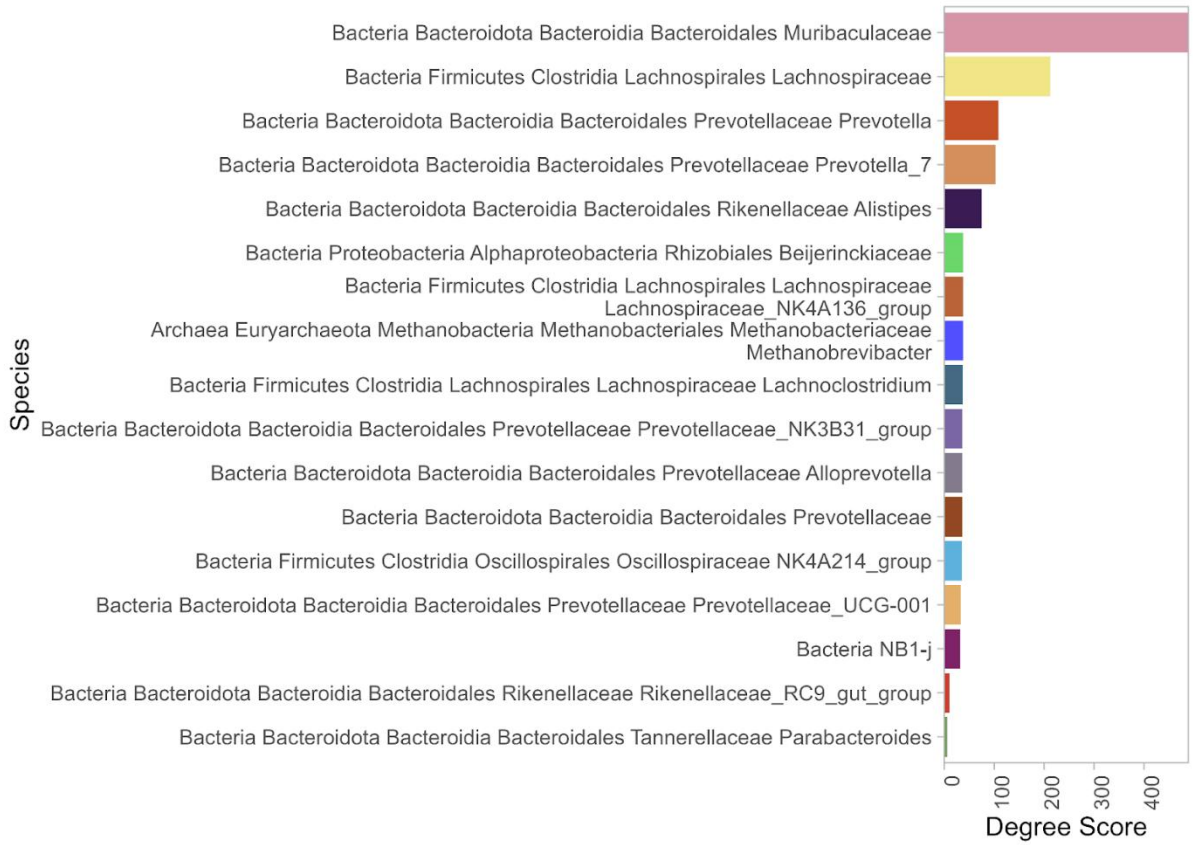

Figure 2.11 Saddlebrown Species Degree Score. Bar chart of degree scores calculated for the saddlebrown module at genus level. The highest degree score for the saddlebrown module, found at the top of the graph, is *Muribaculaceae* (family) with a degree score of 489.

Figure 2.12 Skyblue Species Degree Score. Bar chart of degree scores calculated for the skyblue module at genus level. The highest degree score for the skyblue module, found at the top of the graph, is *Lachnospiraceae* (family) with a degree score of 225.

Figure 2.13 Steelblue Species Degree Score. Bar chart of degree scores calculated for the steelblue module at family level. The highest degree score for the steelblue module, found at the top of the graph, is *Lactobacillaceae* (family) with a degree score of 67.

3.4 Discussion

3.4.1 Correlation between Modules and Traits - darkgrey, steelblue and lightyellow associated with disease, while saddlebrown and skyblue linked to health

The correlation between modules and traits were assessed to identify modules of interest that may shed light on the aim of confirming whether 2,6-DHBA impacts the presence of microbes. This resulted in highlighting five modules for further analysis: darkgrey, negatively correlated with health and 2,6-DHBA inoculation; steelblue, also negatively correlated with health and 2,6-DHBA as well as positively correlated with *R. solanacearum* inoculation; lightyellow, negatively correlated with 2,6-DHBA and positively correlated with *R. solanacearum*; saddlebrown and skyblue, both positively correlated with 2,6-DHBA inoculation. Initially, there were two modules significantly associated with only disease and 2,6-DHBA inoculation: lightcyan, and darkgrey. However, the lightcyan module is less correlated and had lower significance, albeit slightly, so only the darkgrey module progressed for further analysis. The composition of the rhizosphere can both positively and negatively influence a plant, resulting in plants adapting the surrounding rhizosphere by the production of root exudates (Prashar, 2013). Only 2-5% of rhizobacteria are found to promote growth through indirect and direct mechanisms such as outcompeting harmful pathogens and improving nutrient uptake, respectively (Beneduzi, 2012). Therefore, understanding the composition of each module may shed light on their correlations with each treatment.

The darkgrey and steelblue modules are negatively correlated with 2,6-DHBA. As this links to plant health promotion, the negative correlation identified between these modules and the healthy status was expected, indicating that influential taxa in these modules may be linked to disease and symptom proliferation. The lightyellow module is also negatively correlated with 2,6-DHBA but not with the disease status, indicating that taxa belonging to this module are less likely to have a clear link to disease. However, both the lightyellow and steelblue modules are significantly positively correlated with *R. solanacearum* inoculation. This link would be interesting to explore, potentially highlighting taxa that are aiding the proliferation of *R. solanacearum*, are mutualistic towards *R. solanacearum* or are an example of *S. lycopersicum's* immune response to infection. However, mutualistic relationships between pathogenic microbes and non-pathogenic microbes have been previously identified, but few in the rhizosphere. For example, Scherlach (2017) highlights the relationship between *Clostridium difficile* and *Candida albicans* in the human gut where *C. albicans* allows *C.*

difficile to survive in previously hostile conditions and the lightyellow module may aid the identification of a similar mutualistic relationship, that assists growth, formed with *R. solanacearum* (Scherlach, 2017).

The skyblue and saddlebrown modules are significantly positively correlated with 2,6-DHBA inoculation. As this improved resistance to *R. solanacearum* inoculation, these modules may be home to taxa that promote health and immune defence as Sun (2021) highlighted the abundance of research that indicates root exudates' ability to change and recruit nutrient fixing bacteria (Franco Ortega, in press; Sun, 2021). For example, strigolactones are a class of hormones that, when artificially applied, inhibit pathogenic fungal growth (Olanrewaju, 2019). This highlights plants' ability to change the secretion of chemicals and influence the surrounding microbiome to promote growth from improved access to nutrients, or to have a supporting rhizosphere which may be the case in these modules of interest (Sun, 2021; Olanrewaju, 2019).

These five modules can be split into two groups: those theorised to promote disease (darkgrey, steelblue and lightyellow) and those theorised to promote defence (saddlebrown and skyblue). To shed light on these theories, identification of taxa that make up these modules is required so the influence they have on disease proliferation and plant defence can be deduced.

3.4.2 Module Composition and Hub Taxa - validating the prediction of module of interest's role in disease

An overview of each module of interest's composition was used to highlight the influential phyla to indicate module function. As the modules positively associated with disease (darkgrey, lightyellow and steelblue) have a similar composition to each other (Fig. 2.5) and modules positively associated with 2,6-DHBA (saddlebrown and skyblue), also have a similar composition to each other, it can be predicted that these two groups are likely to have similar functions which can be explored through preexisting literature (Table 2.1). This highlights that splitting further analysis into a disease associated and not associated group was appropriate.

Module	Hub Taxa	Resolution	Degree Score	Relevant Literature
darkgrey	*Aquicella*	genus	219	Little specifics are known but they belong to the *Diplorickettsiaceae* family which is associated with inducing invertebrate, human and sometimes plant disease. For examples, *Rickettsia* infect *Empoasca* planthoppers which feed on papaya and cause papaya bunchy top disease (Perlman, 2006; Davis, 1998).
	Gammaproteobacteria	class	211	Encompasses *Ralstonia solanacearum* and many other plant pathogens such as: *Pseudomonas syringae*, *Xanthomonas campestris*, and *Xylella fastidiosa* (Buttimer, 2017). However, some have ben found in *Fusarium oxysporum* infected soil where plants resisted infection (Köberl, 2017).
lightyellow	*Gemmata*	genus	57	*Gemmata* are found in many environmental niches including wetlands, rivers, wastewater treatment plant, and even in the human gut with no direct link to disease (Peprah, 2025; Kulichevskaya, 2017). *Gemmataceae* (family) has also has no links to disease but has been found to degrade polysaccharides, chitin and biopolymers. This aids the degradation of persistent chemicals, such as pesticides, reducing the level of protection (Chang, 2023)
	Phenylobacterium	genus	54	Heavily linked to nitrogen fixation, aiding plant growth (Yang, 2017). However, an excess has been found to causes disease in two varieties of sesame, Jinhuagma and Zhongzhi (Wang, 2018).
saddlebrown	*Muribaculaceae*	family	489	Mostly associated with human gut health but found to remove heavy metal compounds from contaminated soils, aiding plant growth (Zhu, 2024; Gong, 2021). This enhances physicochemical parameters, making necessary elements accessible for the plant, and has been found to promote health (Das, 2022)
	Lachnospiraceae	family	212	Abundance associated with reductive soil disinfection (RSD) treatment but is unclear if this aids disease control or is a result of treatment creating anaerobic conditions (Huang, 2019). *Lachnospiraceae* has also been linked to reducing pH due to their production of short chain fatty acids which influences disease pressure (Huang, 2019).
skyblue	*Lachnospiraceae*	family	225	Abundance associated with reductive soil disinfection (RSD) but unclear if this is aiding disease control or a result of RSD treatment creating anaerobic conditions (Huang, 2019). *Lachnospiraceae* has also been linked to reducing pH due to their production of short chain fatty acids (Huang, 2019).
	Muribaculaceae	family	179	Mostly associated with human gut health but found to remove heavy metal compounds from contaminated soils, aiding plant growth (Zhu, 2024; Gong, 2021). This enhances physicochemical parameters, making necessary elements accessible for the plant, and has been found to promote health (Das, 2022)
steelblue	*Lactobacillaceae*	family	67	Strong link to promoting health in humans and prolonging the viability of food produce, rarely associated with disease (Walter, 2023). Increasingly used as a biological control agent (Gobbi, 2020).

Table 2.1 Summary of Hub Taxa Literature. A summary of the relevant literature of each hub taxa for the modules of interest is displayed alongside the taxonomic level and degree score.

3.4.3 Darkgrey Module - hub taxa associated with disease

The darkgrey module is largely made up of *Proteobacteria* without any other standout phyla, making up 44.9% of the darkgrey module abundance (Fig. 2.3). This is the largest and most phenotypically diverse phyla, encompassing over 1,600 species and dividing into six classes, so interpreting function at this level of taxonomic classification is difficult (Kersters, 2006; Rizzatti, 2017). This phylum is home to a range of species with varying links to plant immunity. An example of this includes *Paraburkholderia phytofirmans* which is known to elicit an immune response in plants but has been linked to short term, detrimental impacts on plant growth, and this promotion of the immune system may be due to inciting the plants immune response due to its pathogenicity (Cheng, 2021; Orellana, 2022). Furthermore, this phylum is home to our pathogen of interest, *R. solanacearum,* so to truly understand the link

between the darkgrey module and the largest linked phylum, further analysis into the keystone taxa was required (Cheng, 2021).

The top two hub taxa in this module are: *Aquicella* (genus) (Fig. 2.9, represented in yellow *); followed by *Gammaproteobacteria* (class) (Fig. 2.9, represented in green *). The second hub taxon, *Gammaproteobacteria*, is broad and encompasses our pathogen of interest, *R. solanacearum*, making it unsurprising that there is a strong correlation with disease outcome (Fig. 2.2: correlation = 0.37, pval = 0.01). However, *R. solanacearum* was sorted into the magenta module so the species that make up these *Gammaproteobacteria* are likely to be closely related rather than *R. solanacearum*. This close relation may mean the species in this module share some similar mechanisms which may be similarly impacted by 2,6-DHBA. This could explain the negative correlation with 2,6-DHBA (Fig. 2.2: correlation = -0.45, pval = <0.01) and positive correlation to disease (Fig. 2.2: correlation = 0.37, pval = 0.01) as they may thrive under similar conditions as *R. solanacearum*. *Gammaproteobacteria* includes plant pathogens but has also been found in fields that resist pathogen infection, theorised to be protecting roots from colonisation (Table 2.1; Burrimer, 2017; Köberl, 2017). Therefore, looking further to the most influential hub genus, *Aquicella*, should be able to shed light on the impact of bacteria such as *Gammaproteobacteria* in this module. Little is known about *Aquicella*, but its family *Diplorickettsiaceae*, which include diseases such as *Rickettsia* which infects *Empoasca* planthoppers causing papaya bunchy top disease, the first known example of *Rickettsia* being a plant pathogen (Table 2.1; Perlman, 2006 ; Davis, 1998). This, also considering darkgrey's correlation with disease, further indicates that this module is home to taxa linked with disease proliferation and it is likely that some *Aquicella* and *Gammaproteobacteria* species are likely to promote disease and will exhibit suppressed growth under 2,6-DHBA inoculation.

3.4.4 Steelblue Module - high levels of beneficial hub taxon linked to disease but 2,6-DHBA may be reducing abundance to a plant promoting level

The steelblue module is mostly composed of *Firmicutes* (38.3%), with *Proteobacteria* (27.7%) being the second most abundant taxon and making up the majority of the top hub taxa (Fig. 2.13). *Firmicutes* are often linked to disease suppression, with examples of reductions in *Firmicutes* abundance being linked to higher disease susceptibility and the promotion of *R. solanacearum* (Lee, 2021). This link to soilborne disease control makes this large allocation to the steelblue module surprising as it is so strongly and significantly correlated with disease and *R. solanacearum* inoculation (Fig. 2.2: correlation = 0.42, pval = <0.01), and is negatively correlated with the application of the beneficial metabolite, 2,6-

DHBA (Fig. 2.2: correlation = -0.54, pval = <0.1) (Yang, 2023). However, there have been instances where *Firmicute* abundance has been linked to diseases, including when *Firmicute* abundance rose by 20% in symptomatic samples, as well as some *Firmicute* species, such as *Clostridium puniceum*, being linked to cases of rot in potatoes and carrots (Bez, 2021; Seong, 2018; Lund, 1981). Therefore, despite the longstanding belief that *Firmicutes* are plant growth promoting and can promote plant immunity, there are examples of *Firmicutes* that promote disease which is likely to be the case with the *Firmicute* species found in the steelblue module.

To understand the steelblue module's function, the hub taxa were identified. This module, however, only had one main hub taxon, *Lactobacillaceae* (family) (Fig. 2.13, represented in blue *), with no clear second most connected taxon. *Lactobacillaceae* is a *Firmicute*, which are known to have strong links to plant immunity, so it is unsurprising that *Lactobacillaceae* are strongly linked to human health, the longevity of food produce, and increased use as a biological control, rarely exhibiting pathogenic traits (Table 2.1; Walter, 2023; Gobbi, 2020). Furthermore, as *Firmicutes* are the most prevalent taxon in the steelblue module, it is expected that the hub taxon is a *Firmicute* linked with plant protection. However, considering the significant positive correlation with diseases and *R. solanacearum* infection as well as significant negative correlation with 2,6-DHBA inoculation, makes this unexpected. *Lactobacillaceae*, the primary hub, produces lactic acid which, when increased over their normal amount, can cause a reduction in pH that has been found to promote disease (Zhang, et al., 2022). Therefore, artificial inoculation of *R. solanacearum* may have initiated dysbiosis, shifting the microbiome which results in a rise in *Lactobacillaceae* and a decrease in pH. The inoculation of 2,6-DHBA without *R. solanacearum* causes a reduction in *Lactobacillaceae* and likely rise in pH, explaining the negative correlation that this module has with 2,6-DHBA inoculation. As 2,6-DHBA reduces *Lactobacillaceae* while *R. solanacearum* increases *Lactobacillaceae*, the addition of both may cause an intermediate response, similar to those seen in the control samples. This indicates that 2,6-DHBA is beneficial in the presence of disease pressure but may be detrimental if not counteracted by the infection.

3.4.5 Lightyellow Module - hub taxa associated with innate immune response or *R. solanacearum* mutualism

The lightyellow modules' largest phyla are *Proteobacteria* (23.4%) and *Chloroflexi* (22.3%), both contributing largely to the top hub taxa (Fig. 2.10). *Chloroflexi* are another diverse phylum which is home to many different organisms, but Yang (2024) found that an increase in unclassified *Chloroflexi* species was linked to metabolic pathways, biosynthesis of

secondary metabolites, and microbial metabolism, known mostly for their role in carbon and geochemical cycles with little information on plant defence (Hug, 2013). Furthermore, as the lightyellow module is not linked to a clear diseased outcome, this may indicate that this module is instead linked to general plant growth or the presence of *R. solanacearum*. Additionally, the negative correlation with 2,6-DHBA may be due to 2,6-DHBA inhibiting the growth of this taxon so the positive correlation found in samples only inoculated with *R. solanacearum* may be due to 2,6-DHBA not being present and, therefore, not inhibiting growth. By this logic, all samples without 2,6-DHBA inoculation would see a positive correlation, including the control samples. However, this was not the case for the lightyellow module, which suggests that *R. solanacearum* and *Chloroflexi* exhibit a mutualistic behaviour, benefiting from each other's presence. This may also explain the lack of correlation between the samples inoculated with both 2,6-DHBA and *R. solanacearum* as they counteract each other, balancing to neutral, as seen in the control samples. Looking at a higher resolution may shed light on the species found in this module and indicate if the lightyellow module is truly linked to a diseased outcome.

To assess this link, the lightyellow module's two hub taxa were analysed: *Gemmata* (genus) (Fig. 2.10, represented in dark purple *); and *Phenylobacterium* (genus) (Fig. 2.10, represented in green *). *Gemmata* is a genus with limited links to plant disease and is found in a range of environmental niches (Table 2.1; Peprah, 2025; Kulichevskaya, 2017). This implies that the *Gemmata* genus is mostly in the background of the system and not necessarily linked to plant immunity or defence stress. *Gemmataceae* also has limited links to plant disease but has been found to degrade pesticides, increasing the level of disease (Table 2.1;Chang, 2023). However, there were no persistent chemicals identified in this experiment so it is unclear if these functions are what links it with the lightyellow module here. Therefore, further work would be required to assess if *Gemmataceae Gemmata* increases disease pressure as expected with the strong positive correlation with *R. solanacearum* inoculation and negative correlation with 2,6-DHBA. Additionally, *Phenylobacterium* has been linked to plant growth promotion but high abundance has occasionally been associated with plant disease (Table 2.1; Yang, 2017). This counteracts the initial suggestion that it is beneficial to plants, further solidified by being a hub taxon for the module correlated with *R. solanacearum* inoculation. This indicates that the lightyellow module may be linked to the plants' innate immune response or have a mutualistic relationship with *R. solanacearum,* and an analysis of *Gemmata* and *Phenylobacterium* species, with and without the addition of 2,6-DHBA, would be insightful to both understand how these bacteria influence the plant and surrounding microbes as well as how 2,6-DHBA is interacting with them specifically.

3.4.6 Disease associated modules - *Actinobacteriota* theorised to exploit diseased plants

It is interesting to note that all three modules that are hypothesised to be linked to disease, also contained *Actinobacteriota* and *Acidobacteriota* and are often found in the top hub taxa (Fig. 2.9; 2.10; 2.13). These two taxa have formed a strong link between the three modules originally hypothesised to be associated with disease, therefore resulting in the expectation of clear links to disease proliferation.

Actinobacteriota has mostly been associated with defence against disease, where a reduction in abundance has caused an increase in *R. solanacearum* (Lee, 2021). This again is unexpected, especially in the darkgrey and steelblue modules that are significantly correlated to diseased plants and, for steelblue, *R. solanacearum* infection. It should be considered again that the lightyellow module is significantly positively correlated with *R. solanacearum* infection and not disease status. Therefore, the large proportion of *Actinobacteriota* found in this module may contain beneficial species of the phylum which correlate with disease suppression or is another example of a mutualistic relationship with *R. solanacearum* (Lee, 2021). Despite the strong association with plant defence, there are species belonging to the *Actinobacteriota* phylum which are associated with disease, such as *Streptomyces scabies* which cause the common scab found on potatoes (Lambert, 1989). As these modules are hypothesised to be linked to disease, and *R. solanacearum* inoculation, the *Actinobacteriota* found in these modules may be species associated with disease and taking advantage of the weakened *R. solanacearum* infected plant, causing a secondary disease incidence. This requires further analysis of the taxa present in these modules to assess which interactions they participate in. Finally, *Acidobacteriota* are often found in soils, but little is known about their roles except indications of influence on plant growth and biogeochemical cycling (Kielak, 2016; Gonçalves, 2024). However, as this phylum is found in all three modules positively correlated with disease, *R. solanacearum* inoculation, or negatively correlated with 2,6-DHBA, it can be assumed that some of these species cause disease or do not align to the category of plant growth promoting or biochemical cycling. Furthermore, *Acidobacteriota* are such a diverse phylum that generalising functions is unwise and some *Acidobacteriota* may have a detrimental impact on plants (Kielak,2016).

3.4.7 Saddlebrown Module - hub taxa associated with plant growth promoting soil environments

The saddlebrown module is significantly and positively correlated to 2,6-DHBA and is largely composed of *Bacteridota* (84.2%) *and Firmicutes* (8.3%) as the two largest phyla, contributing to the majority of top hub taxa (Fig. 2.11). *Bacteroidota* has been found to promote growth and disease control, with little indication of negative interactions with plants (Martin, et al., 2025; Seo, 2024; Han, 2025). As previously established, *Firmicutes* are well known for their link with plant defence and growth promotion which validates our findings of 2,6-DHBA showing disease suppression (Hashmi, 2020). This further solidifies this module, which is correlated with 2,6-DHBA (Fig. 2.2: correlation = 0.38, pval = 0.01), is linked to beneficial bacteria, indicating that 2,6-DHBA is likely to recruit beneficial bacteria.

The hub taxa of the saddlebrown modules, correlated to 2,6-DHBA and therefore linked to health, is *Muribaculaceae* (family) (Fig. 2.11, represented in pink *), followed by *Lachnospiraceae* (family) (Fig. 2.11, represented in yellow *). *Muribaculaceae* is often associated with a healthy human gut but also has been found to reduce contamination in soils, promoting plant growth (Table 2.1; Zhu, 2024; Gong, 2021; Das, 2022). Despite most research focusing on *Muribaculaceae's* link to gut health, being the main hub taxon for the saddlebrown module and the second hub taxon in skyblue, both modules positively correlated with the beneficial metabolite 2,6-DHBA, indicates that *Muribaculaceae* is likely to be attracted by 2,6-DHBA and may contribute to a defensive microbiome in the rhizosphere. The second hub taxon of the saddlebrown module is *Lachnospiraceae* which belongs to the *Firmicutes* phylum, known for their links in promoting defence against harmful soilborne pathogens (Huang, 2019; Yang, 2023). *Lachnospiraceae* abundance has been associated with reductive soil disinfection (RSD) treatment to control soil disease but it is unclear whether *Lachnospiraceae* contribute to disease protection or if it is attracted to the anaerobic conditions created by RSD treatment (Table 2.1; Huang). When undergoing RSD assessments, *Ruminococcaceae* and *Lachnospiraceae* were both associated with a reduction in pH (Table 2.1; Huang, 2019). As previously mentioned, lower pH has been linked to disease proliferation, with increasing soil pH observed to initially reduce symptoms of *R. solanacearum* while promoting well known beneficial microbes in the Firmicutes phylum (Zhang, 2022). Therefore, *Lachnospiraceae's* strong link to reducing pH could be seen as detrimental, implying 2,6-DHBA inoculation is promoting disease and inhibiting microbial protection. However, 2,6-DHBA has been found to reduce disease outcome, and it is not clear if previous studies considered that *Lachnospiraceae* may be attracted to low pH, rather than causing it, as discussed above. Furthermore, alternative control methods such as

RSD have reported a reduction in pH despite improving disease control (Huang, 2019). Therefore, further work should assess the link between: pH and *Lachnospiraceae* to understand if *Lachnospiraceae* produces or is attracted to high acidity; if one of the mechanisms 2,6-DHBA harnesses to reduce *R. solanacearum* pathogenicity is by promoting acidic conditions; and if *Lachnospiraceae*, and acidic conditions, are effective at reducing the pathogenicity of *R. solanacearum*. It is expected that there are other mechanisms behind 2,6-DHBA that promote the reduction in *R. solanacearum* infection severity but this may shed light on one section of a complex interaction.

3.4.8 Skyblue Module - hub taxa linked to plant growth promoting soil environments

The skyblue module is mostly composed of *Firmicutes* (84.3%) followed by *Bacteroidota* (12.2%) which are the two largest phyla found in the saddlebrown module and make up a large proportion of top hub taxa (Fig. 2.12; 2.13) which is also significantly positively correlated with 2,6-DHBA. As previously discussed, these taxa are linked to recruiting beneficial bacteria but to understand the extent of this, the hub taxa should be analysed.

In this module, the two hub taxa are *Lachnospiraceae* (family) (Fig. 2.12, represented in pink *), followed by *Muribaculaceae* (family) (Fig. 2.12, represented in grey *). Both *Lachnospiraceae* and *Muribaculaceae* are also hub taxa for the saddlebrown module (Table 2.1). This is likely to be due to there being multiple ASV with the same genus allocation, but may be different species as reliably identifying organisms down to species level is difficult to achieve. Therefore, despite being the same genus, the organisms are likely to be different species which is why the same genus is allocated to different modules. This further solidifies the reasoning for further investigations regarding *Lachnospiraceae's* role against *R. solanacearum*, if they truly lower pH, and if this impacts the surrounding microbiota.

3.5 Conclusion

The initial predictions were that the darkgrey, steelblue and lightyellow modules were likely to contain taxa associated with disease proliferation. While this may still be true for the darkgrey and steelblue modules, the interpretation of the lightyellow module suggests a more complex relationship.

The hub taxon for the darkgrey module is *Gammaproteobacteria*, and more specifically *Dipolrickettseace*, which has been linked to inducing plant disease. The steelblue and lightyellow modules were also linked to microbes that promote disease but by specifically inducing acidity. This is expected for the steelblue module which is correlated with disease

and *R. solanacearum* inoculation, as well as negatively correlated with 2,6-DHBA inoculation. Similarly, the lightyellow module is positively correlated with *R. solanacearum* and negatively correlated with 2,6-DHBA but is not correlated with disease. This suggests that the steelblue module is promoting a disease environment, potentially by reducing the pH. The lightyellow module, however, is more likely to be linked to a mutualistic relationship and being promoted by *R. solanacearum*, or promoting plant growth rather than inducing disease via aiding *R. solanacearum* growth as the hub genes were linked to nitrogen fixing and degradation of persistent chemicals (Yang, 2017; Chang, 2023). Therefore, the lightyellow module is likely to not be linked to promoting disease as first thought.

The saddlebrown and skyblue modules were predicted to be linked to defence which is further suggested from this work due to the hub taxa, *Lachnospiraceae*, established links to preexisting methods of defence. However, there is some uncertainty regarding the influence of pH which requires further investigation to definitively state that these modules induce defence.

3.5.1 Suggestions for Further Work

This work has highlighted six taxa of interest linked to *R. solanacearum* and 2,6-DHBA inoculation: *Aquicella, Gemmata, Phenylobacterium, Lactobacillaceae, Muribaculaceae,* and *Lachnospiraceae*. However, soil is a complex, everchanging system. This limitation was mediated by the use of a PHCbi cabinet to reduce the variability of external factors. However, this work only focused on bacteria which equates to 70-90% of the microbiome of soil, leaving fungi, the second largest group by abundance, unexplored (Wang, 2024). Despite having a lower abundance, fungi have been found to contribute 62.3% to the ecological uniqueness, 24.6% more than bacteria (Li, 2024). It would, therefore, be beneficial to expand this search and conduct a CANA on fungal taxa for a more comprehensive understanding of the influence the rhizosphere's microbiome has on *R. solanacearum* infection and resistance.

Further work should also be conducted on the hub taxa identified so far (*Aquicella, Gemmata, Phenylobacterium, Lactobacillaceae, Muribaculaceae,* and *Lachnospiraceae*). This should be assessed in microbial interaction assays to understand their connection to *R. solanacearum.* However, 99% of rhizobacteria are difficult to culture so additional time may be required to identify the optimal growing conditions for each taxon (Prashar, 2013). The *Aquicella* genus has been found to be culturable between 30 ºC and 45 ºC, around 7 pH, but some species require activated charcoal and α-ketoglutarate (Santos, 2003). *Gemmata*, on the other hand, are often found in a range of habitats, making their nutrient requirement

difficult to interpret, but have been found to grow well at 28 ºC in M1, R2A and PYGV media and sterile water (Mishek, 2018; Wang, 2002). The *Phenylobacterium* genus has been found to grow slowly but is improved when supplemented with chloridazon, antipyrin, or pyramidon at between 28 ºC and 30 ºC with a pH of 6.8 to 7 (Lingens, 1985). Some genera of *Lactobacillaceae* have been found to grow in M17 media for 2 days at 30 ºC, shaking before being inoculated on a plate and stored for up to 3 days at 37 ºC (Kim, 2018). However, little is reported about isolating *Muribaculaceae* species from soil but as mammalian strains are often grown on blood agar, this would require some additional experiments to identify an effective culturing method for soil specific strains (Park, 2021). Finally, *Lachnospiraceae* has been found to grow in anaerobic conditions between 30 ºC and 45 ºC with strains isolated from humans being the most viable from Yeast Casitone Fatty Acid (YCFA) but this would also have to be tested on soil isolated strains (Zaplana, 2024). Therefore, all of these bacteria have been found to be culturable except soil based *Muribaculaceae* and *Lachnospiraceae*, therefore, multiple growth media, temperatures and pH would most likely be required to optimise growth. Once isolated and cultured, assays designed to assess the relationship between *R. solanacearum* and 2,6-DHBA should be conducted with each taxa. These should include a liquid culture assay, assessing the differences of OD of the taxon of interest in both the presence and absence of fluorescent *R. solanacearum*. Additionally, a spot-on-the-lawn assay should be conducted, requiring the inoculation of *R. solanacearum* on solid agar and adding a 5 uL spot of each taxon of interest. The presence of a zone of inhibition would shed light on the interaction between *R. solanacearum* and each taxon of interest. These two assays should then be conducted with 2,6-DHBA to understand how each taxon interacts with the beneficial metabolite.

As a final step, in-planta experiments should be conducted which would require four treatments: taxon of interest; taxon of interest and *R. solanacearum*; *R. solanacearum*; and a control (CPG). This should assess pH levels as well as indicators of plant health such as: green leaf area; expected growth pattern; signs of stress; signs of damage (disease, pest, or nutrient deficiencies) (Fuentes, 2025). This may then shed light on how each taxon: interacts with *R. solanacearum*, inhibiting, promoting or mutualistically co-existing; interacts with 2,6-DHBA and if 2,6-DHBA promotes or reduces the abundance of the taxon of interest; and finally, how these interactions influence *S. lycopersicum's* susceptibility to *R. solanacearum*, including the impact of acidity. This may then confirm that 2,6-DHBA promotes protection against *R. solanacearum* by influencing the microbes present in the rhizosphere of *S.lycopersicum* which is vital to the commercialisation of metabolites such as 2,6-DHBA.

Overall, this work highlighted the importance of understanding how abundance changes under different treatments and how CANA can be utilised to identify changes of important taxa that may protect the susceptible *S. lycopersicum* from *R. solanacearum* infection.

4 General Discussion

4.1 Summary

This work assessed the uses and benefits of biological network analysis, shedding a light on how diverse its application can be. While this work is highly adaptable and can provide insights into complex interactions, no two analyses are the same and require case specific analysis. The specificity required for network analysis can be taxing but when used appropriately, can be an effective way to analyse interactions.

4.1.1 WGCNA

This work used WGCNA which highlighted five candidate genes that are likely to be involved in *S. dulcamara's* resistance: Solyc10G001528, Solyc10G000984, Solyc05G001746, Solyc11G001222, and Solyc01G003106. Influencing the expression of these genes in *S. lycopersicum* to mimic *S. dulcamara's* expression may then increase resistance to *R. solanacearum* in *S. lycopersicum*.

Solyc10G001528, Solyc10G000984, and Solyc05G001746 were genes identified from the green module in the *S. dulcamara* network and were not found in the *S. lycopersicum* network due to the low level of expression not satisfying the threshold (1 < LFC and 0.05 > pval). These genes were strongly linked to Ca^{2+}-dependent protein kinase 1 (CDPK1) which have previously been associated with plant immunity and the promotion of signalling stress (Boudsocq, 2012). As the expression of these genes were so low in *S. lycopersicum* compared to *S. dulcamara*, further work should be conducted to increase the expression of Solyc10G001528, Solyc10G000984, and Solyc05G001746 with the hypothesis that up regulation of these genes will promote signalling and boost the plants immune response to stress.

The gene Solyc11G001222, a hub gene in the lightyellow module in the *S. dulcamara* network which, in the *S. lycopersicum* network, is found in the thistle2 module saw very different responses between species when infected and not infected with *R. solanacearum.* Where *S. dulcamara* saw an overall increase in expression when inoculated, *S. lycopersicum* only saw a rise towards 48 hours. This gene was linked to SINA1, an E3 ubiquitin ligase, known for causing post-translational changes to ubiquitin, which has been linked to the suppression of cell death and defence signalling (Wang, 2018). As *R. solanacearum* is a hemitrophic bacteria, the promotion of cell death is likely to inhibit *R.*

solanacearum, and as we see a decrease of Solyc11G001222 in infected *S. dulcamara*, cell death is likely to be less suppressed. To fully understand Solyc11G001222 and the impact it has on the proliferation of *R. solanacearum*, knocking out this gene and assessing the interaction between the mutant *S. lycopersicum* and *R. solanacearum* would be beneficial.

Finally, Solyc01G003106, the hub gene in the steelblue module in the *S. lycopersicum* network which is found in the grey60 module in the *S. dulcamara* network, is likely to be a putative peptide:N-glycanase (PNGase) (Joshi, 2005). This promotes deglycosylation which has been linked to fruit ripening, seed development and innate immunity (Hirayama, 2015; Strasser, 2014). When inoculated with *R. solanacearum*, both species changed but interestingly, *S. dulcamara* had a reduction in expression which could be a result of *S. dulcamara's* partial resistance, highlighting that there are still mechanisms that can be harnessed by *S. dulcamara* in its drive to complete resistance, but may be due to this link between fruit ripening and seed development. These two processes are likely to be unimportant when combating infection so may be downregulated when infected. Therefore, downregulating Solyc01G003106 in *S. lycopersicum* may improve resource allocation and aid resistance to *R. solanacearum*.

To conclude, further work would require in-planta inoculation of *R. solanacearum* with mutants containing: upregulated Solyc10G001528, Solyc10G000984 and Solyc05G001746; knocked out Solyc11G001222; and downregulated Solyc01G003106. Analysis of plants with single and multiple mutations may shed light on each gene's role in immunity, and the additive effect which gives *S. dulcamara* its quantitative resistance.

4.1.2 CANA

This work also used CANA which highlighted six taxa that were linked to *R. solanacearum* and 2,6-DHBA inoculation: *Aquicella, Gemmata, Phenylobacterium, Lactobacillaceae, Muribaculaceae,* and *Lachnospiraceae*. This analysis was conducted to shed light on whether this metabolite is both beneficial and marketable as protection from *R. solanacearum* in *S. lycopersicum*.

Aquicella (genus) was the hub taxon of the darkgrey module but has not been previously well explored. Therefore, the family, *Diplorickettsiaceae*, also referred to as *Rickettsiaceae*, was assessed, highlighting links to plant pathogens, including papaya bunchy top disease (Perlman, 2006). This module was positively correlated with disease but negatively correlated with 2,6-DHBA and as this hub taxon is linked to disease, 2,6-DHBA is likely to be providing protection against the disease-associated impact of this taxon.

The lightyellow module was initially thought to be linked to *R. solanacearum* proliferation but the hub taxa are *Gemmata* (genus) and *Phenylobacterium* (genus). *Gemmata* has rarely been linked to disease, and further investigations at higher taxonomic levels found them to be present in both inoculated and non-inoculated soil where they promoted the degradation of chemicals which are likely to aid plant growth (Peprah, 2025; Chang, 2023). The second hub taxon, *Phenylobacterium*, is linked to plant health by promoting nitrogen fixation (Yang, 2017). With both hub taxa linked to plant promotion, but this module being positively correlated to *R. solanacearum* inoculation and negatively correlated to 2,6-DHBA inoculation, it is likely that these taxa are forming a mutualistic relationship or being promoted by *R. solanacearum* which is creating ideal growing conditions. *R. solanacearum* infection has been previously linked to a reduction in ammonium nitrogen and total nitrogen in the soil (Wang, 2022). Certain nitrogen-fixing bacteria, such as *Rhizobium*, are more likely to thrive in low nitrogen conditions, while others, such as *Proteobacteria*, see a decline in abundance with nitrogen availability (Zahran, 1999; Wang, 2024). This is an example of how *R. solanacearum* may be influencing the surrounding soil microbiome, providing the ideal conditions for other bacteria even if they are not pathogenic. Further work identifying the impact *R. solanacearum* has on nutrient availability and conditions of the soil, and then how these conditions impact other soil borne microbes may shed light on potential mutualistic relationships.

The hub taxon for the steelblue module is *Lactobacillaceae* (family) which has been used previously for effective disease control (Gobbi, 2020). However, *Lactobacillaceae* produces lactic acid, reducing pH in the rhizosphere which is often linked to soil borne disease promotion (Zhang, et al., 2022). As this module is positively correlated with *R. solanacearum* inoculation and negatively correlated with 2,6-DHBA, it is expected that this hub taxon is linked to disease proliferation. This contradiction requires further analysis, involving: the inoculation of *Lactobacillaceae* into *S. lycopersicum's* rhizosphere while infected with *R. solanacearum*; and competition assays between *Lactobacillaceae* and *R. solanacearum.*

The saddlebrown and skyblue modules were both predicted to promote plant growth and reduce disease due to the positive correlation with 2,6-DHBA. Both modules had the same hub taxa: *Muribaculaceae* and *Lachnospiraceae*. *Muribaculaceae* has been found to promote plant growth by removing contaminants from the soil while *Lachnospiraceae* is often promoted in reductive soil disinfection (RSD) treatment (Gong, 2021; Huang, 2019). Both align with the prediction of plant growth promotion and disease reduction, but *Lachnospiraceae* has been found to reduce pH which is linked to disease proliferation (Zhang, et al., 2022). This would require similar further assessments as *Lactobacillaceae* to assess the influence of pH.

To conclude, all taxa identified would benefit from in-planta experiments, comparing: *R. solanacearum* infected soil; *R. solanacearum* and microbe infected soil; and non-inoculated soil. Additional competition assays would shed light on how these microbes interact with *R. solanacearum* which may aid the understanding of the interesting interactions, especially with *Lactobacillaceae* and *Lachnospiraceae*. However, from this work, we can conclude that 2,6-DHBA promotes a healthy microbiome by recruiting known beneficial microbes (*Muribaculaceae,* and *Lachnospiraceae*) and suppressing microbes linked to disease (*Diplorickettsiaceae Aquicella*).

4.2 Limitations

4.2.1 WGCNA limitations

It should be noted that *R. solanacearum* is a soil borne disease and a quarantine pathogen in the UK which meant gaining access to root RNA seq data unnecessarily increased risk of contamination from requiring excessive amounts of water to thoroughly clean the roots (Huet, 2014). Therefore, RNA seq data was collected from the leaves to reduce risk to the surrounding ecosystem. However, *R. solanacearum* has been found in leaves only hours after inoculation, making this method still appropriate to measure differences in immune response in plants (Tans-Kersten, 2001). This work did not find an immediate response but saw a slight delay in gene expression starting at around 6 hours, confirming that this is likely to be the case. Despite this reassurance, it would be beneficial to assess the RNA seq data from the roots but this is not a requirement as the leaf data was able to successfully identify candidate genes.

4.2.2 CANA limitations

The difficulty with soil abundance data is that the soil is a complex system which constantly changes. These fluctuations were mediated by using a PHCbi cabinet, limiting external influences but this does not completely isolate the relationships between 2,6-DHBA, *R. solanacearum* and *S. lycopersicum*. However, filtering of the data was conducted to reduce unusual occurrences, and only modules that were significantly and strongly correlated with traits of interest were kept for further analysis. Therefore, this method is likely to be effective at identifying species with links to the traits of interest, but robust filtering of the data and analysis of each species is required to validate the correlations found. Additional work should also consider the impact *R. solanacearum* and 2,6-DHBA has on the abundance of fungi. This is likely to shed light on even more microbial interactions, gaining a clearer indication of the interactions with the rhizosphere as a whole community. Furthermore, soil is

complex and there are many soil types all with different structures and microbiomes, so, it would be interesting to understand the influence of 2,6-DHBA across different soil types to see if its benefits persist.

4.2.3 Overall limitations

Networks have received mixed reviews, where praise for identifying correlations between complex communities and traits are met with scepticism due to unclear methods of analysing often complex outcomes. Therefore, work like this highlights both the adaptability of networks and how they can effectively narrow the search for candidates linked to specific traits of interest. As a network's influence may not always be clear after initial analysis, further work is often required to gain clarity which unfortunately was beyond the scope of this investigation due to time constraints. To further validate these findings, alternative networks, such as gene regulatory networks (GRN), may be beneficial to gain a deeper understanding of specific biochemical processes, bringing clarity to the often complex outcome of networks. GRNs incorporate transcriptomic and epigenomic data, providing key insight into gene expression and regulation by considering transcription factor binding sites and directional regulation (Higgs, 2023). This aids the identification of key genes as well as how their expression is controlled. WGCNA, however, is restricted to highlighting groups of genes with interesting expression patterns in relation to treatment while, GRN aims to understand why these genes highlighted in the WGCNA may be co-expressed, exploring the potential for regulatory influences (Higgs, 2023).

4.3 Conclusion

This project has successfully highlighted the diversity of network analysis which has emphasised the complexity of resistance to *R. solanacearum* infection, in particular, highlighting the importance of variation in genetic and microbial composition. This work has further highlighted that identifying a form of sustainable resistance requires the incorporation of multiple aspects. This can be time consuming but the use of both the WGCNA and CANA networks are an efficient way of streamlining the process of identifying selective candidates from an initially large data set. These processes can then be an affordable and relatively efficient way of identifying an abundance of potential resistance mechanisms, not just for *S. lycopersicum*, but for many species with close relatives that are resistant to harmful pathogens. This project in particular used network analysis to identify five genes which, when expression is modified, may protect *S. lycopersicum* against *R. solanacearum*, as well as identifying six key microbes, some of which are recruited by 2,6-DHBA and are likely to

be providing protection against *R. solanacearum*. This is, therefore, paving the way for potentially long term resistance to *R. solanacearum* for *S. lycopersicum*.

5. References

Artal, R. (2012). An efficient inoculation method to screen tomato, brinjal and chilli entries for bacterial wilt resistance. *Pest Management in Horticultural Ecosystems*, 18(1), pp.70–73.

Arwiyanto, T. (2017). Resistance Test of Several Tomato Varieties to Bacterial Wilt Diseases Caused by Ralstonia solanacearum Uji Ketahanan Beberapa Varietas Tomat terhadap Penyakit Layu Bakteri yang Disebabkan oleh Ralstonia solanacearum. *Jurnal Perlindungan Tanaman Indonesia,* 21(1), pp.51–53. doi:https://doi.org/10.22146/jpti.23171.

Ashida, H., Mimuro, H., Ogawa, M., Kobayashi, T., Sanada, T., Kim, M. and Sasakawa, C. (2011). Cell death and infection: A double-edged sword for host and pathogen survival. *The Journal of Cell Biology,* 195(6), pp.931–942. doi:https://doi.org/10.1083/jcb.201108081.

Aslam, M.N., Mukhtar, T., Hussain, M.A. and Raheel, M. (2017). Assessment of resistance to bacterial wilt incited by Ralstonia solanacearum in tomato germplasm. *Journal of Plant Diseases and Protection*, 124(6), pp.585–590. doi:https://doi.org/10.1007/s41348-017-0100-1.

Barberán, A., Bates, S.T., Casamayor, E.O. and Fierer, N. (2012). Using network analysis to explore co-occurrence patterns in soil microbial communities. *The ISME Journal*, 8(4), p.952.

Beneduzi, A., Ambrosini, A. and Passaglia, L.M.P. (2012). Plant growth-promoting rhizobacteria (PGPR): their potential as antagonists and biocontrol agents. *Genetics and Molecular Biology*, 35(4), pp.1044–1051. doi:https://doi.org/10.1590/s1415-47572012000600020.

Berger, S., Menudier, A., Julien, R. and Karamanos, Y. (1995). Do de-N-glycosylation enzymes have an important role in plant cells? *Biochimie*, 77(9), pp.751–760. doi:https://doi.org/10.1016/0300-9084(96)88193-4.

Berry, D. and Widder, S. (2014). Deciphering microbial interactions and detecting keystone species with co-occurrence networks. *Frontiers in Microbiology*, 5. doi:https://doi.org/10.3389/fmicb.2014.00219.

Bez, C., Esposito, A., Thuy, H.D., Hong, M.N., Valè, G., Licastro, D., Bertani, I., Piazza, S. and Venturi, V. (2021). The rice foot rot pathogen *Dickeya zeae* alters the in-field plant microbiome. *Environmental Microbiology*, 23(12), pp.7671–7687. doi:https://doi.org/10.1111/1462-2920.15726.

Bigeard, J., Colcombet, J. and Hirt, H. (2015). Signaling mechanisms in pattern-triggered immunity (PTI). *Molecular plant*, 8(4), pp.521–39. doi:https://doi.org/10.1016/j.molp.2014.12.022.

Boudsocq, M. and Sheen, J. (2012). CDPKs in immune and stress signaling. *Trends in Plant Science*, 18(1), pp.30–40. doi:https://doi.org/10.1016/j.tplants.2012.08.008.

Boyd, L.A., Ridout, C., O'Sullivan, D.M., Leach, J.E. and Leung, H. (2013). Plant–pathogen interactions: disease resistance in modern agriculture. *Trends in Genetics*, 29(4), pp.233–240. doi:https://doi.org/10.1016/j.tig.2012.10.011.

Brookbank, B.P., Patel, J., Gazzarrini, S. and Nambara, E. (2021). Role of Basal ABA in Plant Growth and Development. *Genes*, 12(12), p.1936. doi:https://doi.org/10.3390/genes12121936.

Brunson JC, Read QD (2023). "ggalluvial: Alluvial Plots in 'ggplot2'." R package version 0.12.5, http://corybrunson.github.io/ggalluvial/.

Buttimer, C., McAuliffe, O., Ross, R.P., Hill, C., O'Mahony, J. and Coffey, A. (2017). Bacteriophages and Bacterial Plant Diseases. Frontiers in Microbiology, 8(34). doi:https://doi.org/10.3389/fmicb.2017.00034.

Byth-Illing, H.-A. and Bornman, L. (2013). Heat shock, with recovery, promotes protection of Nicotiana tabacum during subsequent exposure to Ralstonia solanacearum. *Cell Stress and Chaperones*, 19(2), pp.193–203. doi:https://doi.org/10.1007/s12192-013-0445-8.

Caldwell, D., Kim, B.-S. and Iyer-Pascuzzi, A.S. (2017). Ralstonia solanacearum Differentially Colonizes Roots of Resistant and Susceptible Tomato Plants. *Phytopathology*, 107(5), pp.528–536. doi:https://doi.org/10.1094/phyto-09-16-0353-r.

Chang, J., Shen, F.-T., Lai, W.-A., Liao, C.-S. and Chen, W.-C. (2023). Co-exposure of dimethomorph and imidacloprid: effects on soil bacterial communities in vineyard soil. *Frontiers in microbiology*, 14. doi:https://doi.org/10.3389/fmicb.2023.1249167.

Chen, Y., Zhang, W.Z., Liu, X., Ma, Z.H., Li, B.o., Allen, C. et al (2010) A real-time PCR assay for the quantitative detection of *Ralstonia solanacearum* in the horticultural soil and plant tissues. *Journal of Microbiology and Biotechnology*, 20, 193–201.

Cheng, J.H.T., Bredow, M., Monaghan, J. and diCenzo, G.C. (2021). Proteobacteria Contain Diverse flg22 Epitopes That Elicit Varying Immune Responses in Arabidopsis thaliana. *Molecular plant-microbe interactions: MPMI*, 34(5), pp.504–510. doi:https://doi.org/10.1094/MPMI-11-20-0314-SC.

Dachineni, R., Kumar, D.R., Callegari, E., Kesharwani, S.S., Sankaranarayanan, R., Seefeldt, T., Tummala, H. and Bhat, G.J. (2017). Salicylic acid metabolites and derivatives inhibit CDK activity: Novel insights into aspirin's chemopreventive effects against colorectal cancer. *International Journal of Oncology*, 51(6), pp.1661–1673. doi:https://doi.org/10.3892/ijo.2017.4167.

Das, G. and Dhal, P.K. (2022). Salinity Influences Endophytic Bacterial Communities in Rice Roots from the Indian Sundarban Area. *Current Microbiology*, 79. doi:https://doi.org/10.1007/s00284-022-02936-z.

Davis, M.J., Ying, Z., Brunner, B.R., Pantoja, A. and Ferwerda, F.H. (1998). Rickettsial Relative Associated with Papaya Bunchy Top Disease. *Current Microbiology*, 36, pp.80–84. doi:https://doi.org/10.1007/s002849900283.

Diepold, A., Li, G., Lennarz, W.J., Thorsten Nürnberger and Brunner, F. (2007). The Arabidopsis *AtPNG1* gene encodes a peptide: *N*-glycanase. *The Plant Journal*, 52(1), pp.94–104. doi:https://doi.org/10.1111/j.1365-313x.2007.03215.x.

Dontoro Dekomah, S., Bi, Z., Dormatey, R., Wang, Y., Fasih Ullah Haider, Sun, C., Yao, P. and Bai, J. (2022). The role of CDPKs in plant development, nutrient and stress signaling. *Frontiers in Genetics*, 13. doi:https://doi.org/10.3389/fgene.2022.996203.

Doornbos, R.F., van Loon, L.C. and Bakker, P.A.H.M. (2011). Impact of root exudates and plant defense signaling on bacterial communities in the rhizosphere. A review. *Agronomy for Sustainable Development*, 32(1), pp.227–243. doi:https://doi.org/10.1007/s13593-011-0028-y.

Fernandez-Pozo, N., Menda, N., Edwards, J.D., Saha, S., Tecle, I.Y., Strickler, S.R., Bombarely, A., Fisher-York, T., Pujar, A., Foerster, H., Yan, A. and Mueller, L.A. (2014). *The Solanum lycopersicoides Genome Consortium*. [online] Solgenomics.net. Available at: https://solgenomics.net/organism/Solanum_lycopersicoides/genome.

Ferreira, V., Pianzzola, M.J., Vilaró, F.L., Galván, G.A., Tondo, M.L., Rodriguez, M.V., Orellano, E.G., Valls, M. and Siri, M.I. (2017). Interspecific Potato Breeding Lines Display Differential Colonization Patterns and Induced Defense Responses after Ralstonia solanacearum Infection. *Frontiers in Plant Science*, 8. doi:https://doi.org/10.3389/fpls.2017.01424.

Ficke, A., Cowger, C., Bergstrom, G. and Brodal, G. (2018). Understanding Yield Loss and Pathogen Biology to Improve Disease Management: Septoria Nodorum Blotch - A Case Study in Wheat. *Plant Disease*, 102(4), pp.696–707. doi:https://doi.org/10.1094/pdis-09-17-1375-fe.

Filion, M., Hamelin, R.C., Bernier, L. and St-Arnaud, M. (2004). Molecular Profiling of Rhizosphere Microbial Communities Associated with Healthy and Diseased Black Spruce (Picea mariana) Seedlings Grown in a Nursery. *Applied and Environmental Microbiology*, 70(6), pp.3541–3551. doi:https://doi.org/10.1128/aem.70.6.3541-3551.2004.

Franco Ortega S, James S, Gilbert L, Hogg K, Stevens H, Daff J, Friman VP, Harper AL. 2025. Assembly and annotation of *Solanum dulcamara* and *Solanum nigrum* plant genomes, two nightshades with contrasting susceptibilities to *Ralstonia solanacearum*. G3 Genes|Genomes|Genetics15: jkaf119.

Franco Ortega, in press.

Franco Ortega, S., James, S., Gilbert, L., Hogg, K., Stevens, H., Daff, J., Friman, V.-P. and Harper, A.L. (2025). Assembly and annotation of Solanum dulcamara and Solanum nigrum plant genomes, two nightshades with contrasting susceptibilities to Ralstonia solanacearum. *G3 Genes Genomes Genetics*, 15(7). doi:https://doi.org/10.1093/g3journal/jkaf119.

Frey, P., Prior, P., Marie, C., Kotoujansky, A., Trigalet-Demery, D. and Trigalet, A. (1994). Hrp- Mutants of Pseudomonas solanacearum as Potential Biocontrol Agents of Tomato

Bacterial Wilt. *Applied and Environmental Microbiology*, 60(9), pp.3175–3181. doi:https://doi.org/10.1128/aem.60.9.3175-3181.1994.

Fuentes, A., Asgher, S.A., Dong, J., Jeong, Y., Lee, M.H., Kim, T., Yoon, S. and Park, D.S. (2025). Comprehensive plant health monitoring: expert-level assessment with spatio-temporal image data. *Frontiers in Plant Science*, 16. doi:https://doi.org/10.3389/fpls.2025.1511651.

Galán, J.E. (1999). Type III Secretion Machines: Bacterial Devices for Protein Delivery into Host Cells. *Science*, 284(5418), pp.1322–1328. doi:https://doi.org/10.1126/science.284.5418.1322.

Gobbi, A., Kyrkou, I., Filippi, E., Ellegaard-Jensen, L. and Lars Hestbjerg Hansen (2020). Seasonal epiphytic microbial dynamics on grapevine leaves under biocontrol and copper fungicide treatments. *Scientific Reports*, 10. doi:https://doi.org/10.1038/s41598-019-56741-z.

Gonçalves, O.S., Fernandes, A.S., Tupy, S.M., Ferreira, T.G., Almeida, L.N., Creevey, C.J. and Santana, M.F. (2024). Insights into plant interactions and the biogeochemical role of the globally widespread Acidobacteriota phylum. *Soil biology and biochemistry*, 192. doi:https://doi.org/10.1016/j.soilbio.2024.109369.

Gong, W.-J., Niu, Z.-F., Wang, X.-R. and Zhao, H.-P. (2021). How the Soil Microbial Communities and Activities Respond to Long-Term Heavy Metal Contamination in Electroplating Contaminated Site. *Microorganisms*, 9(2), p.362. doi:https://doi.org/10.3390/microorganisms9020362.

Gu, Y., Banerjee, S., Dini-Andreote, F., Xu, Y., Shen, Q., Jousset, A. and Wei, Z. (2022). Article Navigation Journal Article Small changes in rhizosphere microbiome composition predict disease outcomes earlier than pathogen density variations. *Oxford Academic*, 16(10), pp.2448–2456.

Gu, Y., Wei, Z., Wang, X., Friman, V.-P., Huang, J., Wang, X., Mei, X., Xu, Y., Shen, Q. and Alexandre Jousset (2016). Pathogen invasion indirectly changes the composition of soil microbiome via shifts in root exudation profile. *Biology and Fertility of Soils*, 52(7), pp.997–1005. doi:https://doi.org/10.1007/s00374-016-1136-2.

Han, X., Shen, Y., Sun, L., Shen, J., Mao, Y., Fan, K., Wang, S., Ding, Z. and Wang, Y. (2025). Phyllospheric application of Bacillus mucilaginosus mediates the recovery of tea plants exposed to low-temperature stress by alteration of leaf endophytic community and plant physiology. *BMC Microbiology*, 25. doi:https://doi.org/10.1186/s12866-025-03880-1.

Hashmi, I., Bindschedler, S. and Junier, P. (2020). Chapter 18 - Firmicutes. *ScienceDirect*, pp.363–396.

Hegenauer, V., Furst, U., Kaiser, B., Smoker, M., Zipfel, C., Felix, G., Stahl, M. and Albert, M. (2016). Detection of the plant parasite *Cuscuta reflexa* by a tomato cell surface receptor. *Science*, 353(6298), pp.478–481. doi:https://doi.org/10.1126/science.aaf3919.

Hegenauer, V., Slaby, P., Körner, M., Bruckmüller, J.-A., Burggraf, R., Albert, I., Kaiser, B., Löffelhardt, B., Droste-Borel, I., Sklenar, J., Menke, F.L.H., Maček, B., Ranjan, A., Sinha, N.,

Nürnberger, T., Felix, G., Krause, K., Stahl, M. and Albert, M. (2020). The tomato receptor CuRe1 senses a cell wall protein to identify Cuscuta as a pathogen. *Nature Communications*, 11(1). doi:https://doi.org/10.1038/s41467-020-19147-4.

Hegenauer, V., Slaby, P., Körner, M., Bruckmüller, J.-A., Burggraf, R., Albert, I., Kaiser, B., Löffelhardt, B., Droste-Borel, I., Sklenar, J., Menke, F.L.H., Maček, B., Ranjan, A., Sinha, N., Nürnberger, T., Felix, G., Krause, K., Stahl, M. and Albert, M. (2020). The tomato receptor CuRe1 senses a cell wall protein to identify Cuscuta as a pathogen. *Nature Communications*, 11(1). doi:https://doi.org/10.1038/s41467-020-19147-4.

Higgs, M. (2023). How-to: Infer Gene Regulatory Networks from Omics Data - Front Line Genomics. Front Line Genomics.

Hirayama, H., Hosomi, A. and Suzuki, T. (2015). Physiological and molecular functions of the cytosolic peptide:N-glycanase. *Seminars in Cell & Developmental Biology*, 41, pp.110–120. doi:https://doi.org/10.1016/j.semcdb.2014.11.009.

Horvath, S. (2011). *Weighted Network Analysis: Applications in genomics and systems biology*. 2011th ed. USA: Springer.

Huang, X., Liu, L., Zhao, J., Zhang, J. and Cai, Z. (2019). The families Ruminococcaceae, Lachnospiraceae, and Clostridiaceae are the dominant bacterial groups during reductive soil disinfestation with incorporated plant residues. *Applied Soil Ecology*, 135, pp.65–72. doi:https://doi.org/10.1016/j.apsoil.2018.11.011.

Hueck, C.J. (1998). Type III Protein Secretion Systems in Bacterial Pathogens of Animals and Plants. *Microbiology and Molecular Biology Reviews*, 62(2), pp.379–433. doi:https://doi.org/10.1128/mmbr.62.2.379-433.1998.

Huet, G. (2014). Breeding for resistances to Ralstonia solanacearum. *Frontiers in Plant Science*, 5. doi:https://doi.org/10.3389/fpls.2014.00715.

Hug, L.A., Castelle, C.J., Wrighton, K.C., Thomas, B.C., Sharon, I., Frischkorn, K.R., Williams, K.H., Tringe, S.G. and Banfield, J.F. (2013). Community genomic analyses constrain the distribution of metabolic traits across the Chloroflexi phylum and indicate roles in sediment carbon cycling. *Microbiome*, 1. doi:https://doi.org/10.1186/2049-2618-1-22.

Ishihara, T., Mitsuhara, I., Takahashi, H. and Nakaho, K. (2012). Transcriptome Analysis of Quantitative Resistance-Specific Response upon Ralstonia solanacearum Infection in Tomato. *PLoS ONE*, 7(10). doi:https://doi.org/10.1371/journal.pone.0046763.

Jin, Z., Liu, S., Zhu, P., Tang, M., Wang, Y., Tian, Y., Li, D., Zhu, X., Yan, D. and Zhu, Z. (2019). Cross-Species Gene Expression Analysis Reveals Gene Modules Implicated in Human Osteosarcoma. *Frontiers in Genetics*, 10. doi:https://doi.org/10.3389/fgene.2019.00697.

Jin, Z., Liu, S., Zhu, P., Tang, M., Wang, Y., Tian, Y., Li, D., Zhu, X., Yan, D. and Zhu, Z. (2019). Cross-Species Gene Expression Analysis Reveals Gene Modules Implicated in Human Osteosarcoma. *Frontiers in Genetics*, 10. doi:https://doi.org/10.3389/fgene.2019.00697.

Joshi, S., Katiyar, S. and Lennarz, W.J. (2005). Misfolding of glycoproteins is a prerequisite for peptide: N-glycanase mediated deglycosylation. *FEBS Letters*, 579(3), pp.823–826. doi:https://doi.org/10.1016/j.febslet.2004.12.060.

Juurlink, B.H., Azouz, H.J., Aldalati, A.M., AlTinawi, B.M. and Ganguly, P. (2014). Hydroxybenzoic acid isomers and the cardiovascular system. *Nutrition Journal,* 13(63). doi:https://doi.org/10.1186/1475-2891-13-63.

Kersters, K., De Vos, P., Gillis, M., Swings, J., Vandamme, P., Stackebrandt, E. (2006). Introduction to the Proteobacteria. In: Dworkin, M., Falkow, S., Rosenberg, E., Schleifer, KH., Stackebrandt, E. (eds) The Prokaryotes. Springer, New York, NY. https://doi.org/10.1007/0-387-30745-1_1

Kielak, A.M., Cipriano, M.A.P. and Kuramae, E.E. (2016). Acidobacteria strains from subdivision 1 act as plant growth-promoting bacteria. *Archives of Microbiology*, 198(10), pp.987–993. doi:https://doi.org/10.1007/s00203-016-1260-2.

Kim, H.-J., Lee, H.J., Lim, B., Kim, E., Kim, H.-Y., Suh, M. and Hur, M. (2018). Lactobacillus terrae sp. nov., a novel species isolated from soil samples in the Republic of Korea. *INTERNATIONAL JOURNAL OF SYSTEMATIC AND EVOLUTIONARY MICROBIOLOGY*, 68(9). doi:https://doi.org/10.1099/ijsem.0.002918.

Kim, S., Hur, O.-S., Ro, N.-Y., Ko, H.-C., Rhee, J.-H., Sung, J.-S., Ryu, K.-Y., Lee, S.-Y. and Baek, H.-J. (2016). Evaluation of Resistance to Ralstonia solanacearum in Tomato Genetic Resources at Seedling Stage. *Plant Pathol J.*, 32(1), pp.58–64. doi:https://doi.org/10.5423/ppj.nt.06.2015.0121.

Köberl, M., Dita, M., Martinuz, A., Staver, C. and Berg, G. (2017). Members of Gammaproteobacteria as indicator species of healthy banana plants on Fusarium wilt-infested fields in Central America. *Scientific Reports*, 7. doi:https://doi.org/10.1038/srep45318.

Kuhn, Max (2008). “Building Predictive Models in R Using the caret Package.” *Journal of Statistical Software*, **28**(5), 1–26. doi:10.18637/jss.v028.i05, https://www.jstatsoft.org/index.php/jss/article/view/v028i05.

Kulichevskaya, I.S., Ivanova, A.A., Baulina, O.I., Rijpstra, I.C., Sinninghe Damsté, J.S. and Dedysh, S.N. (2017). Fimbriiglobus ruber gen. nov., sp. nov., a Gemmata-like planctomycete from Sphagnum peat bog and the proposal of Gemmataceae fam. nov. *INTERNATIONAL JOURNAL OF SYSTEMATIC AND EVOLUTIONARY MICROBIOLOGY*, 67(2). doi:https://doi.org/10.1099/ijsem.0.001598.

Kumar, N. and Shahid Mukhtar, M. (2023). Ranking Plant Network Nodes Based on Their Centrality Measures. *Entropy*, 25(4), pp.676–676. doi:https://doi.org/10.3390/e25040676.

Kwak, M.-J., Kong, H.G., Choi, K., Kwon, S.-K., Song, J.Y., Lee, J., Lee, P.A., Choi, S.Y., Seo, M., Lee, H.J., Jung, E.J., Park, H., Roy, N., Kim, H., Lee, M.M., Rubin, E.M., Lee, S.-W. and Kim, J.F. (2018). Rhizosphere microbiome structure alters to enable wilt resistance in tomato. *Nature Biotechnology*, 36(11), pp.1100–1109. doi:https://doi.org/10.1038/nbt.4232.

Lambert, D.H. and Loria, R. (1989). Streptomyces scabies sp. nov., nom. rev. *International journal of systematic bacteriology*, 39(4). doi:https://doi.org/10.1099/00207713-39-4-387.

Langfelder P, Horvath S (2008). “WGCNA: an R package for weighted correlation network analysis.” *BMC Bioinformatics*, 559. https://bmcbioinformatics.biomedcentral.com/articles/10.1186/1471-2105-9-559.

Langfelder, P., Horvath S. (2012). Fast R Functions for Robust Correlations and Hierarchical Clustering. Journal of Statistical Software, 46(11), 1-17. URL http://www.jstatsoft.org/v46/i11/.

Langfelder, P., Luo, R., Oldham, M.C. and Horvath, S. (2011). Is My Network Module Preserved and Reproducible? *PLoS Computational Biology*, 7(1), p.e1001057. doi:https://doi.org/10.1371/journal.pcbi.1001057.

Lebeau, A., Gouy, M., Daunay, M.C., Wicker, E., Chiroleu, F., Prior, P., Frary, A. and Dintinger, J. (2012). Genetic mapping of a major dominant gene for resistance to Ralstonia solanacearum in eggplant. *Theoretical and Applied Genetics*, 126, pp.143–158. doi:https://doi.org/10.1007/s00122-012-1969-5.

Lee, S.-M., Kong, H.G., Song, G.C. and Ryu, C.-M. (2021). Disruption of Firmicutes and Actinobacteria abundance in tomato rhizosphere causes the incidence of bacterial wilt disease. *The ISME Journal*, 15(1), pp.330–347. doi:https://doi.org/10.1038/s41396-020-00785-x.

Li, J., Yang, H., Duan, Y.Y., Dan Sun, X., Pang, X.P. and Guo, Z.G. (2024). Fungi contribute more than bacteria to the ecological uniqueness of soil microbial communities in alpine meadows. *Global Ecology and Conservation*, 55. doi:https://doi.org/10.1016/j.gecco.2024.e03246.

Li, S., Wu, P., Yu, X., Cao, J., Chen, X., Gao, L., Chen, K. and Grierson, D. (2022). Contrasting Roles of Ethylene Response Factors in Pathogen Response and Ripening in Fleshy Fruit. *Cells*, 11(16), p.2484. doi:https://doi.org/10.3390/cells11162484.

Lingens, F., Blecher, R., Blecher, H., Blobel, F., Eberspächer, J., Fröhner, C., Görisch, H., Görisch, H. and Layh, G. (1985). Phenylobacterium immobile gen. nov., sp. nov., a Gram-Negative Bacterium That Degrades the Herbicide Chloridazon. *International journal of systematic bacteriology*, 35(1). doi:https://doi.org/10.1099/00207713-35-1-26.

Liu, C., Li, C., Jiang, Y., Zeng, R.J., Yao, M. and Li, X. (2023). A guide for comparing microbial co-occurrence networks. *iMeta*, 2(1). doi:https://doi.org/10.1002/imt2.71.

Liu, Y., Gu, H.-Y., Zhu, J., Niu, Y.-M., Zhang, C. and Guo, G.-L. (2019). Identification of Hub Genes and Key Pathways Associated With Bipolar Disorder Based on Weighted Gene Co-expression Network Analysis. *Frontiers in Physiology*, 10. doi:https://doi.org/10.3389/fphys.2019.01081.

Love MI, Huber W, Anders S (2014). “Moderated estimation of fold change and dispersion for RNA-seq data with DESeq2.” *Genome Biology*, **15**, 550. doi:10.1186/s13059-014-0550-8.

Lund, B.M., Brocklehurst, T.F. and Wyatt, G.M. (1981). Characterization of Strains of Clostridium puniceum sp.no v., a Pink-pigmented, Pectolytic Bacterium. *Microbiology*, 122(1), pp.17–26. doi:https://doi.org/10.1099/00221287-122-1-17.

Luo, D., Zhang, X., Li, X.-K. and Chen, G. (2021). Identification of Key Functional Modules and Immunomodulatory Regulators of Hepatocellular Carcinoma. *Journal of Immunology Research*, 2021(1), pp.1–21. doi:https://doi.org/10.1155/2021/1801873.

Martin, H., Rogers, L.A., Moushtaq, L., Brindley, A.A., Forbes, P., Quintion, A.R., Murphy, A.R.J., Hipperson, H., Daniell, T.J., Ndeh, D., Amsbury, S., Hitchcock, A. and Ian (2025). Metabolism of hemicelluloses by root-associated *Bacteroidota* species. *The ISME Journal*, 19(1). doi:https://doi.org/10.1093/ismejo/wraf022.

Meng, H.-L., Sun, P.-Y., Wang, J.-R., Sun, X.-Q., Zheng, C.-Z., Fan, T., Chen, Q.-F. and Li, H.-Y. (2022). Comparative physiological, transcriptomic, and WGCNA analyses reveal the key genes and regulatory pathways associated with drought tolerance in Tartary buckwheat. *Frontiers in plant science*, 13. doi:https://doi.org/10.3389/fpls.2022.985088.

Micheli, F. (2001). Pectin methylesterases: cell wall enzymes with important roles in plant physiology. *Trends in Plant Science*, 6(9), pp.414–419. doi:https://doi.org/10.1016/s1360-1385(01)02045-3.

Milling, A., Babujee, L. and Allen, C. (2011). Ralstonia solanacearum Extracellular Polysaccharide Is a Specific Elicitor of Defense Responses in Wilt-Resistant Tomato Plants. *PLoS ONE*, 6(1), p.e15853. doi:https://doi.org/10.1371/journal.pone.0015853.

Mishek, H.P., Stock, S.A., Florick, J.D.E., Blomberg, W.R. and Franke, J.D. (2018). Development of a chemically-defined minimal medium for studies on growth and protein uptake of Gemmata obscuriglobus. *Journal of Microbiological Methods*, 145, pp.40–46. doi:https://doi.org/10.1016/j.mimet.2017.12.010.

Nakaho, K. (1997). Distribution and Multiplication of Ralstonia solanacearum in Stem-inoculatedTomato Rootstock Cultivar LS-89 Resistant to Bacterial Wilt. *Japanese Journal of Phytopathology*, 63(4), pp.341–344. doi:https://doi.org/10.3186/jjphytopath.63.341.

Narancio, R., Zorrilla, P., Robello, C., Gonzalez, M., Vilaró, F., Pritsch, C. and Dalla Rizza, M. (2013). Insights on gene expression response of a characterized resistant genotype of Solanum commersonii Dun. against Ralstonia solanacearum. *European Journal of Plant Pathology*, 136(4), pp.823–835. doi:https://doi.org/10.1007/s10658-013-0210-y.

Olanrewaju, O.S., Ayangbenro, A.S., Glick, B.R. and Babalola, O.O. (2018). Plant health: feedback effect of root exudates-rhizobiome interactions. *Applied Microbiology and Biotechnology*, 103, pp.1155–1166. doi:https://doi.org/10.1007/s00253-018-9556-6.

Orellana, D., Machuca, D., Ibeas, M.A., Estevez, J.M. and Poupin, M.J. (2022). Plant-growth promotion by proteobacterial strains depends on the availability of phosphorus and iron in Arabidopsis thaliana plants. *Frontiers in Microbiology*, 13. doi:https://doi.org/10.3389/fmicb.2022.1083270.

Park, J.K., Chang, D.-H., Rhee, M.-S., Jeong, H., Song, J., Ku, B.J., Kim, S.B., Lee, M. and Kim, B.-C. (2021). Heminiphilus faecis gen. nov., sp. nov., a member of the family Muribaculaceae, isolated from mouse faeces and emended description of the genus Muribaculum. *Antonie van Leeuwenhoek*, 114, pp.275–286. doi:https://doi.org/10.1007/s10482-021-01521-x.

Pascale, A., Proietti, S., Pantelides, I.S. and Stringlis, I.A. (2020). Modulation of the Root Microbiome by Plant Molecules: The Basis for Targeted Disease Suppression and Plant Growth Promotion. *Frontiers in Plant Science*, 10. doi:https://doi.org/10.3389/fpls.2019.01741.

Peprah, S., Addo-Fordjour, P., Fei-Baffoe, B., Boampong, K., Avicor, S.W. and Damsere-Derry, J. (2025). Effects of pesticide application on soil bacteria community structure in a cabbage-based agroecosystem in Ghana. *PLoS ONE*, 20(5), pp.e0323936–e0323936. doi:https://doi.org/10.1371/journal.pone.0323936.

Perlman, S.J., Hunter, M.S. and Zchori-Fein, E. (2006). The emerging diversity of Rickettsia. *Proceedings of the Royal Society B*, 273(1598). doi:https://doi.org/10.1098/rspb.2006.3541.

Persson, P. (2008). Successful eradication of Ralstonia solanacearum from Sweden. *EPPO Bulletin*, 28(1-2). doi:https://doi.org/10.1111/j.1365-2338.1998.tb00713.x.

Pickart, C.M. and Eddins, M.J. (2004). Ubiquitin: structures, functions, mechanisms. *Biochimica et Biophysica Acta (BBA) - Molecular Cell Research*, 1695(1-3), pp.55–72. doi:https://doi.org/10.1016/j.bbamcr.2004.09.019.

Porteous, L.A. and Armstrong, J.L. (1991) Recovery of bulk DNA from soil by a rapid, small-scale extraction method. Current Microbiology 22: 345–348.

Prashar, P., Kapoor, N. and Sachdeva, S. (2013). Rhizosphere: its structure, bacterial diversity and significance. *Reviews in Environmental Science and Bio/Technology*, 13, pp.63–77. doi:https://doi.org/10.1007/s11157-013-9317-z.

Qi, F. and Zhang, F. (2020). Cell Cycle Regulation in the Plant Response to Stress. *Frontiers in Plant Science*, 10. doi:https://doi.org/10.3389/fpls.2019.01765.

R Core Team (2024). _R: A Language and Environment for Statistical Computing_. R Foundation for Statistical Computing, Vienna, Austria. <https://www.R-project.org/>.

Rizzatti, G., Lopetuso, L.R., Gibiino, G., Binda, C. and Gasbarrini, A. (2017). Proteobacteria: a Common Factor in Human Diseases. *BioMed Research International*, 2017, pp.1–7. doi:https://doi.org/10.1155/2017/9351507.

Roche, J., Guérin, C., Dupuits, C., Elmodafar, C., Goupil, P. and Mouzeyar, S. (2023). In silico analysis of the Seven IN Absentia (SINA) genes in bread wheat sheds light on their structure in plants. *PloS one*, 18(12), p.e0295021. doi:https://doi.org/10.1371/journal.pone.0295021.

Santos, P., Pinhal, I., Rainey, F.A., Empadinhas, N., Costa, J., Fields, B., Benson, R., VeríssimoA. and Milton (2003). Gamma-Proteobacteria Aquicella lusitana gen. nov., sp.

nov., and Aquicella siphonis sp. nov. Infect Protozoa and Require Activated Charcoal for Growth in Laboratory Media. *Applied and Environmental Microbiology*, 69(11), pp.6533–6540. doi:https://doi.org/10.1128/aem.69.11.6533-6540.2003.

Santoso, S.P., Ismadji, S., Angkawijaya, A.E., Soetaredjo, F.E., Go, A.W. and Ju, Y.H. (2016). Complexes of 2,6-dihydroxybenzoic acid with divalent metal ions: Synthesis, crystal structure, spectral studies, and biological activity enhancement. *Journal of Molecular Liquids*, 221, pp.617–623. doi:https://doi.org/10.1016/j.molliq.2016.06.015.

Scherlach, K. and Hertweck, C. (2017). Mediators of mutualistic microbe–microbe interactions. *Natural Product Reports*, 35(4), pp.303–308. doi:https://doi.org/10.1039/c7np00035a.

Sebastià, P., de Pedro-Jové, R., Daubech, B., Kashyap, A., Coll, N.S. and Valls, M. (2021). The Bacterial Wilt Reservoir Host Solanum dulcamara Shows Resistance to Ralstonia solanacearum Infection. *Frontiers in Plant Science*, 12. doi:https://doi.org/10.3389/fpls.2021.755708.

Seo, H., Kim, J.H., Lee, S.-M. and Lee, S.-W. (2024). The Plant-Associated Flavobacterium: A Hidden Helper for Improving Plant Health. *The Plant Pathology Journal*, 40(3), pp.251–260. doi:https://doi.org/10.5423/ppj.rw.01.2024.0019.

Seong, C.N., Kang, J.W., Lee, J.H., Seo, S.Y., Woo, J.J., Park, C., Bae, K.S. and Kim, M.S. (2018). Taxonomic hierarchy of the phylum Firmicutes and novel Firmicutes species originated from various environments in Korea. *Journal of Microbiology (Seoul, Korea)*, 56(1), pp.1–10. doi:https://doi.org/10.1007/s12275-018-7318-x.

Serin, E.A.R., Nijveen, H., Hilhorst, H.W.M. and Ligterink, W. (2016). Learning from Co-expression Networks: Possibilities and Challenges. *Frontiers in Plant Science*, 7. doi:https://doi.org/10.3389/fpls.2016.00444.

Shi, H., Liu, Y., Ding, A., Wang, W. and Sun, Y. (2023). Induced defense strategies of plants against Ralstonia solanacearum. *Frontiers in Microbiology*, 14, p.1059799. doi:https://doi.org/10.3389/fmicb.2023.1059799.

Stephens M, Carbonetto P, Gerard D, Lu M, Sun L, Willwerscheid J, Xiao N (2023). _ashr: Methods for Adaptive Shrinkage, using Empirical Bayes_. R package version 2.2-63, <https://CRAN.R-project.org/package=ashr>.

Strasser, R. (2014). Biological significance of complex N-glycans in plants and their impact on plant physiology. *Frontiers in Plant Science*, 5. doi:https://doi.org/10.3389/fpls.2014.00363.

Sun, H., Jiang, S., Jiang, C., Wu, C., Gao, M. and Wang, Q. (2021). A review of root exudates and rhizosphere microbiome for crop production. *Environmental Science and Pollution Research*, 28, pp.54497–54510. doi:https://doi.org/10.1007/s11356-021-15838-7.

Suzuki, T., Huang, C. and Haruhiko Fujihira (2017). The cytoplasmic peptide:N-glycanase (NGLY1) — Structure, expression and cellular functions. *Gene*, 577(1), pp.1–7. doi:https://doi.org/10.1016/j.gene.2015.11.021.

Tans-Kersten, J., Huang, H. and Allen, C. (2001). Ralstonia solanacearum Needs Motility for Invasive Virulence on Tomato. *Journal of Bacteriology*, 183(12), pp.3597–3605. doi:https://doi.org/10.1128/jb.183.12.3597-3605.2001.

Tien, C.C., Chao, C.C., and Chao, W.L. (1999) Methods for DNA extraction from various soils: a comparison. J Appl Microbiol 86: 937–943.

Tominello-Ramirez, C.S., Hoyos, L.M., Oubounyt, M. and Stam, R. (2024). Network analyses predict major regulators of resistance to early blight disease complex in tomato. *BMC Plant Biology*, 24. doi:https://doi.org/10.1186/s12870-024-05366-0.

Vailleau, F., Sartorel, E., Jardinaud, M.-F., Chardon, F., Genin, S., Huguet, T., Gentzbittel, L. and Petitprez, M. (2007). Characterization of the interaction between the bacterial wilt pathogen Ralstonia solanacearum and the model legume plant Medicago truncatula. *Molecular plant-microbe interactions: MPMI*, 20(2), pp.159–167. doi:https://doi.org/10.1094/MPMI-20-2-0159.

van Elsas, J.D., Chiurazzi, M., Mallon, C.A., Elhottova, D., Kristufek, V. and Salles, J.F. (2012). Microbial diversity determines the invasion of soil by a bacterial pathogen. *Proceedings of the National Academy of Sciences*, 109(4), pp.1159–1164. doi:https://doi.org/10.1073/pnas.1109326109.

Walter, J. and O'Toole, P.W. (2023). Microbe Profile: The Lactobacillaceae. *Microbiology*, 169(12). doi:https://doi.org/10.1099/mic.0.001414.

Wang, H., Wu, C., Zhang, H., Xiao, M., Ge, T., Zhou, Z., Liu, Y., Peng, S., Peng, P. and Chen, J. (2022). Characterization of the belowground microbial community and co-occurrence networks of tobacco plants infected with bacterial wilt disease. *World Journal of Microbiology and Biotechnology,* 38(155). doi:https://doi.org/10.1007/s11274-022-03347-9.

Wang, H., Wu, C., Zhang, H., Xiao, M., Ge, T., Zhou, Z., Liu, Y., Peng, S., Peng, P. and Chen, J. (2022). Characterization of the belowground microbial community and co-occurrence networks of tobacco plants infected with bacterial wilt disease. *World Journal of Microbiology and Biotechnology,* 38(155). doi:https://doi.org/10.1007/s11274-022-03347-9.

Wang, J., Jenkins, C., Webb, R.I. and Fuerst, J.A. (2002). Isolation of Gemmata-Like and Isosphaera-Like Planctomycete Bacteria from Soil and Freshwater. *Applied and environmental microbiology*, 68(1), pp.417–422. doi:https://doi.org/10.1128/aem.68.1.417-422.2002.

Wang, J., Xie, R., He, N., Wang, W., Wang, G., Yang, Y., Hu, Q., Zhao, H. and Qian, X. (2023). Five years nitrogen reduction management shifted soil bacterial community structure and function in high-yielding 'super' rice cultivation. *Agriculture, Ecosystems & Environment*, 360, p.108773. doi:https://doi.org/10.1016/j.agee.2023.108773.

Wang, J., Zhang, Y., Pan, X., Du, J., Ma, L. and Guo, X. (2019). Discovery of leaf region and time point related modules and genes in maize (Zea mays L.) leaves by Weighted Gene Co-expression Network analysis (WGCNA) of gene expression profiles of carbon metabolism.

Journal of Integrative Agriculture, 18(2), pp.350–360. doi:https://doi.org/10.1016/S2095-3119(18)62029-5.

Wang, J.-P., Xu, Y.-P., Munyampundu, J.-P., Liu, T.-Y. and Cai, X.-Z. (2015). Calcium-dependent protein kinase (CDPK) and CDPK-related kinase (CRK) gene families in tomato: genome-wide identification and functional analyses in disease resistance. *Molecular Genetics and Genomics*, 291(2), pp.661–676. doi:https://doi.org/10.1007/s00438-015-1137-0.

Wang, T., Liu, S., Ke, Y., Ali, S., Wang, R., Hong, T., Liu, Z., Ma, G., Lan, T.-H., Wang, F., Zhu, M.X., Huang, Y. and Zhou, Y. (2025). Repurposing salicylic acid as a versatile inducer of proximity. *Nature Chemical Biology.* doi:https://doi.org/10.1038/s41589-025-01918-z.

Wang, W., Fan, Y., Niu, X., Miao, M., Kud, J., Zhou, B., Zeng, L., Liu, Y. and Xiao, F. (2018). Functional analysis of the seven in absentia ubiquitin ligase family in tomato. *Plant, cell & environment*, 41(3), pp.689–703. doi:https://doi.org/10.1111/pce.13140.

Wang, X., Chi, Y. and Song, S. (2024). Important soil microbiota's effects on plants and soils: a comprehensive 30-year systematic literature review. *Frontiers in Microbiology*, 15. doi:https://doi.org/10.3389/fmicb.2024.1347745.

Wang, Z., Zhang, Y., Bo, G., Zhang, Y., Chen, Y., Shen, M., Zhang, P., Li, G., Zhou, J., Li, Z. and Yang, J. (2022). Ralstonia solanacearum Infection Disturbed the Microbiome Structure Throughout the Whole Tobacco Crop Niche as Well as the Nitrogen Metabolism in Soil. *Frontiers in Bioengineering and Biotechnology*, 10. doi:https://doi.org/10.3389/fbioe.2022.903555.

Wenneker, M., Verdel, M.S.W., Groeneveld, R.M.W., Kempenaar, C., van Beuningen, A.R. and Janse, J.D. (1999). Ralstonia (Pseudomonas) solanacearum Race 3 (Biovar 2) in Surface Water and Natural Weed Hosts: First Report on Stinging Nettle (Urtica dioica). *European Journal of Plant Pathology*, 105(3), pp.307–315. doi:https://doi.org/10.1023/a:1008795417575.

Wickham H, François R, Henry L, Müller K, Vaughan D (2023). _dplyr: A Grammar of Data Manipulation_. R package version 1.1.4, <https://CRAN.R-project.org/package=dplyr>.

Wickham H, Vaughan D, Girlich M (2024). _tidyr: Tidy Messy Data_. R package version 1.3.1, <https://CRAN.R-project.org/package=tidyr>.

Wickham, H. ggplot2: Elegant Graphics for Data Analysis. Springer-Verlag New York, 2016.

Wildermuth, M.C., Dewdney, J., Wu, G. and Ausubel, F.M. (2001). Isochorismate synthase is required to synthesize salicylic acid for plant defence. *Nature*, 414, pp.562–565. doi:https://doi.org/10.1038/35107108.

Wing, I.S., De Cian, E. and Mistry, M.N. (2021). Global Vulnerability of Crop Yields to Climate Change. *Journal of Environmental Economics and Management*, 109. doi:https://doi.org/10.1016/j.jeem.2021.102462.

Xue, B., Zhou, Y., Xie, Y., Huang, X., Zhang, J., Zhang, Y., Zhong, W., Zhao, J., Zheng, D. and Ruan, L. (2025). A Ralstonia solanacearum effector regulates plant cell death by disrupting the homeostasis of the BPA1-ACD11 complex. *PMC*. doi:https://doi.org/10.1128/mbio.03665-24.

Xue, D., Wu, W. and Kong, D. (2025). Strategies utilized by plants to defend against Ralstonia solanacearum. *Frontiers in Plant Science*, 16. doi:https://doi.org/10.3389/fpls.2025.1510177.

Yan L (2025). ggvenn: Draw Venn Diagram by 'ggplot2'. R package version 0.1.19, https://github.com/yanlinlin82/ggvenn.

Yang, B., Zheng, M., Dong, W., Xu, P., Zheng, Y., Yang, W., Luo, Y., Guo, J., Niu, D., Yu, Y. and Jiang, C. (2023). Plant Disease Resistance-Related Pathways Recruit Beneficial Bacteria by Remodeling Root Exudates upon Bacillus cereus AR156 Treatment. *Microbiology Spectrum*, 11(2). doi:https://doi.org/10.1128/spectrum.03611-22.

Yang, X., Yuan, R., Yang, S., Dai, Z., Di, N., Yang, H., He, Z. and Wei, M. (2024). A salt-tolerant growth-promoting phyllosphere microbial combination from mangrove plants and its mechanism for promoting salt tolerance in rice. *Microbiome*, 12, 270. doi:https://doi.org/10.1186/s40168-024-01969-9.

Yang, Y., Wang, N., Guo, X., Zhang, Y. and Ye, B. (2017). Comparative analysis of bacterial community structure in the rhizosphere of maize by high-throughput pyrosequencing. *PLOS ONE*, 12(5). doi:https://doi.org/10.1371/journal.pone.0178425.

Yu, K., Pieterse, C.M.J., Bakker, P.A.H.M. and Berendsen, R.L. (2019). Beneficial microbes going underground of root immunity. *Plant, Cell & Environment,* 42(10), pp.2860–2870. doi:https://doi.org/10.1111/pce.13632.

Zahran, H.H. (1999). Rhizobium-Legume Symbiosis and Nitrogen Fixation under Severe Conditions and in an Arid Climate. *Microbiology and Molecular Biology Reviews*, 63(4), pp.968–989. doi:https://doi.org/10.1128/mmbr.63.4.968-989.1999.

Zaplana, T., Miele, S. and Tolonen, A.C. (2024). Lachnospiraceae are emerging industrial biocatalysts and biotherapeutics. *Frontiers in bioengineering and biotechnology*, 11. doi:https://doi.org/10.3389/fbioe.2023.1324396.

Zeng, F., Shi, M., Xiao, H. and Chi, X. (2021). WGCNA-Based Identification of Hub Genes and Key Pathways Involved in Nonalcoholic Fatty Liver Disease. BioMed Research International, 2021, pp.1–16. doi:https://doi.org/10.1155/2021/5633211.

Zhang, S., Liu, X., Zhou, L., Deng, L., Zhao, W., Liu, Y. and Ding, W. (2022). Alleviating Soil Acidification Could Increase Disease Suppression of Bacterial Wilt by Recruiting Potentially Beneficial Rhizobacteria. *Microbiology Spectrum*, 10(2). doi:https://doi.org/10.1128/spectrum.02333-21.

Zhang, W., Planas-Marquès, M., Liang, M., Zhang, Q., Vermeulen, A., Kaschani, F., Kaiser, M., Takken, F.L.W., Coll, N.S. and Valls, M. (2025). The CAPE1 peptide confers resistance against bacterial wilt in tomato. *PubMed*. doi:https://doi.org/10.1093/jxb/eraf145.

Zhang, Y., Ye, C., Su, Y., Peng, W., Lu, R., Liu, Y., Huang, H., He, X., Yang, M. and Zhu, S. (2022b). Soil Acidification caused by excessive application of nitrogen fertilizer aggravates soil-borne diseases: Evidence from literature review and field trials. *Agriculture, Ecosystems & Environment*, 340, p.108176. doi:https://doi.org/10.1016/j.agee.2022.108176.

Zhou Y, Zhang Z, Bao Z, Li H, Lyu Y, Zan Y, Wu Y, Cheng L, Fang Y, Wu K, et al. 2022. Graph pangenome captures missing heritability and empowers tomato breeding. Nature 2022 606:7914 606: 527–534.

Zhu, B., Zhang, Y., Gao, R., Wu, Z., Zhang, W., Zhang, C., Zhang, P., Ye, C., Yao, L., Jin, Y., Mao, H., Tou, P., Huang, P., Zhao, J., Zhao, Q., Liu, C.-J. and Zhang, K. (2025). Complete biosynthesis of salicylic acid from phenylalanine in plants. *Nature*. doi:https://doi.org/10.1038/s41586-025-09175-9.

Zhu, Y., Chen, B., Zhang, X., Akbar, M.T., Wu, T., Zhang, Y., Zhi, L. and Shen, Q. (2024). Exploration of the Muribaculaceae Family in the Gut Microbiota: Diversity, Metabolism, and Function. *Nutrients*, 16(16). doi:https://doi.org/10.3390/nu16162660.

Zitnik, M., Li, M.M., Wells, A., Glass, K., Gysi, D.M., Krishnan, A., Murali, T.M., Radivojac, P., Roy, S., Baudot, A., Bozdag, S., Chen, D.Z., Cowen, L., Devkota, K., Gitter, A., Gosline, S.J.C., Gu, P., Guzzi, P.H., Huang, H. and Jiang, M. (2024). Current and future directions in network biology. *Bioimage Informatics*, 4(1). doi:https://doi.org/10.1093/bioadv/vbae099.

Zito, A. (2025). WGCNA Tutorial: How It Works, Limitations, and Tools. [online] BigOmics Analytics. Available at: https://bigomics.ch/blog/introduction-to-wgcna-and-its-applications-in-gene-correlation-network-analysis/.

6. Supplementary Material

S.2 Supplementary Material for Chapter 2

Differentially Expressed Genes (DEGs) at 6 hours

Solyc06G001841	Solyc10G000360	Solyc10G002698	Solyc10G002353	Solyc07G002228
Solyc02G002397	Solyc05G002368	Solyc03G003194	Solyc02G001853	Solyc06G002005
Solyc02G001708	Solyc01G004357	Solyc05G002509	Solyc03G002929	Solyc11G001449
Solyc01G002746	Solyc05G000607	Solyc08G001752	Solyc04G001005	Solyc07G001834
Solyc01G002578	Solyc02G002655	Solyc11G000455	Solyc09G002280	Solyc07G001400
Solyc04G002701	Solyc01G003383	Solyc02G000953	Solyc07G000066	Solyc02G002858
Solyc01G002262	Solyc07G001989	Solyc12G002350	Solyc01G002452	Solyc01G003287
Solyc03G001337	Solyc11G001063	Solyc08G000999	Solyc09G002739	Solyc06G001288
Solyc08G000228	Solyc04G001551	Solyc02G001268	Solyc12G002523	Solyc09G001224
Solyc08G000405	Solyc02G001461	Solyc01G004131	Solyc11G000334	Solyc06G002317
Solyc10G000547	Solyc07G000006	Solyc01G004156	Solyc11G002430	Solyc09G001962
Solyc01G002803	Solyc12G000530	Solyc08G002155	Solyc03G003106	Solyc07G002372

Solyc09G001322 Solyc01G001365 Solyc02G001050 Solyc12G001805 Solyc01G002357

Solyc03G000089 Solyc06G001327 Solyc04G002642 Solyc05G001281

Solyc03G002291 Solyc01G002087 Solyc07G002021 Solyc10G000471

Solyc09G000092 Solyc11G000040 Solyc05G002744 Solyc01G000487

Solyc06G000003 Solyc09G001996 Solyc04G002376 Solyc11G001721

Differentially Expressed Genes (DEGs) at 12 hours

Solyc06G001863 Solyc07G002544 Solyc01G003389 Solyc06G001246 Solyc06G000767

Solyc04G001521 Solyc04G002140 Solyc01G003388 Solyc11G001730 Solyc06G000757

Solyc06G000210 Solyc08G001590 Solyc03G002547 Solyc08G000116 Solyc08G001438

Solyc03G002171 Solyc06G001565 Solyc01G002965 Solyc04G002482 Solyc09G000002

Solyc07G002016 Solyc12G000725 Solyc01G002963 Solyc01G003554 Solyc06G000506

Solyc01G000246 Solyc12G000719 Solyc01G002955 Solyc12G002718 Solyc09G001968

Solyc01G000234 Solyc04G001966 Solyc09G001789 Solyc09G000228 Solyc12G002378

Solyc01G001668 Solyc12G001039 Solyc05G002689 Solyc09G001938 Solyc09G000744

Solyc07G002819 Solyc04G000645 Solyc01G001936 Solyc07G000460 Solyc02G002150

Solyc07G002806	Solyc04G000321	Solyc12G000617	Solyc07G000461	Solyc02G002124
Solyc07G002795	Solyc08G001583	Solyc11G002513	Solyc12G002850	Solyc08G000939
Solyc07G002794	Solyc04G000210	Solyc06G002337	Solyc03G000041	Solyc02G002544
Solyc02G002386	Solyc08G002373	Solyc02G002371	Solyc06G000219	Solyc02G002559
Solyc01G003124	Solyc08G002379	Solyc07G001989	Solyc04G002768	Solyc08G001395
Solyc01G003128	Solyc03G002631	Solyc03G002507	Solyc09G002616	Solyc01G000354
Solyc01G003155	Solyc01G001230	Solyc05G002352	Solyc03G002262	Solyc10G002529
Solyc04G001555	Solyc03G002651	Solyc12G002254	Solyc10G000342	Solyc10G002513
Solyc03G001473	Solyc10G000414	Solyc12G000413	Solyc08G000233	Solyc10G002462
Solyc12G002304	Solyc01G001247	Solyc01G001956	Solyc10G002548	Solyc07G000633
Solyc12G002299	Solyc11G000057	Solyc07G001722	Solyc09G000190	Solyc04G002009
Solyc02G001695	Solyc03G002665	Solyc11G000028	Solyc03G003214	Solyc04G001992
Solyc06G002162	Solyc03G003427	Solyc11G001063	Solyc09G002264	Solyc02G000676
Solyc06G002164	Solyc03G003446	Solyc01G002891	Solyc06G000705	Solyc08G001072
Solyc06G002192	Solyc02G000827	Solyc11G000025	Solyc07G001726	Solyc05G001664
Solyc06G002208	Solyc08G000127	Solyc10G002829	Solyc08G001597	Solyc04G000531
Solyc04G000731	Solyc01G004281	Solyc07G001496	Solyc04G000139	Solyc04G000553

Solyc04G000735	Solyc01G004284	Solyc03G000215	Solyc03G000435	Solyc11G001978
Solyc04G000736	Solyc01G004288	Solyc07G001565	Solyc08G002027	Solyc06G001319
Solyc04G000754	Solyc06G002267	Solyc10G002536	Solyc01G003826	Solyc12G001637
Solyc04G000821	Solyc06G002273	Solyc02G002616	Solyc09G000426	Solyc07G002592
Solyc04G000854	Solyc06G002280	Solyc02G001465	Solyc09G000429	Solyc07G002595
Solyc04G000842	Solyc06G001986	Solyc04G002457	Solyc04G000120	Solyc01G002705
Solyc01G002772	Solyc08G001452	Solyc04G002455	Solyc02G001969	Solyc07G002622
Solyc06G000795	Solyc03G002805	Solyc10G001588	Solyc02G001973	Solyc07G002634
Solyc03G000375	Solyc03G000365	Solyc05G002733	Solyc05G000802	Solyc08G000029
Solyc03G000381	Solyc06G001702	Solyc06G001958	Solyc11G001325	Solyc03G002043
Solyc05G000944	Solyc06G001699	Solyc06G001957	Solyc11G001327	Solyc01G001226
Solyc04G000259	Solyc06G001687	Solyc06G001949	Solyc09G001932	Solyc04G000700
Solyc01G002571	Solyc07G000322	Solyc03G001749	Solyc11G000681	Solyc04G000702
Solyc01G002572	Solyc03G002734	Solyc03G001734	Solyc08G000576	Solyc02G001518
Solyc01G002577	Solyc12G000272	Solyc03G003274	Solyc09G002715	Solyc07G002164
Solyc01G002585	Solyc05G002285	Solyc02G001349	Solyc09G002431	Solyc09G002007
Solyc03G002210	Solyc05G002274	Solyc08G001833	Solyc09G002436	Solyc01G000291

Solyc04G002705	Solyc09G001494	Solyc01G001548	Solyc01G001402	Solyc01G000301
Solyc03G003013	Solyc03G003584	Solyc09G002473	Solyc09G002710	Solyc01G000302
Solyc06G002091	Solyc05G000302	Solyc09G002471	Solyc04G000147	Solyc07G001302
Solyc06G002085	Solyc08G000045	Solyc03G001677	Solyc10G002875	Solyc03G001866
Solyc06G002083	Solyc08G000050	Solyc03G001682	Solyc07G002236	Solyc11G001499
Solyc01G003988	Solyc10G002464	Solyc01G004225	Solyc03G001295	Solyc04G002366
Solyc03G001766	Solyc05G002598	Solyc07G001414	Solyc05G001283	Solyc10G002356
Solyc05G000247	Solyc02G000586	Solyc12G000157	Solyc12G002440	Solyc02G002305
Solyc07G000608	Solyc11G002085	Solyc11G000261	Solyc09G000960	Solyc02G002289
Solyc12G001834	Solyc10G000587	Solyc01G003345	Solyc09G002686	Solyc02G002268
Solyc05G001011	Solyc11G000685	Solyc01G003475	Solyc08G002189	Solyc11G000370
Solyc05G000979	Solyc11G000849	Solyc09G000168	Solyc08G002202	Solyc10G000913
Solyc01G002273	Solyc05G001691	Solyc03G003321	Solyc01G001549	Solyc11G000384
Solyc01G002281	Solyc08G001304	Solyc09G000178	Solyc04G000033	Solyc03G000892
Solyc08G002479	Solyc04G002720	Solyc03G003324	Solyc09G002668	Solyc12G001477
Solyc08G002493	Solyc08G001362	Solyc01G003807	Solyc02G000953	Solyc10G001097
Solyc06G001433	Solyc01G003532	Solyc05G002540	Solyc03G000569	Solyc03G000327

Solyc06G001427	Solyc01G003551	Solyc01G002406	Solyc05G001119	Solyc03G000330
Solyc06G000362	Solyc09G000088	Solyc09G000118	Solyc05G001116	Solyc09G001132
Solyc03G001856	Solyc09G000100	Solyc12G000530	Solyc05G001084	Solyc09G002304
Solyc08G000401	Solyc01G000020	Solyc02G002983	Solyc05G001107	Solyc09G002316
Solyc12G002032	Solyc01G000028	Solyc02G002985	Solyc05G001688	Solyc10G001039
Solyc04G000374	Solyc01G002862	Solyc09G000287	Solyc03G001079	Solyc09G002324
Solyc04G000384	Solyc01G002867	Solyc12G000736	Solyc12G002352	Solyc03G002053
Solyc04G000382	Solyc01G002873	Solyc10G000131	Solyc12G002344	Solyc07G001486
Solyc04G000408	Solyc09G001254	Solyc10G000124	Solyc03G002849	Solyc05G001674
Solyc11G001804	Solyc05G000828	Solyc04G002834	Solyc09G000963	Solyc01G001225
Solyc12G002558	Solyc09G002578	Solyc12G001332	Solyc01G001883	Solyc04G001840
Solyc12G002553	Solyc09G002594	Solyc01G002502	Solyc03G001559	Solyc12G000188
Solyc12G002538	Solyc07G002660	Solyc01G002505	Solyc03G001557	Solyc12G000181
Solyc12G002049	Solyc04G002815	Solyc05G000273	Solyc10G001761	Solyc12G000172
Solyc09G002538	Solyc04G002819	Solyc05G002707	Solyc04G000222	Solyc12G000164
Solyc07G000955	Solyc11G000632	Solyc09G002265	Solyc05G001164	Solyc03G000422
Solyc03G001030	Solyc11G000630	Solyc01G000406	Solyc05G001547	Solyc02G001851

Solyc05G000198	Solyc05G000468	Solyc06G002517	Solyc09G000402	Solyc02G000524
Solyc05G000197	Solyc05G000467	Solyc06G001878	Solyc09G000031	Solyc03G002938
Solyc01G003582	Solyc08G000098	Solyc11G000306	Solyc05G002240	Solyc09G000639
Solyc01G003577	Solyc02G001886	Solyc11G000305	Solyc05G002234	Solyc10G000233
Solyc03G003367	Solyc10G002904	Solyc01G003440	Solyc05G002231	Solyc02G000573
Solyc09G002879	Solyc07G002283	Solyc07G001933	Solyc07G000145	Solyc02G000532
Solyc12G000237	Solyc05G002748	Solyc01G002085	Solyc02G002083	Solyc02G001998
Solyc08G000961	Solyc11G001678	Solyc01G000004	Solyc06G000911	Solyc02G001978
Solyc08G000089	Solyc03G003202	Solyc10G002632	Solyc08G000344	Solyc10G000298
Solyc01G003415	Solyc03G003206	Solyc10G002634	Solyc02G002090	Solyc07G000314
Solyc01G003416	Solyc11G000529	Solyc02G001233	Solyc05G001004	Solyc04G002869
Solyc01G003426	Solyc11G000519	Solyc03G000205	Solyc04G000963	Solyc04G002864
Solyc04G002507	Solyc09G001700	Solyc01G000667	Solyc11G001531	Solyc04G002841
Solyc12G001985	Solyc06G002127	Solyc01G000668	Solyc11G001536	Solyc02G000528
Solyc08G000189	Solyc04G000921	Solyc06G002502	Solyc11G001537	Solyc09G000634
Solyc08G000192	Solyc01G002635	Solyc06G002500	Solyc02G001253	Solyc02G002495
Solyc08G000390	Solyc12G000307	Solyc07G002728	Solyc02G001257	Solyc11G000692

Solyc08G000391	Solyc11G000098	Solyc07G002733	Solyc06G000990	Solyc07G001676
Solyc01G002465	Solyc11G000093	Solyc10G002758	Solyc04G001096	Solyc10G000292
Solyc01G001573	Solyc11G000089	Solyc07G002298	Solyc10G000671	Solyc03G000213
Solyc10G000182	Solyc11G000083	Solyc03G002758	Solyc02G000155	Solyc06G000274
Solyc10G000176	Solyc01G004376	Solyc08G001668	Solyc09G000895	Solyc06G000228
Solyc09G002130	Solyc01G002555	Solyc08G001670	Solyc07G001172	Solyc07G002063
Solyc06G000988	Solyc12G002103	Solyc01G003465	Solyc05G001231	Solyc07G002084
Solyc06G000317	Solyc12G002102	Solyc09G000272	Solyc01G004076	Solyc01G000181
Solyc09G002286	Solyc01G004370	Solyc02G000210	Solyc01G004096	Solyc01G000183
Solyc08G000210	Solyc05G002371	Solyc06G000255	Solyc01G004111	Solyc09G002288
Solyc08G000211	Solyc05G002368	Solyc06G000244	Solyc01G004124	Solyc09G002291
Solyc08G000212	Solyc04G000672	Solyc09G002547	Solyc01G004185	Solyc04G002578
Solyc08G002584	Solyc01G004356	Solyc12G000593	Solyc01G004194	Solyc12G002453
Solyc05G000654	Solyc02G001718	Solyc03G000016	Solyc09G001854	Solyc05G000147
Solyc05G000640	Solyc02G001734	Solyc03G000020	Solyc09G001544	Solyc05G000140
Solyc06G002774	Solyc06G001118	Solyc12G002580	Solyc07G000648	Solyc05G000135
Solyc11G000855	Solyc06G001120	Solyc12G002596	Solyc12G001054	Solyc09G002114

Solyc09G002028	Solyc01G004347	Solyc07G001786	Solyc02G000801	Solyc07G000183
Solyc09G002024	Solyc12G000456	Solyc07G001783	Solyc01G000334	Solyc09G002107
Solyc04G002285	Solyc01G004344	Solyc01G002943	Solyc01G000332	Solyc05G002356
Solyc04G002283	Solyc06G001641	Solyc03G002264	Solyc01G000322	Solyc12G001233
Solyc04G002278	Solyc06G001660	Solyc09G000157	Solyc08G002146	Solyc01G002685
Solyc02G002889	Solyc05G000615	Solyc09G002001	Solyc02G001011	Solyc01G002677
Solyc02G002901	Solyc05G000607	Solyc03G001327	Solyc02G001014	Solyc04G000367
Solyc08G000992	Solyc01G004336	Solyc08G001340	Solyc02G001043	Solyc04G003025
Solyc10G002918	Solyc05G002060	Solyc05G000568	Solyc02G001055	Solyc10G002667
Solyc01G002929	Solyc06G002475	Solyc05G000570	Solyc02G001056	Solyc07G000418
Solyc01G002941	Solyc10G002176	Solyc05G000564	Solyc02G000980	Solyc03G003199
Solyc04G001855	Solyc07G001595	Solyc06G001706	Solyc04G000979	Solyc00G000012
Solyc07G000053	Solyc10G002274	Solyc01G002852	Solyc05G002333	Solyc00G000017
Solyc09G001840	Solyc10G002719	Solyc00G000019	Solyc07G001653	Solyc11G001222
Solyc01G001641	Solyc03G000552	Solyc05G001415	Solyc03G002478	Solyc00G000013
Solyc02G000194	Solyc11G002066	Solyc05G001418	Solyc03G002489	Solyc00G000014
Solyc01G002383	Solyc01G004321	Solyc10G000860	Solyc04G002642	Solyc00G000015

Solyc02G000256	Solyc01G004314	Solyc10G000861	Solyc04G002628	Solyc00G000016
Solyc02G000259	Solyc08G002315	Solyc07G000360	Solyc04G002626	Solyc11G001233
Solyc06G000474	Solyc03G003246	Solyc01G001756	Solyc06G002625	Solyc06G001259
Solyc11G001945	Solyc03G003236	Solyc06G001580	Solyc06G000698	Solyc05G002503
Solyc07G000231	Solyc01G002654	Solyc10G002698	Solyc01G001996	Solyc05G002483
Solyc04G002237	Solyc12G000399	Solyc10G002884	Solyc04G001756	Solyc07G000417
Solyc05G000078	Solyc01G002793	Solyc03G000002	Solyc04G001742	Solyc07G001810
Solyc12G000866	Solyc11G002519	Solyc09G000421	Solyc08G001274	Solyc05G001944
Solyc10G002072	Solyc07G001945	Solyc10G002734	Solyc02G000290	Solyc01G003448
Solyc01G003351	Solyc12G002209	Solyc09G002212	Solyc02G000268	Solyc06G002254
Solyc02G001594	Solyc01G003957	Solyc08G000244	Solyc11G000001	Solyc07G000066
Solyc02G001592	Solyc01G000209	Solyc08G001884	Solyc05G000868	Solyc01G003934
Solyc10G000496	Solyc07G000331	Solyc02G002828	Solyc06G000090	Solyc09G001867
Solyc01G002823	Solyc07G001803	Solyc01G003819	Solyc06G000094	Solyc09G000656
Solyc01G002812	Solyc07G000048	Solyc09G000444	Solyc06G002569	Solyc08G001398
Solyc12G000755	Solyc06G001046	Solyc02G002840	Solyc09G002571	Solyc04G000053
Solyc03G003131	Solyc10G000059	Solyc05G002652	Solyc01G003182	Solyc09G002172

Solyc03G003139	Solyc10G000085	Solyc05G002669	Solyc01G003198	Solyc05G000937
Solyc03G003143	Solyc01G004046	Solyc03G001723	Solyc01G003233	Solyc03G000530
Solyc03G003153	Solyc10G000119	Solyc07G002508	Solyc09G001369	Solyc03G000524
Solyc03G003172	Solyc01G004054	Solyc03G001719	Solyc11G002445	Solyc09G002346
Solyc03G003183	Solyc08G000083	Solyc06G000853	Solyc08G001908	Solyc09G002345
Solyc08G000723	Solyc06G000820	Solyc01G000154	Solyc04G001129	Solyc01G002421
Solyc10G002324	Solyc10G000011	Solyc01G000138	Solyc02G001786	Solyc01G002448
Solyc03G002620	Solyc05G001281	Solyc01G001523	Solyc11G002452	Solyc01G002452
Solyc08G001000	Solyc02G001543	Solyc11G002112	Solyc02G001779	Solyc03G001393
Solyc07G002760	Solyc02G001561	Solyc11G002070	Solyc02G001750	Solyc04G001821
Solyc07G001025	Solyc02G001577	Solyc12G000491	Solyc11G000130	Solyc02G001372
Solyc07G002743	Solyc03G002139	Solyc08G002515	Solyc11G000132	Solyc02G001388
Solyc06G001898	Solyc01G002117	Solyc08G002531	Solyc11G000135	Solyc02G001427
Solyc09G002854	Solyc01G002104	Solyc06G001003	Solyc11G000140	Solyc02G001432
Solyc09G002828	Solyc04G000485	Solyc03G002124	Solyc08G002415	Solyc02G001447
Solyc02G002986	Solyc04G000504	Solyc03G002131	Solyc08G002390	Solyc12G000038
Solyc09G000672	Solyc11G000869	Solyc11G002126	Solyc02G000163	Solyc03G003490

Solyc01G002042	Solyc11G000870	Solyc05G000096	Solyc02G000213	Solyc03G003517
Solyc07G000100	Solyc02G002736	Solyc04G000448	Solyc11G002390	Solyc03G003518
Solyc09G000537	Solyc11G001549	Solyc06G000394	Solyc05G000399	Solyc03G003566
Solyc02G001105	Solyc01G002011	Solyc11G002136	Solyc05G000405	Solyc08G001999
Solyc06G002452	Solyc01G002074	Solyc02G001088	Solyc03G002621	Solyc09G002760
Solyc06G002442	Solyc01G002055	Solyc06G001942	Solyc04G001435	Solyc09G002773
Solyc06G002423	Solyc01G003055	Solyc06G001947	Solyc06G000182	Solyc09G002794
Solyc03G000984	Solyc01G003050	Solyc11G002140	Solyc11G002172	Solyc11G002033
Solyc06G002409	Solyc07G002348	Solyc06G001623	Solyc04G003014	Solyc02G000713
Solyc03G002403	Solyc07G002386	Solyc11G002145	Solyc04G002997	Solyc08G000935
Solyc03G002391	Solyc07G002405	Solyc03G002973	Solyc11G002179	Solyc11G000325
Solyc12G001457	Solyc06G001310	Solyc01G003632	Solyc08G001850	Solyc11G000357
Solyc04G001947	Solyc06G001298	Solyc11G002166	Solyc08G001854	Solyc02G001219
Solyc03G003082	Solyc08G000874	Solyc01G003613	Solyc06G001991	Solyc09G000332
Solyc03G003043	Solyc04G002448	Solyc01G003609	Solyc06G001974	Solyc09G000347
Solyc09G001203	Solyc04G000334	Solyc11G002168	Solyc02G002942	Solyc11G002429
Solyc09G001221	Solyc06G002326	Solyc09G000648	Solyc02G002940	Solyc10G001255

Solyc10G000851	Solyc06G002327	Solyc02G000307	Solyc08G002062	Solyc00G000007
Solyc11G001062	Solyc08G001423	Solyc04G003020	Solyc11G001558	Solyc01G003157
Solyc04G001955	Solyc07G002228	Solyc01G003162	Solyc12G000373	Solyc10G002421
Solyc01G001963	Solyc06G002003	Solyc01G003163	Solyc12G000365	Solyc01G003256
Solyc11G001547	Solyc12G001928	Solyc08G001867	Solyc03G002323	Solyc10G001194
Solyc04G001989	Solyc05G001123	Solyc12G002748	Solyc11G000269	Solyc03G000291
Solyc00G000018	Solyc09G002558	Solyc12G002732	Solyc12G001196	Solyc10G001187
Solyc09G000494	Solyc06G000550	Solyc01G003519	Solyc11G001372	Solyc12G001652
Solyc09G000482	Solyc07G002443	Solyc01G003513	Solyc01G003850	Solyc07G002470
Solyc08G001078	Solyc04G000627	Solyc07G000302	Solyc01G003885	Solyc07G002102
Solyc12G002688	Solyc01G002970	Solyc07G001467	Solyc01G003900	Solyc07G002105
Solyc01G001925	Solyc01G002975	Solyc12G002785	Solyc08G000814	Solyc07G002133
Solyc01G001911	Solyc01G002983	Solyc12G002808	Solyc10G002390	Solyc08G001726
Solyc03G002337	Solyc01G003273	Solyc11G002223	Solyc10G002401	
Solyc01G002236	Solyc01G003677	Solyc11G002229	Solyc11G002045	
Solyc07G002482	Solyc04G001303	Solyc11G002230	Solyc01G002872	
Solyc01G003647	Solyc00G000041	Solyc11G001415	Solyc08G001712	

Differentially Expressed Genes (DEGs) at 24 hours

Solyc06G001863	Solyc04G000417	Solyc11G000053	Solyc08G001491	Solyc09G000177
Solyc03G002171	Solyc12G002550	Solyc03G003434	Solyc08G000380	Solyc03G002914
Solyc01G000234	Solyc12G002537	Solyc01G004254	Solyc08G000373	Solyc03G002907
Solyc07G002810	Solyc09G002532	Solyc01G004278	Solyc12G002102	Solyc05G000831
Solyc08G000076	Solyc08G001927	Solyc01G004298	Solyc05G002368	Solyc05G002537
Solyc07G002795	Solyc08G000028	Solyc06G002280	Solyc10G002061	Solyc09G000118
Solyc07G002794	Solyc01G003563	Solyc04G002747	Solyc03G000740	Solyc01G001358
Solyc02G002412	Solyc02G000237	Solyc01G001958	Solyc06G002726	Solyc09G000371
Solyc01G003151	Solyc12G002318	Solyc03G002813	Solyc01G004359	Solyc12G000738
Solyc01G003155	Solyc08G000829	Solyc03G002805	Solyc04G000672	Solyc04G002834
Solyc08G001572	Solyc12G001985	Solyc03G002776	Solyc02G001734	Solyc12G001332
Solyc08G001574	Solyc02G001119	Solyc02G001641	Solyc06G001120	Solyc03G001922
Solyc02G001343	Solyc09G000552	Solyc03G002734	Solyc01G004347	Solyc11G000433
Solyc06G002162	Solyc04G001277	Solyc12G000263	Solyc11G000662	Solyc01G003440
Solyc06G002208	Solyc08G000192	Solyc03G003596	Solyc06G002478	Solyc07G001778
Solyc04G000731	Solyc01G002465	Solyc03G003584	Solyc12G000710	Solyc01G000004

Solyc04G000735	Solyc10G000182	Solyc05G000300	Solyc08G002315	Solyc07G002728
Solyc03G000574	Solyc09G002130	Solyc05G002593	Solyc01G002671	Solyc07G002737
Solyc04G000854	Solyc06G000317	Solyc10G002464	Solyc01G002655	Solyc11G000037
Solyc01G002778	Solyc11G000855	Solyc10G002467	Solyc07G000331	Solyc04G000260
Solyc06G000795	Solyc02G002876	Solyc02G000586	Solyc02G000484	Solyc02G000210
Solyc03G000381	Solyc10G001715	Solyc12G002165	Solyc01G003386	Solyc06G000255
Solyc09G002180	Solyc01G002942	Solyc11G000685	Solyc01G002965	Solyc06G002226
Solyc05G000115	Solyc04G000355	Solyc11G000849	Solyc03G002534	Solyc09G002540
Solyc04G000259	Solyc05G000990	Solyc04G001141	Solyc01G001936	Solyc03G000016
Solyc04G000250	Solyc02G001081	Solyc05G000223	Solyc11G002513	Solyc03G000017
Solyc01G002568	Solyc01G001641	Solyc04G002720	Solyc06G002337	Solyc12G002585
Solyc01G002587	Solyc02G000194	Solyc04G002733	Solyc06G002347	Solyc12G000667
Solyc03G002975	Solyc11G001944	Solyc01G003551	Solyc02G002366	Solyc07G001783
Solyc05G000979	Solyc04G000269	Solyc09G000090	Solyc07G001989	Solyc06G002233
Solyc01G002273	Solyc04G000275	Solyc01G000018	Solyc12G000437	Solyc06G001716
Solyc08G002479	Solyc07G000152	Solyc01G000029	Solyc01G001956	Solyc06G001706
Solyc08G002494	Solyc05G000078	Solyc01G002871	Solyc04G001659	Solyc02G002799

Solyc06G001433	Solyc05G002469	Solyc09G001254	Solyc10G002825	Solyc10G002698
Solyc11G001835	Solyc12G000866	Solyc05G000828	Solyc10G002826	Solyc10G002887
Solyc07G000027	Solyc10G002072	Solyc09G002586	Solyc07G001496	Solyc04G002223
Solyc12G002032	Solyc01G003350	Solyc07G002678	Solyc04G002457	Solyc02G001535
Solyc02G001921	Solyc01G003368	Solyc11G000642	Solyc05G002729	Solyc03G002892
Solyc07G000015	Solyc08G000167	Solyc11G002251	Solyc06G001957	Solyc09G002212
Solyc01G002188	Solyc12G000743	Solyc12G000938	Solyc06G001949	Solyc09G002215
Solyc04G000374	Solyc07G002544	Solyc12G000937	Solyc08G000259	Solyc08G000247
Solyc04G000390	Solyc07G002528	Solyc02G001896	Solyc09G000009	Solyc08G000245
Solyc04G000413	Solyc12G001010	Solyc05G002741	Solyc03G001742	Solyc12G000685
Solyc06G000259	Solyc04G002140	Solyc05G002762	Solyc03G001734	Solyc12G002248
Solyc03G000135	Solyc02G001456	Solyc02G002472	Solyc08G001833	Solyc08G001884
Solyc04G002541	Solyc12G000728	Solyc12G001141	Solyc03G003291	Solyc07G001857
Solyc10G002548	Solyc12G000719	Solyc03G003209	Solyc11G001957	Solyc08G000116
Solyc09G000183	Solyc01G002524	Solyc01G004389	Solyc01G004225	Solyc04G002482
Solyc01G002840	Solyc12G000965	Solyc11G000529	Solyc04G002213	Solyc02G002843
Solyc03G003188	Solyc04G000645	Solyc01G004384	Solyc08G000315	Solyc03G001759

Solyc03G000435	Solyc07G000365	Solyc01G004383	Solyc11G000264	Solyc05G000092
Solyc04G002791	Solyc01G002611	Solyc04G000921	Solyc11G000261	Solyc05G000093
Solyc01G001937	Solyc03G002631	Solyc01G004380	Solyc01G003345	Solyc12G002718
Solyc05G000802	Solyc01G001247	Solyc01G002635	Solyc09G000168	Solyc12G002850
Solyc10G001269	Solyc02G000155	Solyc12G002377	Solyc06G002256	Solyc06G001027
Solyc09G001931	Solyc06G000964	Solyc06G001139	Solyc01G003939	Solyc02G001110
Solyc11G000829	Solyc12G001155	Solyc02G002185	Solyc09G001867	Solyc06G002442
Solyc11G000681	Solyc05G001231	Solyc02G002148	Solyc08G000865	Solyc03G002391
Solyc11G002052	Solyc01G004076	Solyc08G000939	Solyc08G001398	Solyc12G001457
Solyc09G002436	Solyc01G004096	Solyc08G001307	Solyc04G000053	Solyc04G001947
Solyc05G002742	Solyc01G004185	Solyc02G002544	Solyc03G001686	Solyc12G000365
Solyc03G000648	Solyc09G001854	Solyc10G002530	Solyc06G000289	Solyc04G001984
Solyc09G002704	Solyc07G000648	Solyc10G002462	Solyc09G002345	Solyc00G000018
Solyc07G002236	Solyc12G001054	Solyc04G002009	Solyc01G002448	Solyc09G000482
Solyc04G001286	Solyc08G001060	Solyc02G000643	Solyc02G001370	Solyc01G001912
Solyc03G001345	Solyc01G000328	Solyc08G001072	Solyc02G001432	Solyc01G001906
Solyc03G001295	Solyc02G001014	Solyc11G001976	Solyc03G003548	Solyc11G001372

Solyc12G002441	Solyc06G001127	Solyc07G002589	Solyc03G003555	Solyc01G003854
Solyc12G002440	Solyc04G000969	Solyc07G002634	Solyc10G001642	Solyc01G003872
Solyc01G001420	Solyc03G002478	Solyc08G000029	Solyc08G001995	Solyc01G003885
Solyc01G001549	Solyc04G002642	Solyc08G000030	Solyc09G002794	Solyc08G000814
Solyc09G002668	Solyc11G000881	Solyc10G002812	Solyc03G001992	Solyc07G001126
Solyc02G000953	Solyc06G000698	Solyc09G001232	Solyc11G000357	Solyc03G002602
Solyc05G001116	Solyc06G000957	Solyc03G003140	Solyc02G001219	Solyc01G004033
Solyc05G001084	Solyc10G000531	Solyc02G001513	Solyc10G001255	Solyc10G002393
Solyc05G001107	Solyc04G001738	Solyc07G002164	Solyc11G002430	Solyc10G002421
Solyc03G001079	Solyc02G000290	Solyc06G000063	Solyc00G000007	Solyc10G000078
Solyc09G000022	Solyc01G000070	Solyc01G000290	Solyc01G003162	Solyc10G000113
Solyc03G002849	Solyc06G000094	Solyc09G001106	Solyc01G003198	Solyc05G001281
Solyc01G001335	Solyc06G001227	Solyc11G000408	Solyc01G003207	Solyc06G000017
Solyc10G000940	Solyc06G001228	Solyc07G001464	Solyc01G003233	Solyc01G003723
Solyc03G001557	Solyc09G002252	Solyc03G000330	Solyc11G002445	Solyc02G001543
Solyc04G000222	Solyc09G002244	Solyc03G000339	Solyc02G001790	Solyc02G001576
Solyc05G001164	Solyc12G000659	Solyc05G001674	Solyc08G002419	Solyc05G000056

Solyc11G001898	Solyc06G000757	Solyc01G001225	Solyc11G002398	Solyc05G000057
Solyc05G001698	Solyc08G001438	Solyc03G000150	Solyc02G000163	Solyc04G001612
Solyc05G001547	Solyc04G002039	Solyc07G001027	Solyc04G001036	Solyc01G002107
Solyc09G000031	Solyc06G001240	Solyc06G000034	Solyc05G000392	Solyc04G000493
Solyc05G001026	Solyc07G002250	Solyc02G000570	Solyc06G000183	Solyc04G000504
Solyc05G002208	Solyc09G000004	Solyc02G000532	Solyc03G003139	Solyc11G000876
Solyc07G001166	Solyc06G000506	Solyc01G001801	Solyc12G001801	Solyc02G002717
Solyc11G001465	Solyc09G002288	Solyc12G001992	Solyc06G000187	Solyc01G002065
Solyc02G002090	Solyc09G002291	Solyc10G000253	Solyc10G002324	Solyc01G002063
Solyc11G001471	Solyc05G000147	Solyc10G000263	Solyc06G000525	Solyc07G001970
Solyc04G000963	Solyc09G002112	Solyc07G001677	Solyc09G002854	Solyc07G002386
Solyc11G001868	Solyc05G002356	Solyc07G001676	Solyc09G002851	Solyc06G000884
Solyc02G001253	Solyc10G002670	Solyc03G000213	Solyc09G002819	Solyc03G000484
Solyc02G001257	Solyc03G003199	Solyc03G002206	Solyc02G002986	Solyc12G001093
Solyc02G001268	Solyc01G003443	Solyc07G002084	Solyc07G000106	Solyc09G000460
Solyc05G001232	Solyc09G001876	Solyc03G000594	Solyc11G001709	Solyc11G001427
Solyc11G000321	Solyc06G002254	Solyc05G000069	Solyc06G002294	Solyc11G001700

Solyc02G002699	Solyc04G001303	Solyc08G002538	Solyc08G001854	Solyc11G002223
Solyc08G001423	Solyc06G001288	Solyc03G002131	Solyc08G001856	Solyc01G002236
Solyc02G002951	Solyc06G001287	Solyc11G000484	Solyc12G002765	Solyc11G002225
Solyc03G000865	Solyc05G000347	Solyc11G002123	Solyc07G000290	Solyc08G001784
Solyc03G000625	Solyc05G002638	Solyc11G002136	Solyc06G001783	Solyc01G001673
Solyc02G002263	Solyc05G002652	Solyc07G002136	Solyc12G002785	Solyc01G002872
Solyc01G002970	Solyc03G001723	Solyc06G001942	Solyc11G002112	Solyc01G003613
Solyc01G002975	Solyc03G001719	Solyc06G001601	Solyc08G002531	Solyc08G001850
Solyc01G003273	Solyc01G000138	Solyc06G001609	Solyc07G002482	
Solyc03G000291	Solyc01G000135	Solyc03G002973	Solyc01G003677	

Differentially Expressed Genes (DEGs) at 48 hours

Solyc06G001844	Solyc06G002262	Solyc09G001641	Solyc02G002514	Solyc10G000148
Solyc10G002779	Solyc05G002324	Solyc04G002642	Solyc06G000270	Solyc10G001715
Solyc11G002546	Solyc11G002087	Solyc12G002611	Solyc05G000066	Solyc01G002934
Solyc04G000800	Solyc04G001653	Solyc04G001530	Solyc10G000456	Solyc01G002939
Solyc05G000115	Solyc06G002739	Solyc05G000878	Solyc06G001541	Solyc04G002913

Solyc03G000503	Solyc11G001522	Solyc04G002032	Solyc09G002019	Solyc04G000645
Solyc01G003990	Solyc01G004317	Solyc06G001316	Solyc02G001372	Solyc03G002973
Solyc08G002489	Solyc08G002316	Solyc03G002043	Solyc03G003537	Solyc04G002984
Solyc07G000029	Solyc08G000580	Solyc03G000422	Solyc09G002784	Solyc10G002088
Solyc09G002879	Solyc07G001989	Solyc02G001811	Solyc09G000734	Solyc06G002535
Solyc09G000558	Solyc08G001528	Solyc10G000315	Solyc03G001077	Solyc07G001475
Solyc02G002953	Solyc04G002828	Solyc10G000263	Solyc03G003059	Solyc01G002236
Solyc12G001452	Solyc01G000281	Solyc07G000505	Solyc08G002052	Solyc06G002369
Solyc02G002263	Solyc01G002120	Solyc05G001026	Solyc12G000337	Solyc11G001415
Solyc04G000440	Solyc07G002217	Solyc11G002200	Solyc05G000553	

Visual representation of the green in the *S. dulcamara* WGCNA

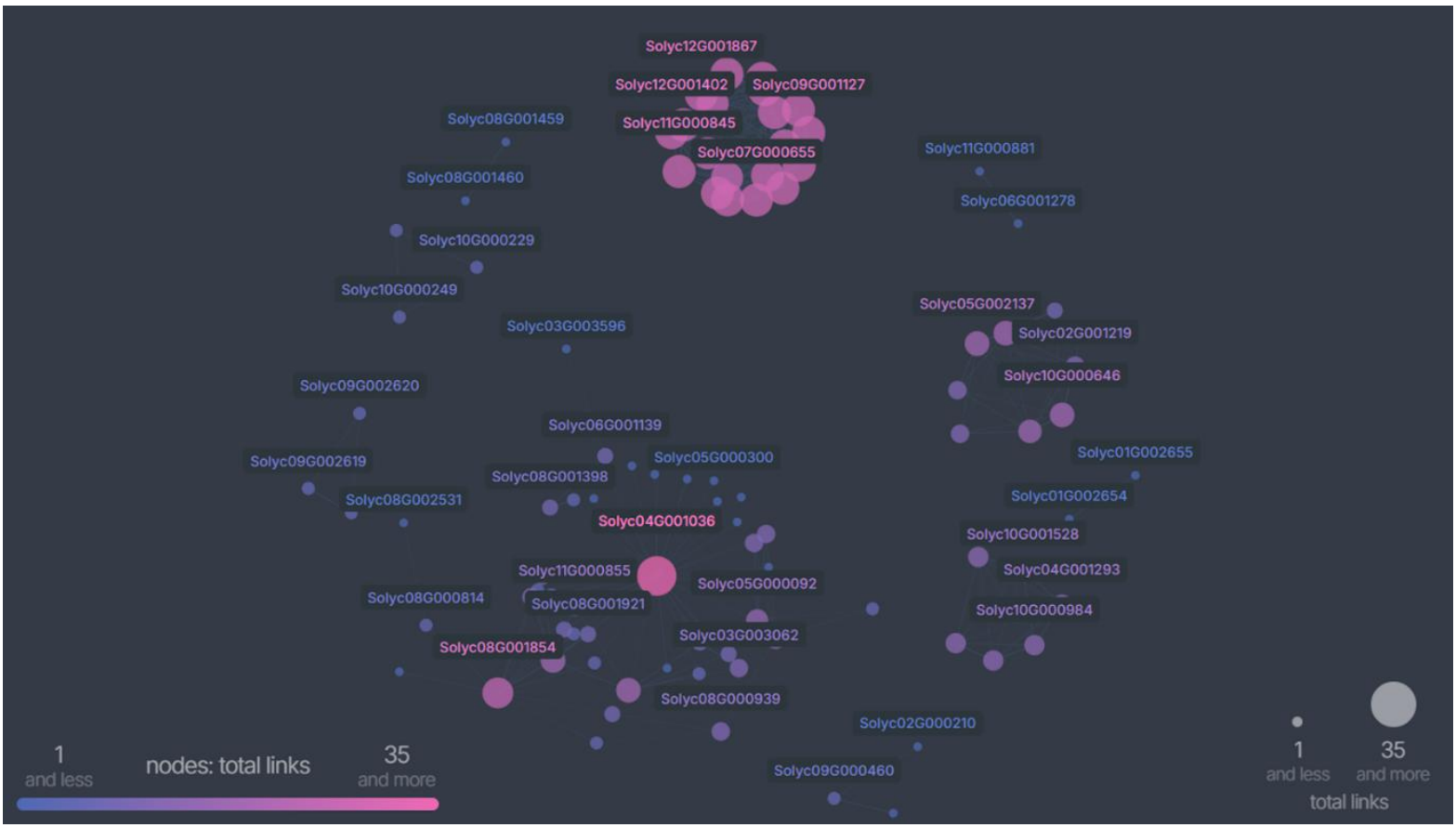

Figure S.2.1 Visual representation of the green module in the *S. dulcamara* network. Each node's connection is represented by lines, indicating which genes are directly and indirectly linked. The size and colour of each node indicate how many connections that gene has within the network, with pink representing more links than blue.

Visual representation of the lightyellow in the *S. lycopersicum* WGCNA

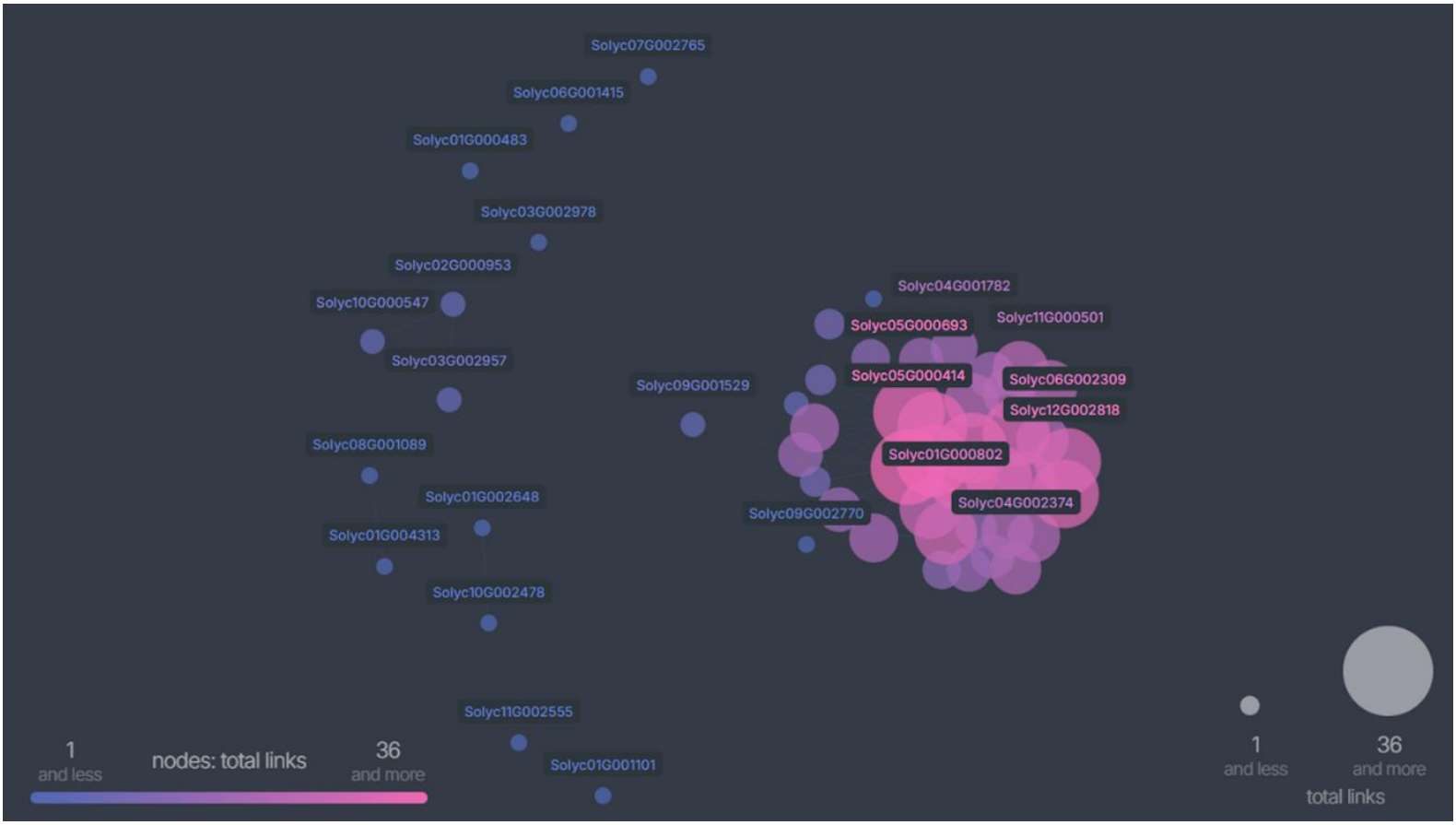

Figure S.2.2 Visual representation of the lightyellow module in the *S. lycopersicum* network. Each node's connection is represented by lines, indicating which genes are directly and indirectly linked. The size and colour of each node indicate how many connections that gene has within the network, with pink representing more links than blue.

Visual representation of the steelblue in the S. lycopersicum WGCNA

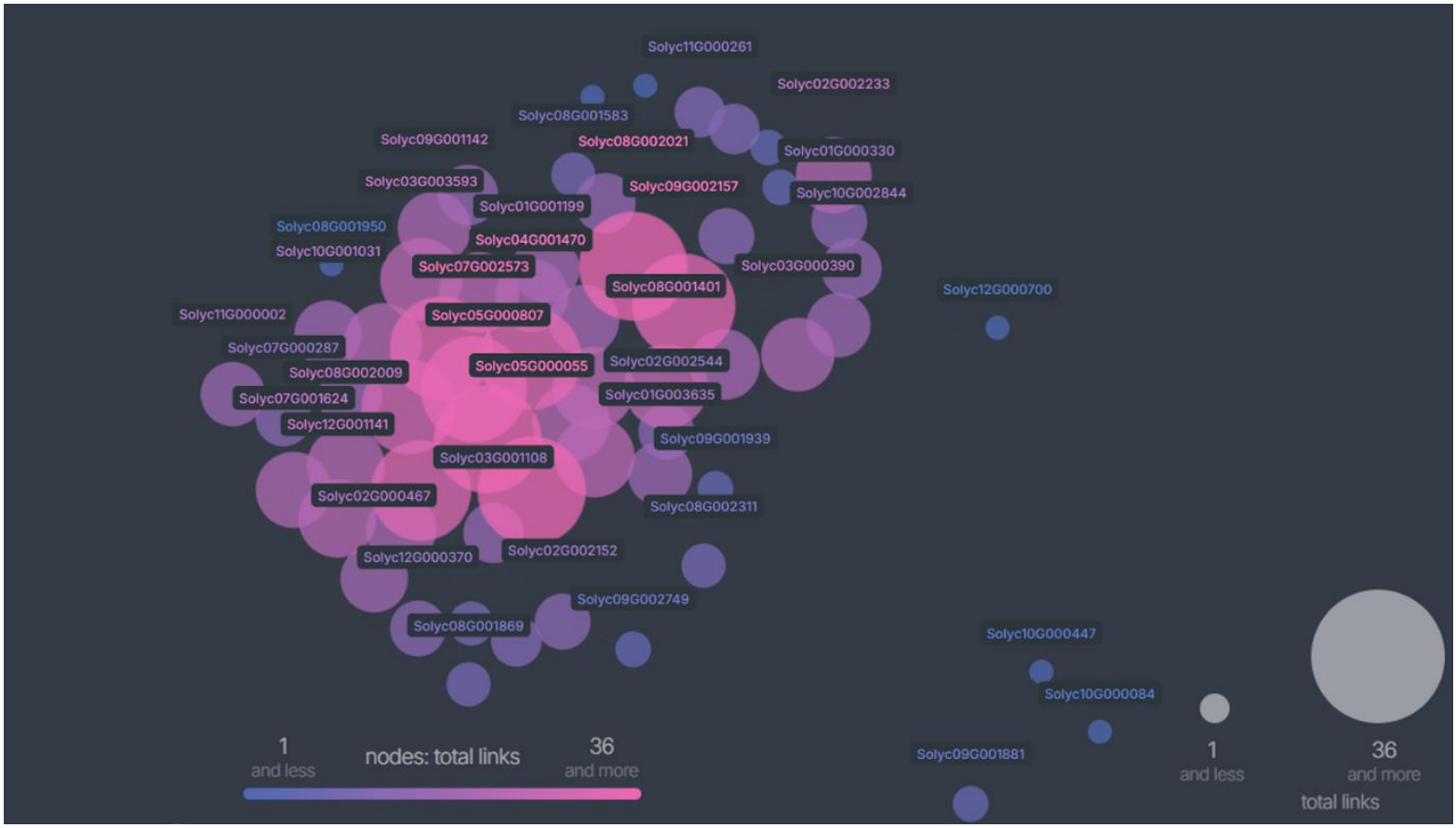

Figure S.2.3 Visual representation of the steelblue module in the *S. lycopersicum* network. Each node's connection is represented by lines, indicating which genes are directly and indirectly linked. The size and colour of each node indicate how many connections that gene has within the network, with pink representing more links than blue.

S.3 Supplementary Material for Chapter 3

Visual representation of the darkgrey in the CANA

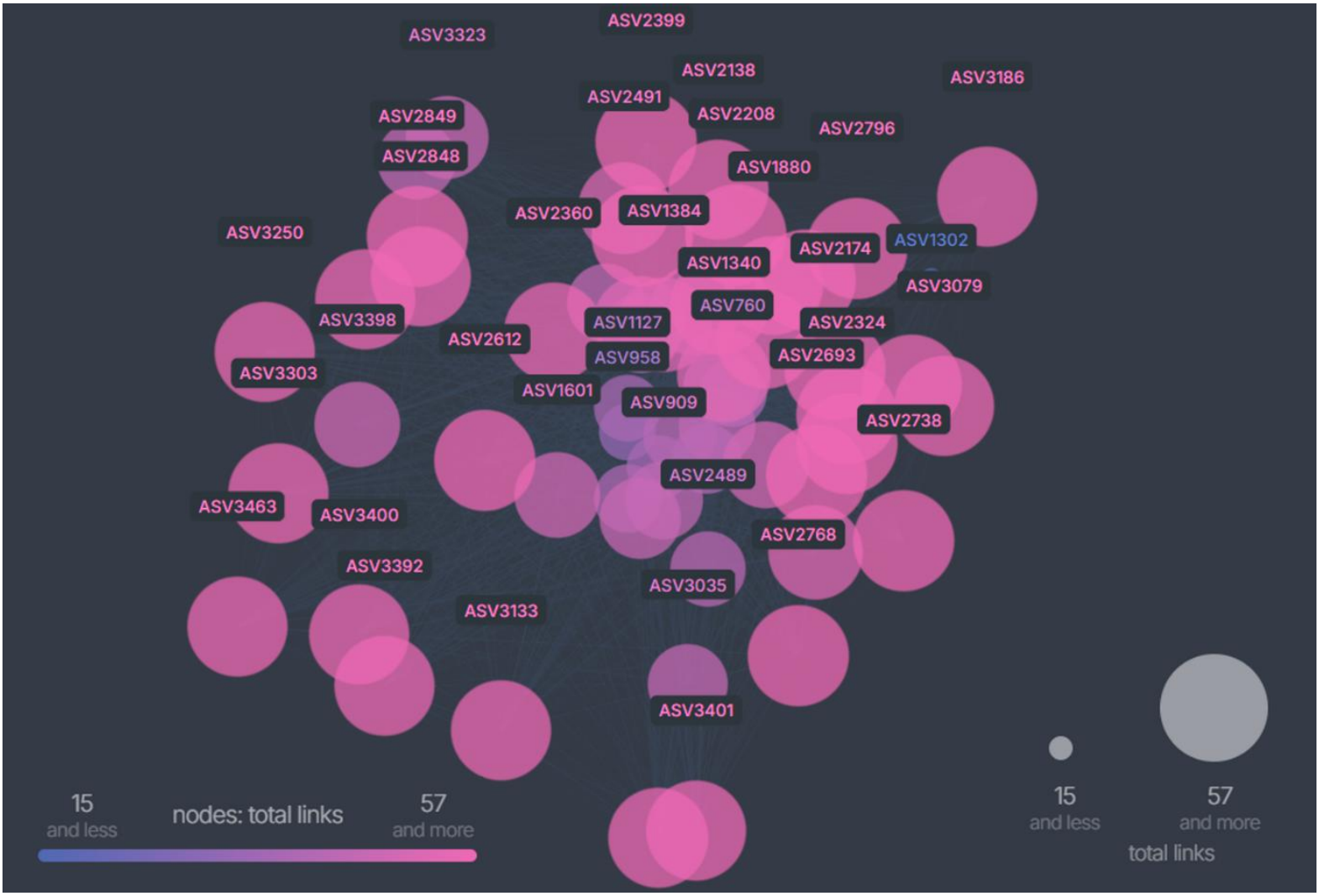

Figure S.3.1 Visual representation of the darkgrey module in the CANA. Each node's connection is represented by lines, indicating which species are directly and indirectly linked. The size and colour of each node indicate how many connections that species has within the network, with pink representing more links than blue.

Visual representation of the steelblue in the CANA

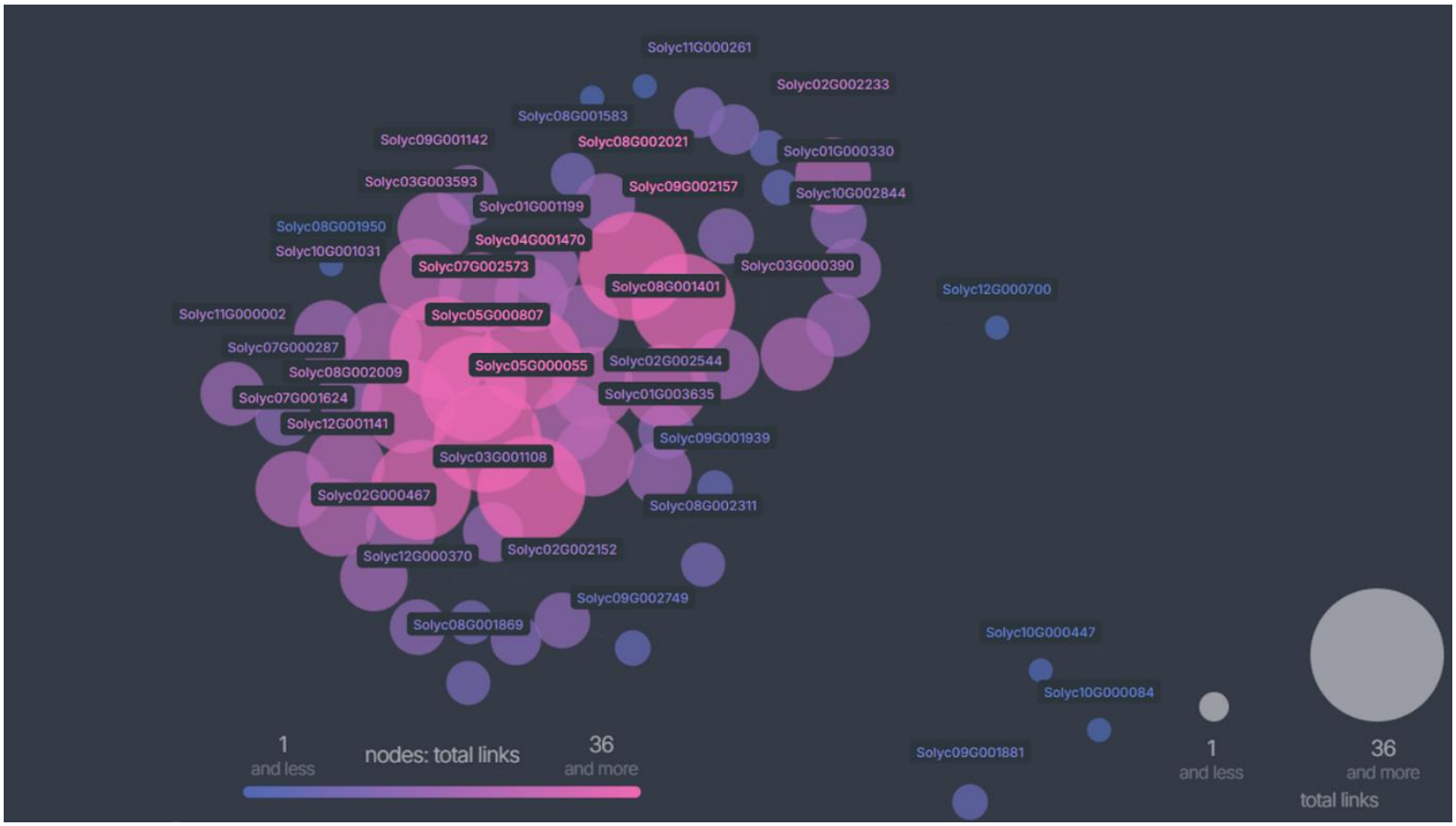

Figure S.3.2 Visual representation of the steelblue module in the CANA. Each node's connection is represented by lines, indicating which species are directly and indirectly linked. The size and colour of each node indicate how many connections that species has within the network, with pink representing more links than blue.

Visual representation of the lightyellow in the CANA

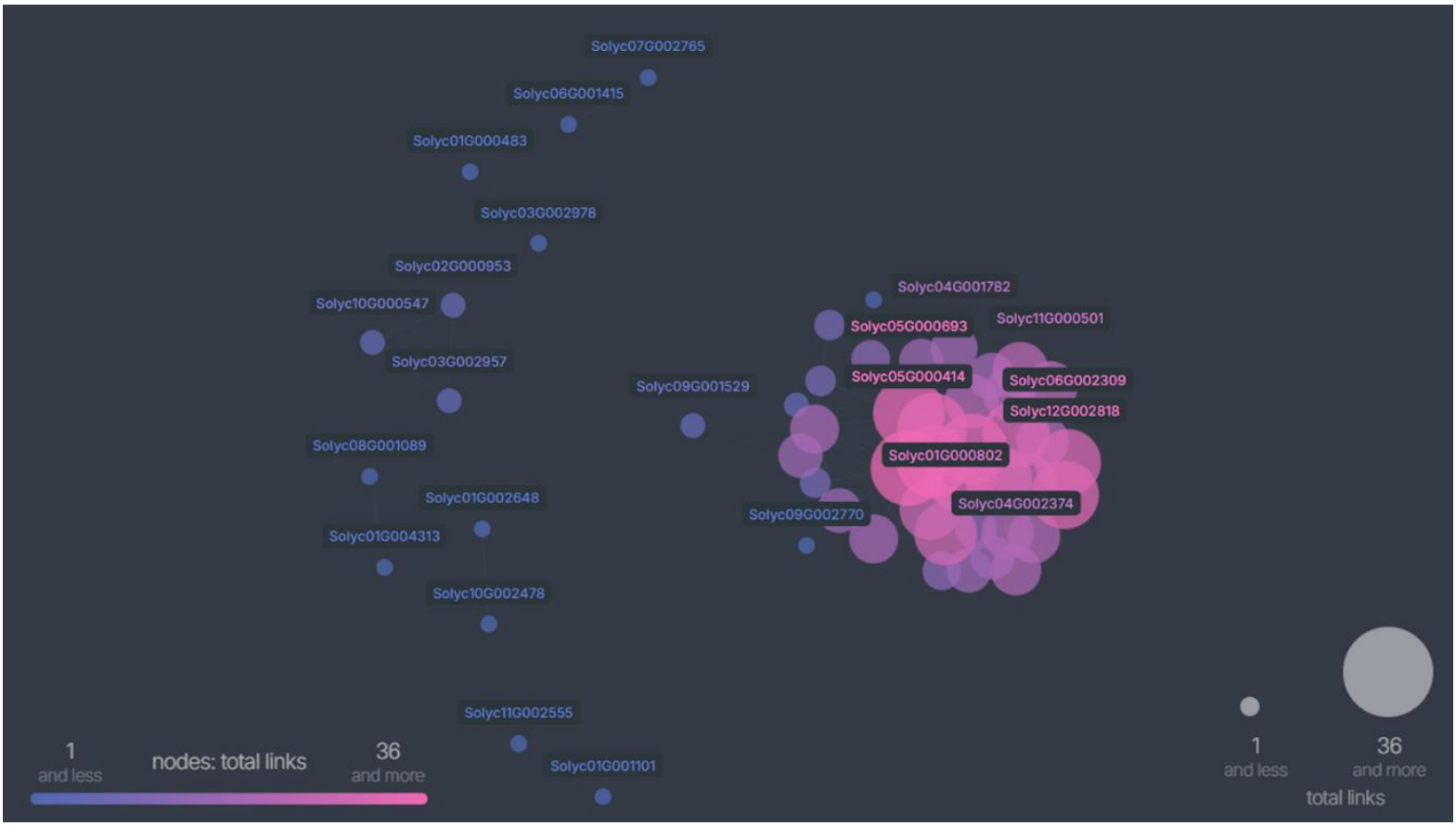

Figure S.3.3 Visual representation of the lightyellow module in the CANA. Each node's connection is represented by lines, indicating which species are directly and indirectly linked. The size and colour of each node indicate how many connections that species has within the network, with pink representing more links than blue.

Visual representation of the saddlebrown in the CANA

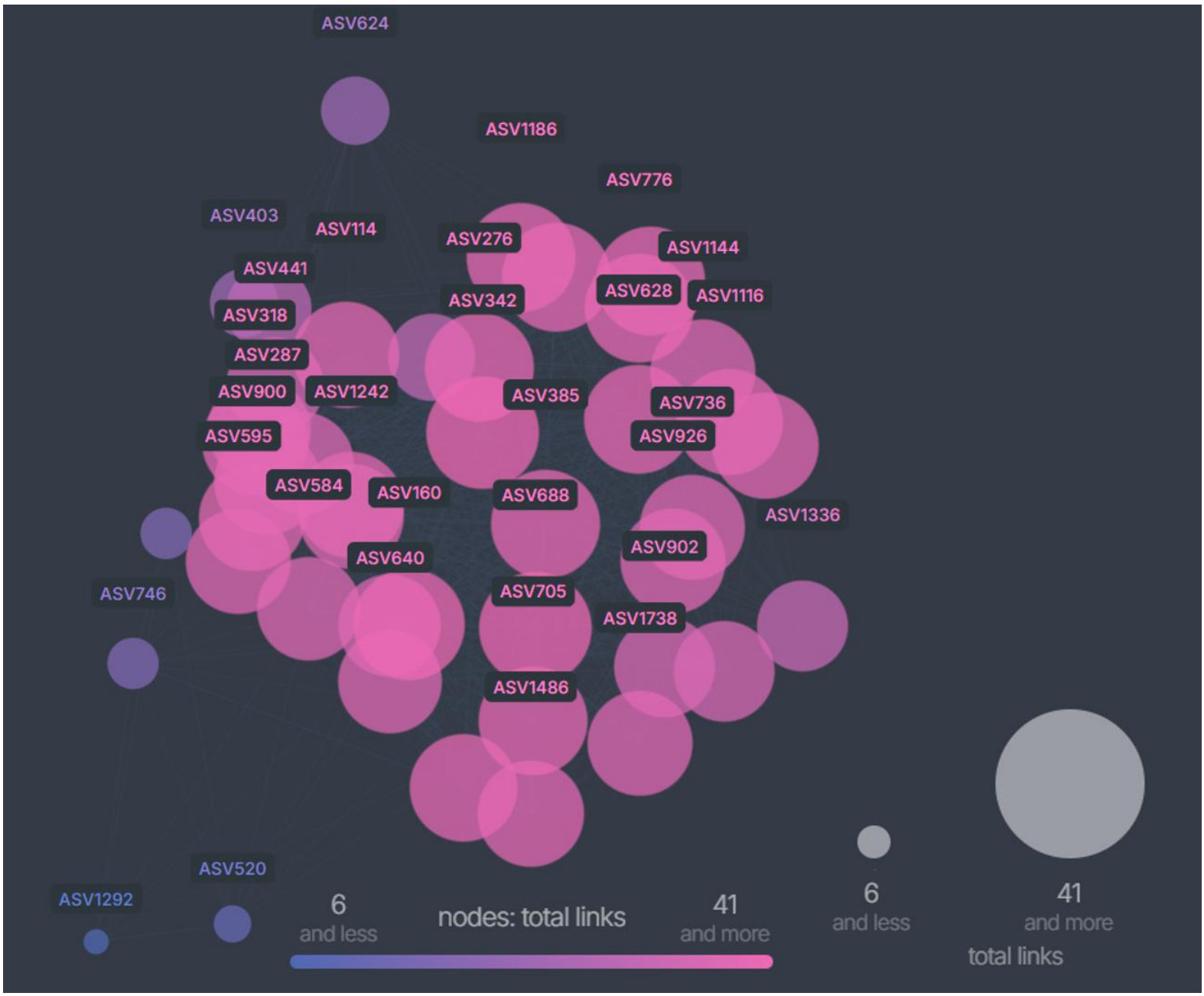

Figure S.3.4 Visual representation of the saddlebrown module in the CANA. Each node's connection is represented by lines, indicating which species are directly and indirectly linked. The size and colour of each node indicate how many connections that species has within the network, with pink representing more links than blue.

Visual representation of the skyblue in the CANA

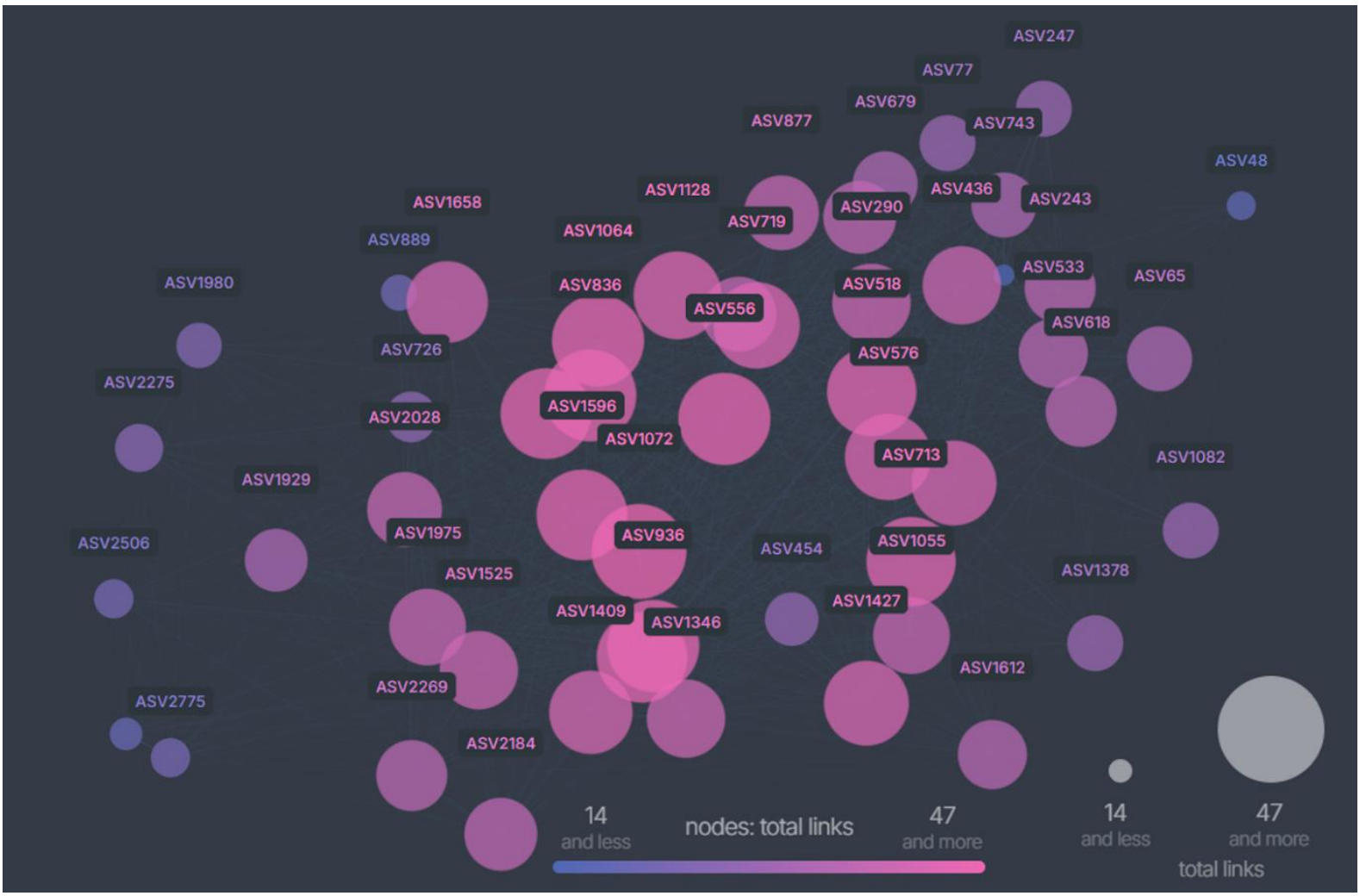

Figure S.3.5 Visual representation of the skyblue module in the CANA. Each node's connection is represented by lines, indicating which species are directly and indirectly linked. The size and colour of each node indicate how many connections that species has within the network, with pink representing more links than blue.